Universitat
de Barcelona

Intrauterine Growth Restriction (IUGR) and imprinted gene expression in the placenta: Role of *PLAGL1* and analysis of the 6q24.2 region

Isabel Iglesias Platas

UNIVERSITAT DE BARCELONA

INTRAUTERINE GROWTH RESTRICTION (IUGR) AND IMPRINTED GENE EXPRESSION IN THE PLACENTA: ROLE OF *PLAGL1* AND ANALYSIS OF THE 6q24.2 REGION

TESIS DOCTORAL

ISABEL IGLESIAS PLATAS

DIRIGIDA POR

PROF. GUDRUN E. MOORE/ DR. MARTÍN IRIONDO SANZ
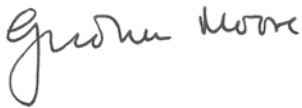
Photograph: Magnification (x400) of a fetoplacental vascular cast in term placenta. From Kaufmann P, Mayhew TM and Charnock-Jones DS, Placenta, 2004. 25: 114-116.

Prof. Gudrun E. Moore, Institute of Child Health (ICH), London,

y Martín Iriondo Sanz, Universitat de Barcelona, acreditan que el trabajo titulado:

CERTIFICAN QUE:

Isabel Iglesias Platas, licenciada con grado en Medicina y especialista en Pediatría, ha trabajado bajo nuestra dirección en el proyecto de investigación titulado "Restricción de crecimiento intrauterino y expresión de genes imprintados: papel de *PLAGL1* y análisis de la region 6q24.2"
 que presenta para optar al grado de Doctora en Medicina por la Universitat de Barcelona.

Prof. G. E. Moore   Dr. M. Iriondo Sanz

Barcelona, octubre de 2011

ACKNOWLEDGEMENTS

CONTENTS

FIGURES

TABLES

ABREVIATIONS

*Gene names in lower case represent murine orthologues, gene names in upper case refer to human orthologues.

ADCY5- adenylate cyclase 5
Air- Antisense to Insulin-like growth factor 2 receptor RNA
ApoE- Apolipoprotein E
ART- Assisted Reproduction Techniques
AS- Angelman Syndrome
Ata3- system A aminoacid transporter 3. *Slc38a4-* solute carrier family 38 (sodium-coupled neutral amino acid transporters), member 4
BAC- Bacterial artificial chromosome
C19MC- chromosome 19 microRNA cluster
Cdkn1c- cyclin-dependent kinase inhibitor 1c (P57)
CMV- Cytomegalovirus
Copg2- coatomer protein complex, subunit gamma 2
CTCF- CCCTC- binding factor
DEADC1/ADAT2- Deaminase domain containing 1/ Adenosine deaminase, tRNA-specific 2.
Dlk1- Delta Drosophila Homolog-like 1
DMR-Differentially Methylated Region
DNA- Deoxyribonucleic Acid
DNMT- DNA Methyl Transferase
ES cells- Embryonic Stem cells
Ezh2- enhancer of zeste homolog 2 (*Drosophila*)
FAM164B- Family with sequence similarity 164, member B.
FUCA2- Fucosidase, α-L-2
GAPDH- Glyceraldehyde-3-phospate dehydrogenase
Gatm- Glycine amidinotransferase
Gnas- Guanine nucleotide binding protein, alpha stimulating
GOM- Gain of Methylation
Grb10- growth factor receptor bound protein 10
Gtl2- Glycosyltransferase type 2
Hotair- HOX (homeobox) transcript antisense RNA
Hottip- HOXA distal transcript antisense RNA
Hoxa- homeobox A gene.
Hoxc- homeobox C gene.
HP1- heterochromatin protein 1
hPL- human Placental Lactogen
*HYMAI-*hydatidiform mole associated and imprinted
IC1/*H19* DMD-Imprinting Control Region 1 (telomeric/distal)/ H19 Differentially Methylated Domain, in the 11p15.5 human region
IC2 (KvDMR1)- Imprinting Control Region 2 (centromeric/ proximal) in the 11p15.5 human region
ICM- Inner Cell Mass
ICR- Imprinting Control Region
ICSI- Intracytoplasmic sperm injection
Igf- Insulin-like Growth Factor gene
Igf1r- Insulin-like Growth Factor receptor type 1 gene

Igf2r/ M6pr - Insulin-like Growth Factor receptor type 2 gene/- mannose 6-phosphate receptor
    gene
Igfbp- Insulin-like Growth Factor Binding Protein.
Ipl/Phlda2- Imprinted in placenta and liver/ Pleckstrin homology-like domain A2.
IUGR- IntraUterine Growth Restriction
IVF- *In vitro* fertilization
Kcnq1- Potassium voltage-gated channel, KQT-like subfamily
Kcnq1ot1- *Kcnq1* opposite strand/antisense transcript 1
LncRNA- long non-coding RNA
LOI- Loss of Imprinting
LOM- Loss of Methylation
LOS- Large Offspring Syndrome
LPL- LipoProtein Lipase
LTV1- LTV1 homolog (*S. cerevisiae*)
Mash1/Ascl2- Mammalian achaete-scute homolog/ Achaete-scute complex homolog 2
    (Drosophila)
Meg- Maternally expressed gene
Mest- Mesoderm specific transcript
MiRNA- micro RNA
MLL/WDR5- myeloid/lymphoid or mixed-lineage leukemia (trithorax homolog, *Drosophila*)
    gene/ WD repeat domain 5 gene
Nlrp- NLR (NOD -like receptor) family, pyrin domain containing gene
Peg- Paternally Expressed Gene
PEX3- Peroxisomal biogenesis factor 3
PGC- Primordial Germ Cells
pGH- placental Growth Hormone
PHACTR2- Phosphatase and actin regulator 2
Phlda2- Pleckstrin homogy-like domain family A member 2
PiRNA- Piwi-associated RNA
PIWI- P-element induced wimpy testis
Plagl1/Lot1/Zac1- Pleomorphic Adenoma Gene- Like 1/ Lost on transformation 1/ Zinc finger
    protein regulator of apoptosis and cell-cycle arrest 1.
PWS- Prader Willi Syndrome
Rasgrf1-RAS protein-specific guanine nucleotide-releasing factor 1
RNA- Ribonucleic acid
SF3B5- Splicing factor 3b, subunit 5
SGA- Small for Gestational Age
SiRNA- small interfering RNA
Slc- Solute carrier gene
SncRNA- short non-coding RNA
SNP- Single Nucleotide Polymorphism
SRS- Silver-Russell Syndrome
STX11- Syntaxin 11
Tet1-tet methylcytosine dioxygenase 1 gene
TNDM- Transient Neonatal Diabetes Mellitus
UPD- uniparental disomy. mUPD- maternal UPD. pUPD- paternal UPD
UTRN- Utrophin.
VLDL- Very Low Density Lipoproteins
Zfp57- Zinc finger protein 57

ABSTRACT

Background: Fetal growth is a complex process which depends on nutrient and oxygen availability and transport from the mother to the fetus across the placenta. This involves hormones and growth factors as well as maternal and fetal genes. The failure of the fetus to reach his or her full potential for growth is called Intrauterine Growth Restriction (IUGR) and implies risks for adverse short- and long- term outcomes. Imprinted genes are a specific subset of genes that display, in mammals and flowering plants, monoallelic expression depending on the parental origin of the allele. The regulation of imprinted expression depends on epigenetic mechanisms, a subset of heritable marks that have the ability to regulate DNA functions without altering its sequence. Imprinted genes tend to cluster in the genome due to coordinated regulation through Imprinting Control Centers, usually in the form of Differentially Methylated Regions between the paternally and maternally inherited alleles. Studies in both animals and humans as well as imprinting syndromes have uncovered a role for this group of genes in prenatal growth. Two imprinted genes (*PLAGL1* and *HYMAI*) have been described in the 6q24 locus. Genetic and epigenetic defects in this region relate to the Transient Neonatal Diabetes Mellitus 1 phenotype, including severe growth restriction. We aimed to study the involvement of this region in non-syndromic IUGR.

Participants and methods: One hundred placental samples from a cohort of healthy term singletons, fetal tissues from fifty-four first trimester terminations and one hundred placental samples from healthy and complicated pregnancies of different gestational ages were used to analyze the role of the 6q24 region in normal fetal growth and IUGR, respectively. Relevant clinical data was obtained after informed consent. The methylation status of the 6q24 CpG islands was studied by array technology and bisulfite sequencing in normal term placenta and in first trimester fetal tissues. Methylation levels in the *PLAGL1* DMR in healthy and IUGR placentas were compared by pyrosequencing. Allelic origin of expression was assessed by heterozygous DNA/cDNA SNP analysis. Levels of expression of imprinted transcripts were analyzed by qRT-PCR.

Results: *PLAGL1* P1, *HYMAI* and two newly described *PLAGL1* isoforms (P3 and P4) were the only transcripts subjected to genomic imprinting in the investigated 6q24 region. Correspondingly, the CpG island associated to the P1 promoter was the only differentially methylated region. There was no correlation between *PLAGL1* expression in the placenta and fetal size in uneventful pregnancies. In placentas from IUGR gestations, expression of *HYMAI* was significantly higher than in those from normally grown fetuses. Levels of expression of

PLAGL1 were lower in IUGR and correlated positively and significantly with the presence of IUGR in placentas from girls, but not boys. These changes in expression were not mediated by Loss of Imprinting or abnormalities in the levels of methylation of the promoter-associated DMR, but possibly by a change in regulatory posttranscriptional mechanisms, as suggested by the loss of correlation of *PLAGL1* P1 and *HYMAI* expression in IUGR.

<u>Conclusions</u>: Imprinted expression in the 6q24 region is limited to the *PLAGL1/HYMAI* locus, maybe due to demarcation of this region by CTCF boundaries. Intrauterine Growth Restriction is associated to abnormalities in expression of *PLAGL1* and *HYMAI* in the placenta, which are not due to LOI or methylation changes.

INTRODUCTION

INTRODUCTION

1   INTRAUTERINE GROWTH RESTRICTION

1.1. NORMAL AND ABNORMAL FETAL GROWTH

Fetal growth is a highly complex process that depends on nutrient and oxygen availability and transport between the mother and the fetus across the placenta. This involves hormone and growth factor regulation as well as both maternal and fetal genetic information. The concept of growth is dynamic and best defined by changes along time (velocity), but birth weight has been broadly used as a proxy because of its accessibility and as an end point of *in utero* development.

Many factors have shown to influence the final fetal size in otherwise normal pregnancies (Gluckman and Hanson, 2004). Maternal weight and weight gain, maternal age, parity and socio-economic status and the gestational age at birth and gender of the fetus are all determinants of birth weight. The mother´s own birth weight also seems to be a factor, but a difficult one to elucidate, because it influences both maternal anthropometry at the time of pregnancy and her risk of other conditions.

1.1.1 GENETIC CONTRIBUTION TO FETAL SIZE

The contribution of genetic inheritance towards birth weight has been estimated to be between 30 to 70% in different studies (Dunger et al., 2006). The particular implications of maternal and fetal genotypes, parent-of-origin effects and the uterine environment are difficult to separate as they are all intertwined. As an example, mutations in the glucokinase gene produce an increase or reduction of the same magnitude in the weight of the newborn when present in the mother or the baby, respectively. If both of them have the mutation, the effect is neutralized, resulting in a normal birth weight (Hattersley et al., 1998).

The discrete effects of both maternal and paternal genetics and of the uterine environment have recently been addressed in an ingenious study assessing data from babies conceived using assisted reproduction techniques. Participants were classified in groups

according to the origin of the gametes (couple´s own vs sperm and/or oocyte donor). The results confirmed the existence of both maternal and paternal genetic influences and uncovered a possible synergy between the mother´s genetic endowment and the uterine environment, acting to diminish paternal contribution. This was suggested by a less evident paternal impact in the group with a homologous (non-donor) oocyte, where both the gamete and the uterus were contributed by the same individual (Rice and Thapar, 2010).

Common variations in genes known to be involved in hormonal pathways of fetal growth or later metabolic disease have been investigated in relation to birth weight with mixed rates of success and reproducibility (Petry et al., 2005; Adkins et al., 2010; Morgan et al., 2010). Recently, a genome-wide scale analysis highlighted the role of two regions on the long arm of chromosome 3 (Freathy et al., 2010). The associations were proven independent of the maternal genotype. One variant mapped to a long non-coding RNA, while the other corresponds to the *ADCY5* gene. The latter has also been identified as a region in linkage disequilibrium for the risk of type 2 diabetes and other measurements of the efficiency of adult glucose metabolism. Each of the Single Nucleotide Polymorphism (SNP) associations explains a percentage of the variance of birth weight that is in the same order of magnitude as maternal age (0,3% and 0,1% for each SNP vs 0,5% for maternal age). The difference in weight between the carriers of the 4 birth weight-lowering alleles (individuals who were homozygous C for both associated SNPs at 3q25 and 3q21) with respect to the ones carrying one or none was approximately 113g, similar to the effect of the mother smoking 4-5 cigarettes a day (Freathy et al., 2010).

1.1.2 HORMONAL FACTORS IN FETAL GROWTH

The placenta plays a major role as an endocrine organ. Some factors act mainly on the mother, like human Placental Lactogen (hPL) and placental Growth Hormone (pGH), contributing to the metabolic adaptation to pregnancy, which ensures availability of substrates for the fetus (Carrascosa, 2003). Maternal plasma levels of these hormones correlate with baby´s weight at mid-gestation and term (Sankaran and Kyle, 2009).

Molecules acting directly in the fetal compartment during prenatal development are usually produced by many of the developing tissues and act through autocrine and paracrine mechanisms, behaving more like growth factors than hormones. To date the best studied

proteins are insulin and the Insulin-like Growth Factor system. This includes 3 ligands (insulin, Insulin-like Growth Factors-I and –II) and at least four receptors (insulin receptor-INSR, type-1 Insulin-like Growth Factor receptor- IGF1R, type 2 Insulin-like Growth Factor receptor or mannose 6-phosphate receptor- IGF2R and hybrid insulin/Insulin-like Growth Factor 1 receptors) and 6 binding proteins (IGFBPs) (Sankaran and Kyle, 2009). Extensive experiments in engineered mouse models have enlightened the differential roles of the components of this axis in different tissues (see *Figure 1*). The effects of insulin and IGF-I on fetal growth are mediated mainly through IGF1R and also the INSR, and insulin-IGF1R dymeric receptors. IGF-II acts through these and an unidentified receptor that mediates its actions on the placenta (reviewed in Efstratiadis, 1998). IGF2R exerts its effect on the extracellular concentration of IGF-II by mediating endocytosis and subsequent lysosomal degradation of excess ligand. Despite its lack of a catalytic domain, recent studies have also pointed to possible additional roles of IGF2R in the regulation of cell motility, TGF-β1 activation and retinoic acid signal transduction (Tong et al., 1998; Ghosh et al., 2003).
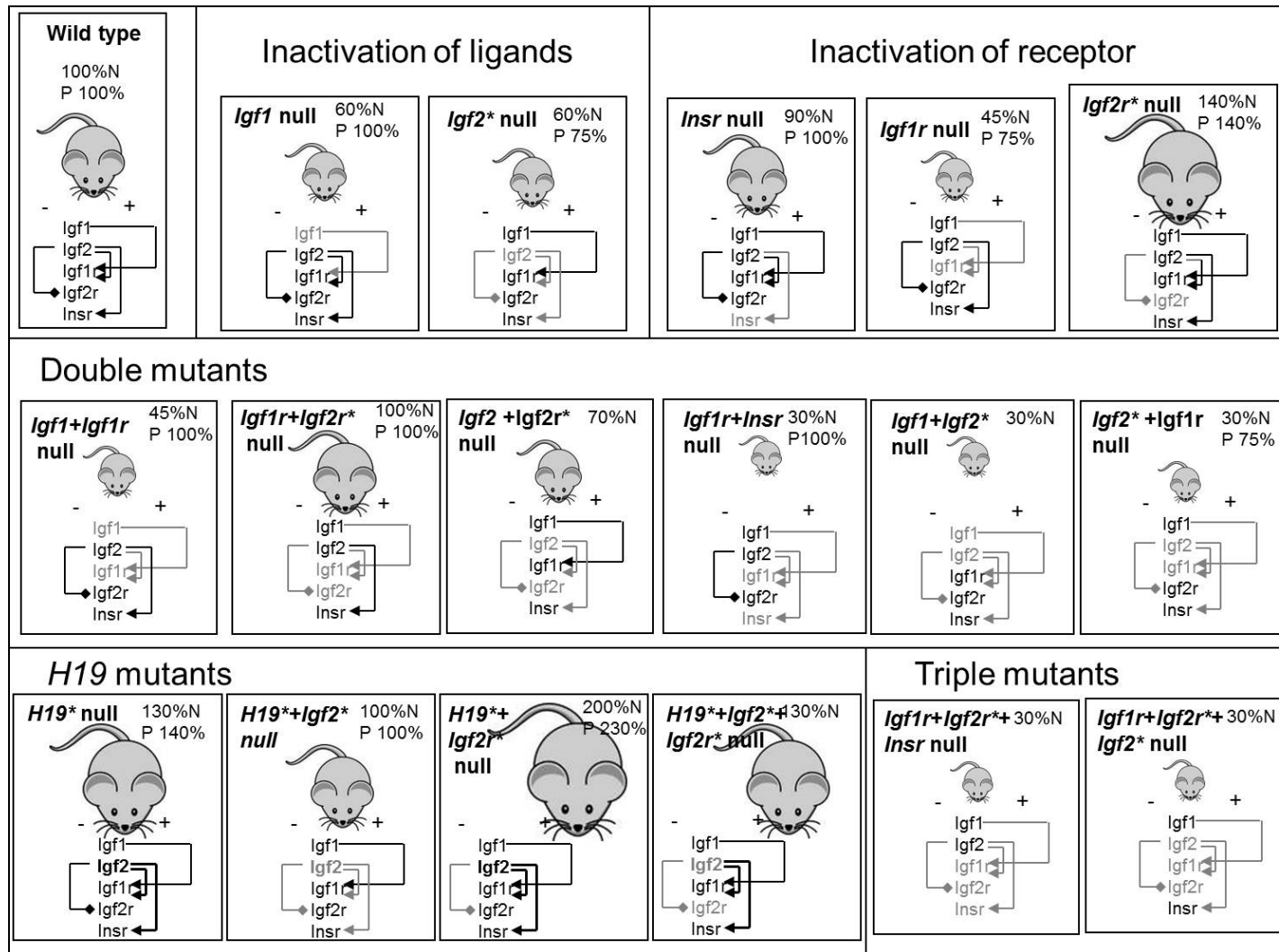
Figure 1: Summary of the growth phenotypes of mice for which different elements of the IGF axis have been knocked out, clarifying their roles in the system.

Figure 1: Summary of the growth phenotypes of mice for which different elements of the IGF axis have been knocked out, clarifying their roles in the system. N: normal size for an embryo at the end of gestation. P: placental size with respect to normal. Due to their imprinted character, Igf2, H19 *and* Igf2r *heterozygotes with an inactivated paternal (for* Igf2*) or maternal (for* H19 *and* Igf2r*) allele will be functionally null. Double mutants for* Igf1 *and* Igf1r *have the same phenotype as* Igf1r *nulls, indicating that the action of Igf1 is only mediated by this receptor. On the contrary, inactivation of both* Igf2 *and* Igf1r *have additive effects, indicating action through another receptor. Cumulative mutations that functionally inactivate this pathway have a maximum phenotype, with embryos* being 30% of the *size of the wild type. This is the case for mice lacking both ligands (*Igf1+Igf2 *null) or* Igf2+Igf1r*. Inactivation of the* Igf2r *is perinatal lethal. This is caused by hyperstimulation of Igf1r by high levels of Igf2, as shown by the fact that Igf2r+Igf2 double mutants are viable dwarfs (reviewed in Efstratiadis, 1998).*

From mid to late gestation, IGF-II is more abundant than IGF-I, and for this reason it has been considered the major driver of fetal growth. IGF-II seems to exert its actions mainly through altering the size and the transport capacity of the placenta, while IGF-I affects fetal growth directly. Nutritional and endocrine conditions can influence this hormonal system mainly by inducing fluctuations in the levels of IGF-I (reviewed in Fowden, 2003). While IGF-I raises in the presence of insulin, increased cellular availability of glucose or deficiency of thyroid hormone, IGF-II is quite insensitive to these stimuli. The IGFBPs are tissue specific and developmentally regulated. IGFBP 1 is the most responsive to environmental signals, and it is increased, while IGFBP-3 is decreased, in intrauterine growth restriction (IUGR) (Giudice et al., 1995). IGFBP-1 is also responsive to hypoxic conditions.

After birth, there is a dramatic decline in expression of IGF-II, which completely disappears in some species and a shift to predominance of IGF-I in others (Beck et al., 1988; Giudice et al., 1995). The mechanism of action of IGF-I changes from paracrine to endocrine and is dependent on the action of GH in the liver (somatothropic axis). Postnatally, IGF-II has a role in tissue differentiation. In the pancreas, for example, the β-cell wave of apoptosis and the evolution of the islets to a non-proliferative mature state at the time of weaning depends on the timed decrease of Igf2 (Fowden, 2003).

1.1.3 THE ROLE OF THE PLACENTA

The placenta constitutes the interface for fetal-maternal interaction and has an active role in the management of fetal resources. The relevance of this organ is such that, until the second trimester of pregnancy, 40% of the oxygen and 70% of the glucose that enter the uterus are solely destined to fulfill its metabolic demands (Sankaran and Kyle, 2009).

The development of the placenta starts around day 6 of gestation with the implantation of the blastocyst. Rapid proliferation of the external layer, the trophoectoderm, gives rise to an inner layer of cytotrophoblast (mononucleated and proliferative) and an outer syncitium (syncytiotrophoblast), multinucleated and with diffuse intercellular limits. Cavities called *trophoblastic lacunae* form inside the syncytiotrophoblast and are occupied by maternal capillary blood, eventually forming the intervillous space.

At around day 13 of gestation, the cytotrophoblast cells start to proliferate and migrate through the overlying syncytium, forming columns that will reach the maternal decidua and establish the basis for the formation of the villous structures (see *Figure 2*). From this moment on, two types of cytotrophoblast can be distinguished: the *villous cytotrophoblast* (replicating layer for the formation of the syncytiotrophoblast) and the extravillous cytotrophoblast. The *extravillous trophoblast* is in charge of the invasion of the maternal decidua starting from the tips of the anchoring villi. These cells can differentiate into multinucleated rounded placental giant cells (*interstitial trophoblast*) or reach the maternal spiral arteries, being responsible for their remodelling. By destroying and replacing the endothelium and the smooth muscle layer, the arteries are rendered unresponsive to maternal vasomotor control (Kauffman et al., 2003). Until 10-12 weeks of pregnancy, the *endovascular trophoblast* plugs the spiral arteries, preventing maternal blood flow from entering the system and thus keeping a low oxygen environment (Malassiné et al, 2003; Gude et al, 2004).

From the end of the first trimester, the haemochorial structure of the human placenta determines the existence of an exchange barrier (see *Figure 2*) devoted to the bidirectional transport of substances between the mother and the fetus. Transplacental nutrient supply is governed by the same rules that apply for other situations of transfer through lipophilic membranes (mainly the microvillous and the basal membranes of the syncytiotrophoblast). Depending on the maternal-fetal concentration difference or on electrochemical gradients, different molecules will be transferred passively or by energy-requiring active transport. The diffusion of very soluble gases, like oxygen, will relate mainly to blood flow rate, while for less

soluble substances the efficiency of transport depends on the surface and thickness of the exchange area, the molecular size and the expression of required channels or transporters. Although information on the fine-tuned regulation of these mechanisms is still scarce, it seems that vascular reactivity of uterine and umbilical vessels, the structural development of the placental barrier and the presence of specific carriers are all regulated by fetal needs through feedback loops (Desforges and Sibley, 2010).
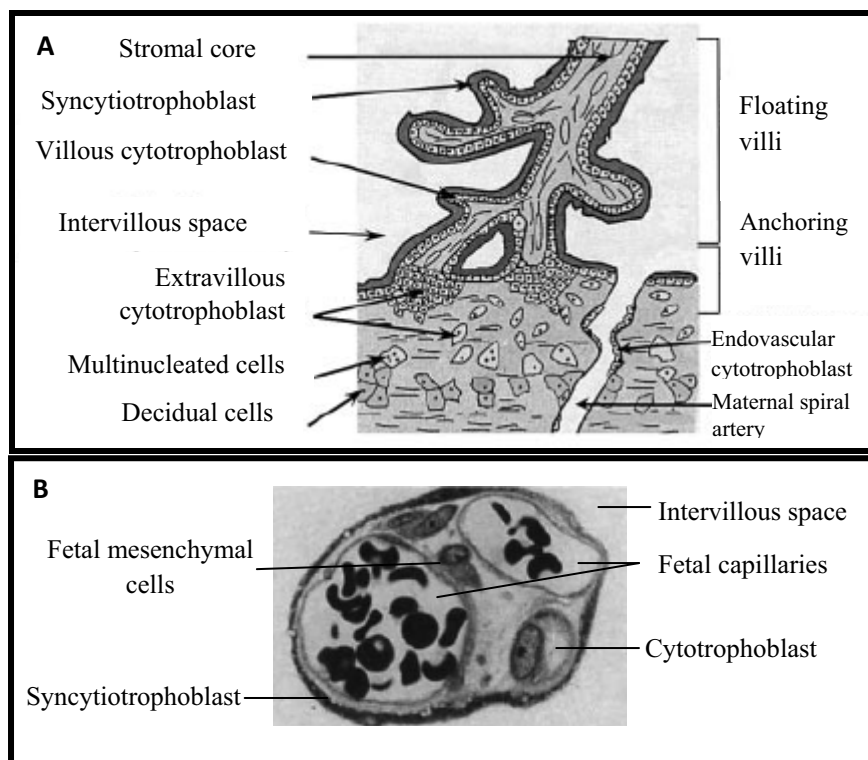
Figure 2: A: Schematic view of the structure of the human placenta. B: Structure of a tertiary (mature) villus.
(From Malassiné et al, 2003 and Kaufman et al, 2004). Microscopy semithin cross section (x800) of a terminal villus. Fetal blood is separated from maternal blood (in the intervillous space) for the so-called "placental barrier": the fetal endothelium and interstitial space, the discontinuous layer of cytotrophoblast and the outer syncytiotrophoblast.

Tight control of the program regulating placental growth and function is required to provide appropriate conditions for the well-being of the fetus while avoiding excessive invasion of maternal tissues. Both intrauterine growth restriction (IUGR) and preeclampsia seem to be a consequence of defective placental development during early pregnancy. Shallow invasion of extravillous trophoblast brings about incomplete remodelling of the spiral arteries and a decrease in the production of vasodilating factors, implying an increased resistance to

blood flow and reduction in the delivery of oxygen to the fetal-placental unit (Kaufmann et al., 2003). Primary or secondary failures in the exchange barrier contribute to placental dysfunction. This causes suboptimal growth of the fetus and, in the presence of certain ill-defined predisposing factors in the mother, such as endothelial or immune dysfunction, leads to a cascade of events ending in pre-eclampsia (Lala and Chakraborty, 2003). The genes involved in both fetal growth restriction and pre-eclampsia are likely to influence the pathways of trophoblast cell proliferation, migration and invasiveness during placentation in the first trimester.

In summary, the placenta is the central organ for successful fetal development and the alteration of the physiologic pathways involved in the healthy interplay between the mother and the fetus will surely play a major role in the route to fetal growth disturbances.

1.2. DEFINITION, DIAGNOSIS AND CAUSES OF IUGR

IUGR is the failure of the fetus to reach his/her full genetic potential for growth (Miller et al, 2008). The first approaches defined this problem as a postnatal concept based on population statistics. Individuals who had a birth weight below the 10th percentile were considered Small for Gestational Age (SGA) and they were shown to carry a higher risk of mortality or adverse neonatal outcome. As ultrasound scans were incorporated into routine pregnancy management, information on prenatal anthropometric parameters (abdominal circumference, biparietal diameter, and estimated fetal weight) could be used to predict final birth weight and identify SGA fetuses prior to the end of gestation (Hadlock et al., 1991)

In time, it became apparent that most SGA fetuses are, in fact, healthy at birth. Efforts were then made to improve the accuracy for the detection of pathologically small babies through mathematical models for individualized assessment (Deter, 2004) or customized prenatal growth charts (Gardosi, 2004). The terms IUGR or FGR (Fetal Growth Restriction) were reserved for babies that showed severe delayed growth (<3rd percentile) or those under the 10th percentile together with other signs of chronic hypoxia or malnutrition, who were indeed at odds for perinatal morbidity (Harkness and Mari, 2004).

Later, incorporation of Doppler studies allowed for the assessment of fetal haemodynamics to help determine the extent of compromise and to guide the management of

the pregnancy. Usually, flow abnormalities appear first in the umbilical artery, followed by the Middle Cerebral Artery and the *ductus venosus*, although this temporal sequence may vary, especially near term (Harkness and Mari, 2004, see Table 1). No effective treatment has been identified for IUGR to date, so the key medical intervention is the decision of when to deliver the baby, in an attempt to find a balance between the risk of stillbirth versus the risk of prematurity (Miller et al., 2008).

Vessel	Waveform characteristics	Proposed mechanism	Outcome/ Clinical relevance
UTERINE ARTERY	↑resistance Early diastolic notch	Failure of trophoblast invasion of spiral arteries	Prediction of IUGR Need for closer surveillance
UMBILICAL ARTERY	↑resistance→ absent end-diastolic flow→ reverse end diastolic flow (ARED)	Low placental –stem artery number/abnormal primary villous development/placental stem-vessel vasoconstriction	↑ mortality ↑ admission ↑altered neurodevelopment (ARED)
MIDDLE CEREBRAL ARTERY (MCA)	↓ resistance (pulsatility index)	Compensatory vasodilation due to blood-flow redistribution	Poor outcome, even if normal umbilical artery waveform Useful up to 34 weeks
DUCTUS VENOSUS	Absent or reversed flow	Right-side heart failure due to myocardial hypoxia	Poor outcome, probably indication for immediate delivery, but trials lacking

Table 1: Haemodynamic assessment of the fetus by Doppler flow study.
Interpretation of findings. Based on Harkness and Mari, 2004.

The causes of IUGR are frequently classified under maternal, fetal or placental in origin, although boundaries between these categories are not well defined and it is likely that one extensively influences the others (Hendrix and Berghella, 2008. See *Table 2*). Severe diseases affecting the baby can alter his or her growth rate, whether caused by chromosomal or genetic abnormalities, major congenital malformations or intrauterine infections. Women suffering from chronic disorders (hypertension, systemic *lupus eritematosus*, renal disease or cardiac malformation) or pregnancy-associated conditions (gestational diabetes, pre-eclampsia) also tend to deliver growth restricted babies (Bryan and Hindmarsh, 2006). Smoking has also been highlighted as a significant but preventable contributor to this problem (Thompson et al., 2001).

Maternal undernutrition is the leading cause of growth restriction in the developing world, while placental insufficiency accounts for more than 80% of IUGR cases in Western countries (Shankaran and Kyle, 2009). Placental insufficiency reflects the end result of an alteration of the complex program of expression of growth factors, hormones and receptors, adhesion molecules and extracellular matrix required for the correct placentation during early pregnancy (Ventolini and Neiger, 2006). Consequences of this malfunction can be monitored indirectly by changes in Doppler waveforms and in other parameters of fetal wellbeing. For example, a shallow invasion of the maternal spiral arteries by the interstitial trophoblast will not achieve the physiologic low resistance utero-placental system and will be reflected in an increase in the pulsatility index of the uterine arteries (Pardi et al., 2002).

Placental transport mechanisms are also affected in *in vitro* studies of isolated microvilli and basal plasma membranes of syncytiotrophoblast from placentas of babies with suboptimal intrauterine growth. The amino acid transporter system A as well as ion transporters (Na^+/K^+ ATPase, Na^+/H^+ exchanger and Ca^{2+} ATPase) and transport of leucine seem to be decreased *in vivo* in human growth restricted pregnancies. A number of other genes related to lipid metabolism –like lipoprotein receptors (*VLDL-ApoE*), lipoprotein lipase (*LPL*) – have also been shown to be abnormally expressed in IUGR placentas in expression array studies, in agreement with data from other studies regarding differences in polyunsaturated fatty acid profiles in IUGR babies (Alvino et al., 2008). It is unclear which changes are causative and which secondary and the exact nature of the processes leading to placental insufficiency remains, at the moment, unknown.

Compartment	Causes
Fetal	Genetic disease (5-20%)
	Chromosomal abnormalities (trisomy 16, 18, 13, 21, deletions,…)
	Single gene disorders
	Uniparental disomies (UPD) 6, 14, 16
	Confined placental mosaicism
	Major congenital malformations (1-2%)
	Fetal infection (up to 10%)
	In developed countries, mostly *Toxoplasma* or CMV (cytomegalovirus)
	Multiple gestation
Maternal	Maternal disease (pre-existing or gestation-induced)
	Hypertension
	Diabetes
	Organ insufficiency
	Sistemic *lupus erytematosus*
	Acquired (but not inherited) trombophilia
	Decreased nutrition
	Smoking, alcohol or other drug abuse
	Short interpregnancy interval
	Maternal periodontal disease
	Previous IUGR (recurrence rate around 25%)
Placental	Placenta and umbilical cord anatomic anomalies
	Placental insufficiency (up to 80%)

Table 2. Classification of causes of and risk factors for IntraUterine Growth Restriction (IUGR). Based on Hendrix and Berghella, 2008 and Shankaran and Kyle, 2009).

1.3. SHORT- AND LONG-TERM CONSEQUENCES OF IUGR: FETAL PROGRAMMING

FGR plays a role in neonatal mortality in both term and preterm babies (Kady and Gardosi, 2004; Berstein et al., 2000). Moreover, neonatal cases might only represent the non-intrauterine-lethal forms of the problem, as half of the "unexpected" or "unexplained"

stillbirths could be directly related to FGR (Kady and Gardosi, 2004). Prematurity is the single largest conditioning of neonatal mortality and evidence from animal work supports the idea that an adverse intrauterine environment could also predispose to an earlier delivery (Bloomfield et al., 2003). Data on humans also point in the same direction, in spite of heterogeneity regarding study populations and definitions of IUGR and spontaneous preterm labour (Zeitlin et al., 2000; Morken et al., 2006; Zhang et al., 2008).

Due to conditions of chronic hypoxemia and malnutrition, babies born after IUGR have an increased prevalence of transitional pathology (Yu and Upadhyay, 2004), the general name given to conditions associated to inadequate adaptation to the extrauterine environment. Uterine contractions during labor are poorly tolerated, and hypoxic-ischemic events may occur, resulting in higher risks of meconium aspiration syndrome, need for resuscitation and subsequent signs of encephalopathy. Fetal adaptation to chronic hypoxia leads to an increase in red blood cell count (Neerhof and Thaete, 2008), which predisposes to neonatal polycythaemia and hyperviscosity and to pathologic hyperbilirrubinemia. Depleted stores of glucose and fat expose the newborn to hypoglycaemia and also to hypothermia. When adjusted for confounding variables, extremely preterm babies (≤ 30 weeks) born small for gestational age are at higher risk of prematurity-associated complications, like respiratory distress syndrome and necrotizing enterocholitis (Bernstein et al., 2000).

Adverse outcomes persist during childhood. Although most babies born small seem to present a subsequent period of accelerated growth ('catch-up') during the first six months to one year of life (Hokken-Koelega et al., 1995), 7-8% of them will remain with a low final height (Yanney and Marlow, 2004). Neurodevelopmental impairment is a rare but remarkable consequence of IUGR after adjustment for other factors, and it is more frequent if microcephaly is present at birth. Different forms of cerebral palsy (Jarvis et al., 2003) and behavioural problems have been shown to be more prevalent among children that were born SGA. In extremely preterm babies, this effect is not consistent, possibly because prematurity has a much bigger impact by itself (Yanney and Marlow, 2004). Later reproductive function can also be affected in children that were small at birth, and both men and women born SGA have a predisposition to adult subfertility (Main et al., 2006; van Weissenbruch and Delemarre-van de Waal, 2006). Being born small and undergoing catch-up growth seem to be factors that facilitate an advanced progression of female puberty (Ibañez and de Zegher, 2006).

Epidemiological evidence has served to uncover further relationships between suboptimal intrauterine growth and predisposition to adult-onset diseases (Barker, 2006) that

could even be transferred to offspring (Drake and Walker, 2004). This is the case for obesity, type 2 diabetes, cardiovascular disease, hypertension and osteoporosis (Ravelli et al., 1999; Barker et al., 1993; Cooper et al., 2002). For some conditions, the risk appears to be modified by postnatal trajectories of growth and, more specifically, by the presence of "catch-up" or accelerated growth during childhood (Barker et al., 2005).

Different theories have tried to explain the link between early life growth trajectories and long-term events (Ong and Dunger, 2002). The fetal insulin hypothesis (Hattersley and Tooke, 1999) was proposed after the discovery of rare glucokinase mutations that could influence size at birth. It was postulated that mutations in genes involved in insulin pathways could both impair fetal growth and contribute to insulin resistance later in life. Loci such as *ADCY5* highlighted by genome-wide studies as contributors to size at birth would fulfil this hypothesis. Conversely, most type 2 diabetes associated loci do not relate to birth weight (Freathy et al., 2010). Our gene of interest, the imprinted *PLAGL1* gene, is responsible for a neonatal transient form of diabetes with defective perinatal insulin secretion and long-term tendency to insulin resistance (Temple *et al.*, 2000; Temple and Mackay, 2010). Through this intermediate mechanism, it may influence fetal growth and relate to adult glucose intolerance. This particular phenotype would fit the occurrence of catch-up growth, a common phenomenon after fetal growth restriction that is not addressed by the fetal insulin hypothesis, being considered its major flaw (Ong and Dunger, 2002).

The "thrifty phenotype" or "fetal programming" hypothesis claims that growth restriction during fetal development brings about a series of changes in organs and systems aimed to help the newborn to better adapt to the expected environment. The ability of the inmmature organ to change according to the surrounding circumstances is known as plasticity. Due to plasticity, one genotype can give rise to a range of phenotypes or physiologic states that better suit a variety of conditions (reviewed in Barker, 2006).

The first response to undernutrition is a reduction in growth, which is asymmetric: total adipose tissue mass is reduced, with a specific preservation of visceral fat (Harrington et al., 2004), maybe in order to protect the transition to extrauterine life. Subsequently, the blood flow is redistributed preferentially to vital organs, mainly heart and brain. In animals, the third strategy for the fetus when faced with a limited nutritional supply is to hasten maturation and shorten gestation (Gluckman and Hanson, 2004). These adjustments are based on a predicted postnatal environment that will threaten immediate neonatal survival, and where life expectancy will be short as a consequence of malnutrition. This response aims to improving

the chances of short-term success at the expense of long-term problems. The faulty information provided to the fetus by an insufficient placenta in IUGR and the ever-increasing life-span of humans cause a mismatch between the intrauterine adaptive responses and the external conditions, which leads to adult-onset metabolic disease.

Different mechanisms have been suggested to explain the molecular basis of developmental plasticity and fetal programming. Among them, there is a recent and increasing focus in the role of epigenetic changes (Fowden et al., 2006; Gicquel et al., 2008).

2   EPIGENETIC MARKERS AND GENOMIC IMPRINTING

Epigenetic modifications are inheritable marks that do not alter the DNA sequence but affect gene activity by favouring or repressing transcription. They can be influenced by environmental exposure, making them good candidates in fetal programming. Epigenetic mechanisms, especially DNA methylation, have been shown to be involved in X inactivation, imprinting and heterochromatin formation, all of which are essential for normal embryonic growth and development.

2.1.   EPIGENETIC MECHANISMS

There are many epigenetic mechanisms, which usually act in a co-ordinated manner. Among them, DNA methylation, non-coding RNAs and histone modification are the best understood.

2.1.1 DNA METHYLATION

Methylation of DNA in mammals occurs mainly at cytosine residues. It is generally located at CpG dinucleotides, although non-CpG methylation has been observed lately in embryonic stem cells (ES cells) and gametes (Tomizawa et al., 2011; Nishino et al., 2011) and shown to be specific and subjected to inheritance (Grandjean et al., 2007). The CpG dinucleotide combination is rare in the genome, because it implies a risk of point mutations, as cytosines tend to be methylated and undergo spontaneous deamination into thymidines (Hermann et al., 2004). Selection pressure has resulted in the clustering of CpG dinucleotides in regions called CpG islands, which are defined as stretches of sequence longer than 200 base pairs and containing a CG percentage of 50% or greater, with an observed to expected ratio of CpG >0.6.

Most DNA methylation occurs in intergenic regions and inactive heterochromatin within the genome and defines the stable global level of DNA methylation. The CpG rich-regions associate with the promoters of approximately 60% of all genes and are generally unmethylated. The methylation of these particular sequences within euchromatin creates

different patterns which have a crucial role in the regulation of gene expression (Hermann et al., 2004).

The group of enzymes responsible for this modification of DNA, the DNA Methyl Transferases (DNMTs), is highly conserved through evolution and three families have been identified so far in mammals. DNMT1 is specific for CpG dinucleotides and, although it likely has a role in *de novo* methylation as well, it acts preferentially on hemimethylated substrates during replication, being in charge of the maintenance of methylation. The DNMT3 family contributes to *de novo* methylation in both CpG and non-CpG cytosines. It seems to target particular compartments of the genome (pericentromeric satellite regions) and both Dnmt3a/b and Dnmt3L are involved in the establishment of maternal and paternal imprints (Kaneda et al, 2004; Bourc'his et al., 2001). Dnmt3L is likely to act by enhancing the activity of Dnmt3a/b and guiding the enzymatic complex to target sites, as it lacks catalytic domains. DNMT2 has been less well described and appears to relate to centromere function (Bestor, 2000; Hermann et al., 2004).

Methylation of CpG island- associated promoters has been shown to have a significant role in the regulation of gene expression (Santos and Dean, 2004) with high levels of methylation being associated with gene silencing. Conversely, methylation of CpG islands embedded in the body of the genes is usually correlated with high rates of activity of an upstream promoter and represses initiation of downstream transcription. This latter mechanism probably evolved in mammals in order to block the promoters of spurious elements without interfering with the elongation of other transcripts (Jones and Takai, 2001).

The totipotent cells required for embryonic development start from the union of highly specialized gametes, which calls for a genome-wide resetting of epigenetic information. The information contained within the pronuclei undergoes erasure immediately after fertilization (Reik et al., 2001). In the paternal pronucleus, this is known to be an active mechanism, involving Tet-associated formation of an intermediate product, 5-hydroximethylcytosine (Wossidlo et al., 2011; Iqbal et al., 2011), although the exact factors for demethylation have not yet been identified (Okada et al., 2010). During this process, the maternal pronucleus is protected by PGC7/STELLA (Nakamura et al., 2007; Wossidlo et al., 2011), but undergoes passive demethylation due to the exclusion of DNA-methyltransferases from the nucleus to the cytoplasm during early divisions (Lepikhov et al., 2010). The start of *de novo* methylation coincides with the first differentiation stages of the embryo, and asymmetrically affects the two newly formed lineages. The inner cell mass (ICM), which gives rise to the embryo,

becomes relatively hypermethylated, in comparison with the trophoectoderm cells, which forms the placenta (Santos and Dean, 2004).

2.1.2 OTHER EPIGENETIC MECHANISMS

NON-CODING RNAs

In the last 50 years, the importance of non-coding RNAs has been uncovered, challenging the classical dogmas of molecular genetics. They have been shown to be involved in transcriptional interference, serve as targeting mechanisms for chromatin modifying enzymes responsible for posttranslational modifications of histones, and be the precursors of small interfering RNAs and microRNAs (Zhou et al., 2010; Kozhiol and Rinn, 2010).

Regulatory RNAs are divided according to their length as long (>200bp) –lncRNAs (long non-coding)- and short –sncRNAs (short non-coding). Specific post-transcriptional machinery is required for the synthesis of sncRNAs (Eddy, 2001) depending on the type of sncRNA produced. For example, the Drosha-Dicer complex is necessary for processing microRNAs, while small-interfering RNAs (siRNAs) need Dicer but not Drosha. The post-transcriptional machinery for the production of mature PIWI-associated RNA (piRNAs) is still unknown. PiRNAs associate specifically with PIWI proteins, a subtype of Argonaute proteins, for inhibition of transcription (Siomi et al., 2011). No particular enzymatic system specifically required for the synthesis or action of lncRNAs has been identified.

ncRNAs play essential roles in fetal and embryonic development, and have been shown to be key factors in cell type-specific gene expression, pluripotency and differentiation, imprinting and X inactivation (Pauli et al., 2011). The lncRNAs can have active or repressive transcriptional functions, through interaction with various chromatin-modifying enzymes (Tsai et al., 2010). For example, *HOTAIR* recruits the EZH2 repressor complex to the *HOXC* gene locus (Gupta et al., 2010), whereas *HOTTIP* interacts with MLL/WDR5 to create a permissive transcriptional state at the *HOXA* cluster (Wang et al., 2011).

HISTONE MODIFICATIONS

DNA is arranged in higher-order structures within the nucleus. The smallest unit of this organization is the nucleosome, which contains approximately 2 helix turns of DNA wrapped

around an octamer of proteins called histones. Histones are basically charged globular proteins with a flexible amino terminus that protrude from the nucleosome. These histone "tails" have been found to be subjected to several covalent modifications including methylation, acetylation, phosphorylation and others at specific positions. Some of these changes can undergo mitotic inheritance (Jenuwein and Allis, 2001).

Specific associations appear to exist between DNA methylation, transcriptional state and chromatin structure. Transcriptionally inactive regions usually display methylated DNA, and silencing histone modifications, like methylation of histone 3 in lysine 9 (H3K9me) and hypoacetylation of H3 and H4. K4 methylation and hyperacetylation on H3 mark the actively transcribed regions (Zhou et al., 2011) (see Figure 3). Histone modifications can exert their regulatory action by direct alteration of the chromatin conformation or by facilitating or obstructing the binding of other factors (Bannister and Kouzarides, 2011). Protein domains capable of specific interactions with modified histone tails have been described in both chromatin regulators, including histone modifying enzymes themselves, and transcription factors. Trithorax proteins, for example, are involved in the establishment of euchromatic signals and contain bromodomains, which interact with acetylated lysines on histone tails (Jenuwein and Allis, 2001). Bromodomains are also found in histone acetyl-transferases (HATs). On the contrary, heterochromatin-binding protein 1 (HP1) and polycomb proteins, such as EZH2, play a role in establishing heterochromatic marks and they contain chromodomains, which recognize specific methylation patterns in histones (Beisel and Paro, 2011).
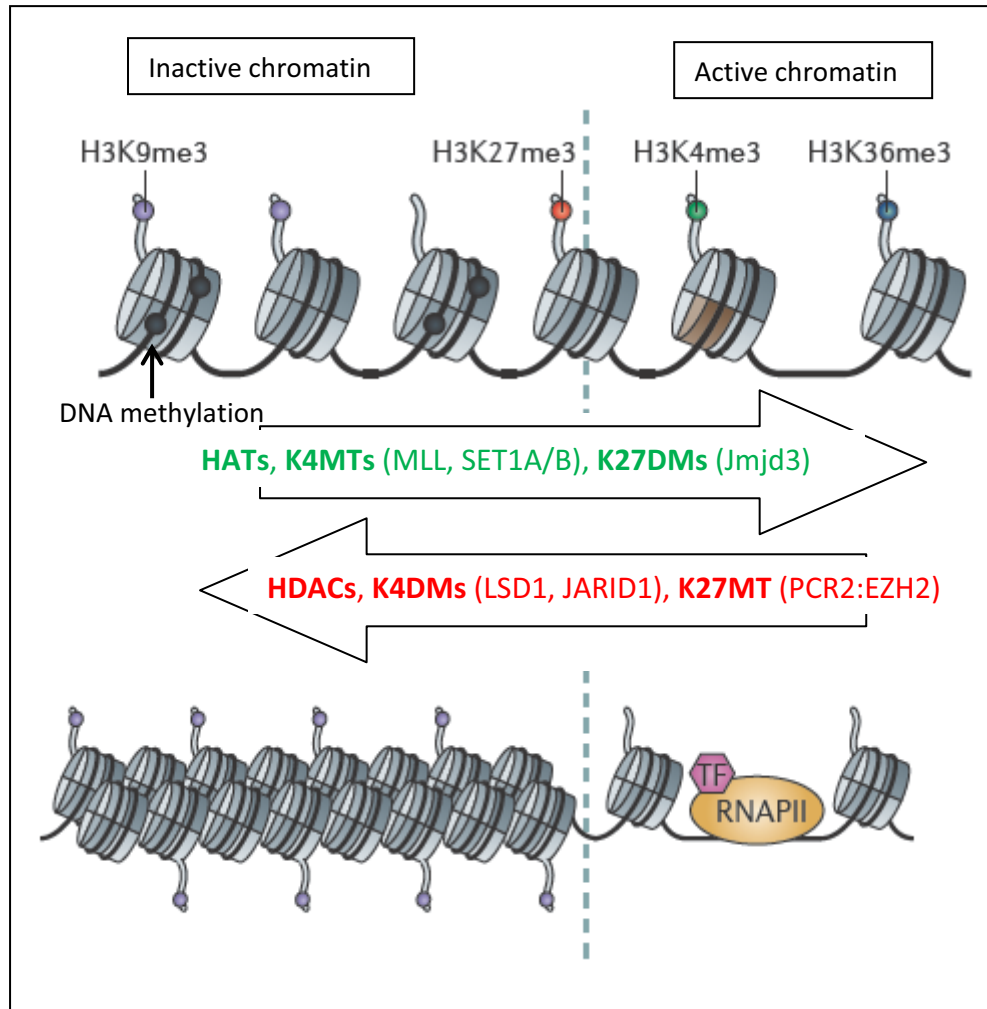
Figure 3: Histone modifications associated with active and inactive chromatin states.
(Modified from Zhou et al., 2011). H3K9me3: histone 3 lysine 9 tri-methylation. H3K27me3: histone 3 lysine 27 tri-methylation. H3K4me3: histone 3 lysine 4 tri-methylation. H3K36me3: histon3 lysine 36 tri-methylation. In green, enzymes that deposit histone modifications associated to chromatin activity: HATs: histone acetyl-transferases, K4MTs: lysine 4 methyl-transferases. MLL: myeloid/lymphoid or mixed-lineage leukemia (trithorax homolog, Drosophila). SET1A/B: SET (Su(var)3-9, Enhancer of Zeste and Trithorax) domain histone lysine methyltransferase . K27DMs: lysine 27 demethylases. Jmjd3: Jumonji domain containing 3. In red, enzymes responsible for histone modifications that associate to inactive chromatin: HDACs: histone deacetylases. K4DMs: K4 demethylases. LSD1: lysine specific demethylase 1. JARID1: Jumonji ARID (A/T Rich Interaction Domain) 1. K27MT: lysine 27 methyltransferases. PCR2: Polycomb repressor complex 2. EZH2: Enhancer of Zeste Homolog 2.

2.2. DISCOVERY OF GENOMIC IMPRINTING

During the 1980s, embryo manipulation studies in mice led to the discovery of the non-equivalence of the maternal and paternal genomes (Surani et al, 1984; McGrath and Solter, 1984). Using pronuclear transfer techniques, zygotes were created that were gynogenetic (with two female pronuclei) or androgenetic (with two male pronuclei), both of which failed to give rise to normal conceptuses. Possessing a normal diploid number of chromosomes was not enough to warrant full embryonic development: half of the set had to come from a male individual and the other half from a female. This led to the conclusion that the genetic material received a mark or "imprint" depending on its parental origin.

It was later shown that this parental marking involves a restricted subset of genes which display a parent-of-origin dependent expression. These imprinted genes are expressed monoallelically from either the maternal or the paternal chromosome. This mechanism helps achieve a balanced expression of these genes during normal embryonic and fetal development (Hitchins and Moore, 2002).

Imprinted genes tend to be found in clusters, associated with an Imprinting Control Regions (ICRs) which direct the allelic regulation throughout large domains (Verona et al., 2003). The maintenance of a particular pattern of expression relies on the efficient adaptation of the epigenetic mechanisms that are common to the transcriptional regulation of the whole genome.

2.3. EPIGENETIC REGULATION OF IMPRINTING CLUSTERS

Imprinted expression is regulated by the differential setting of epigenetic marks in the two chromosomes of different parental origin. Differentially methylated regions (DMRs) between paternal and maternal alleles can be found in most imprinted clusters (Brannan and Bartolomei, 1999). There are two main mechanistic models that have been described in the control of imprinted expression: the insulator model and the non-coding RNA model (Ideraabdullah et al., 2008).

The best known example of the insulator model operates in the *IGF2/H19* cluster (domain 1, telomeric or distal -see *Figure* 4 *4*- in chromosome 11p15.5). Imprinted expression is controlled by the paternally methylated *IC1* –imprinting control region 1-, also known as the *H19* DMD, which acts as a methylation-sensitive insulator. The *IC1* region contains multiple binding sites for the insulator factor CTCF (CCCTC- binding factor), which is inactivated by methylation in the paternal allele. The CTCF binding to the unmethylated maternal allele facilitates higher order chromatin loops, which regulate the reciprocal interaction of *IGF2* or *H19* promoters to upstream enhancers, resulting in paternal or maternal transcription, respectively (Verona et al., 2003).
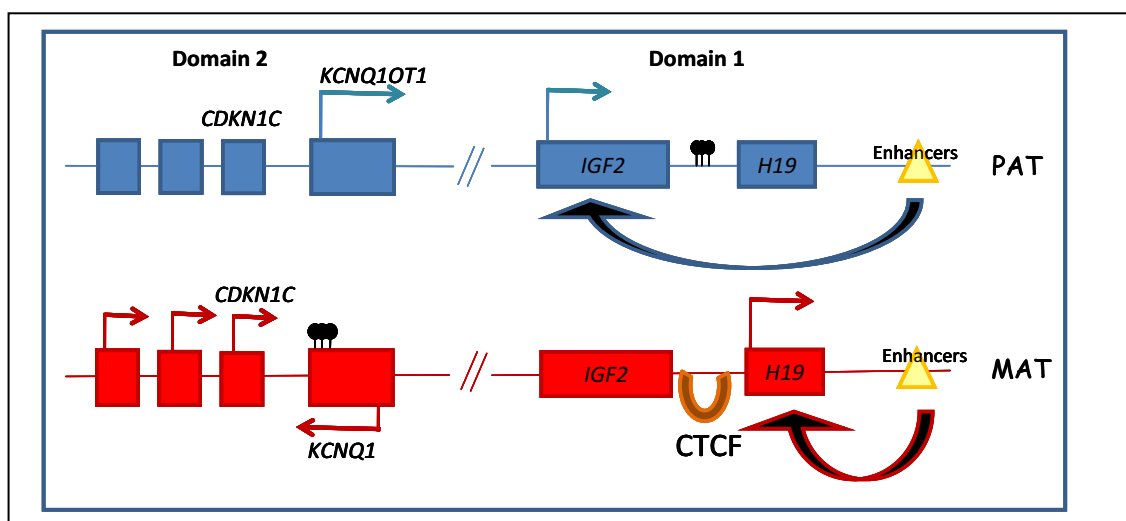
Figure 4: Structure of the 11p15.5 imprinted region.
Colour coding represents paternally (blue) and maternally (red) inherited homologue alleles. Arrows indicated active transcription. IC1 is methylated (black lollipops) on the paternal allele, preventing the binding of CTCF and allowing the access of IGF2 *to enhancers. IC2 is methylated in the maternal allele, which prevents expression of* KCNQ1OT1 *and allows expression of other genes in the cluster (*KCNQ1*,* CDKN1C*).*

Imprinting involving non-coding RNAs is seen in many clusters, frequently with antisense transcription originating from DMRs and regulated by their methylation status (O'Neill, 2005). Maternally methylated ICRs giving rise to the paternally expressed ncRNAs *Air* and *Kcnq1ot1*, have been shown to regulate allelic repression of other transcripts throughout their respective imprinted domains (Fitzpatrick et al., 2002; Mancini-DiNardo et al., 2003; Wutz et al., 1997). It is currently unknown if the process of active transcription is necessary for parental allele repression, but premature truncation of the RNAs has shown that they are indispensable for allelic silencing (Mancini-DiNardo et al., 2006; Kanduri et al., 2006; Sleutels et al., 2002). The proposed model for *Air* is that the transcription of the ncRNA physically displaces essential

factors required for *Igf2r* expression. The centromeric domain at 11p15.5 is regulated by *Kcnq1ot1* (see Figure 4), which recruits repressive histone-modifying enzymes to the paternal chromosome, silencing multiple other genes, including *Cdkn1c*, *Phlda2* and *Slc22a18* (Umlauf et al, 2004; Lewis et al., 2004).

Other kinds of untranslated RNAs, such as microRNAs and components of PIWI-interacting RNA (piRNA) pathway have recently been shown to have a role as an imprinting mechanism (Seitz et al., 2004; Noguer-Dance et al., 2010; Watanabe et al., 2011).

2.4. THE LIFE CYCLE OF IMPRINTS

The transmission of gender-specific methylation patterns implies that some resetting has to take place in the passage from generation to generation. The acquisition of imprints occurs during the development of germ cells. Methylation marks are set earlier in the male germline, before meiotic division, while the process occurs during late maturation in the oocyte (Lees-Murdoch and Walsh, 2008). All imprinted control regions are germline DMRs and are maintained throughout development after fertilization. Somatic DMRs, which can contribute to tissue- or developmental- specific imprinted expression, appear later during embryonic development. The Primordial Germ Cells (PGCs), which are the precursors of gametes, undergo a first wave of DNA demethylation with extensive epigenetic reprogramming, from which imprints and some repetitive sequences are spared. After this, specific erasure of methylation of the ICRs in early primordial germ cells is followed by the acquisition of *de novo* methylation in agreement with the gender of the fetus (see <u>*Figure* 5</u>) . The timings for erasure and acquisition of methylation seem to be specific to each ICR (Kelly and Trasler, 2004; Arnaud and Feil, 2005). Once established, the germline DMRs are protected from global post-fertilization demethylation waves (see section 2.1.1. DNA methylation) by specific factors, such as ZFP57 and members of the NLRP family (Li et al., 2008; Meyer et al., 2009).
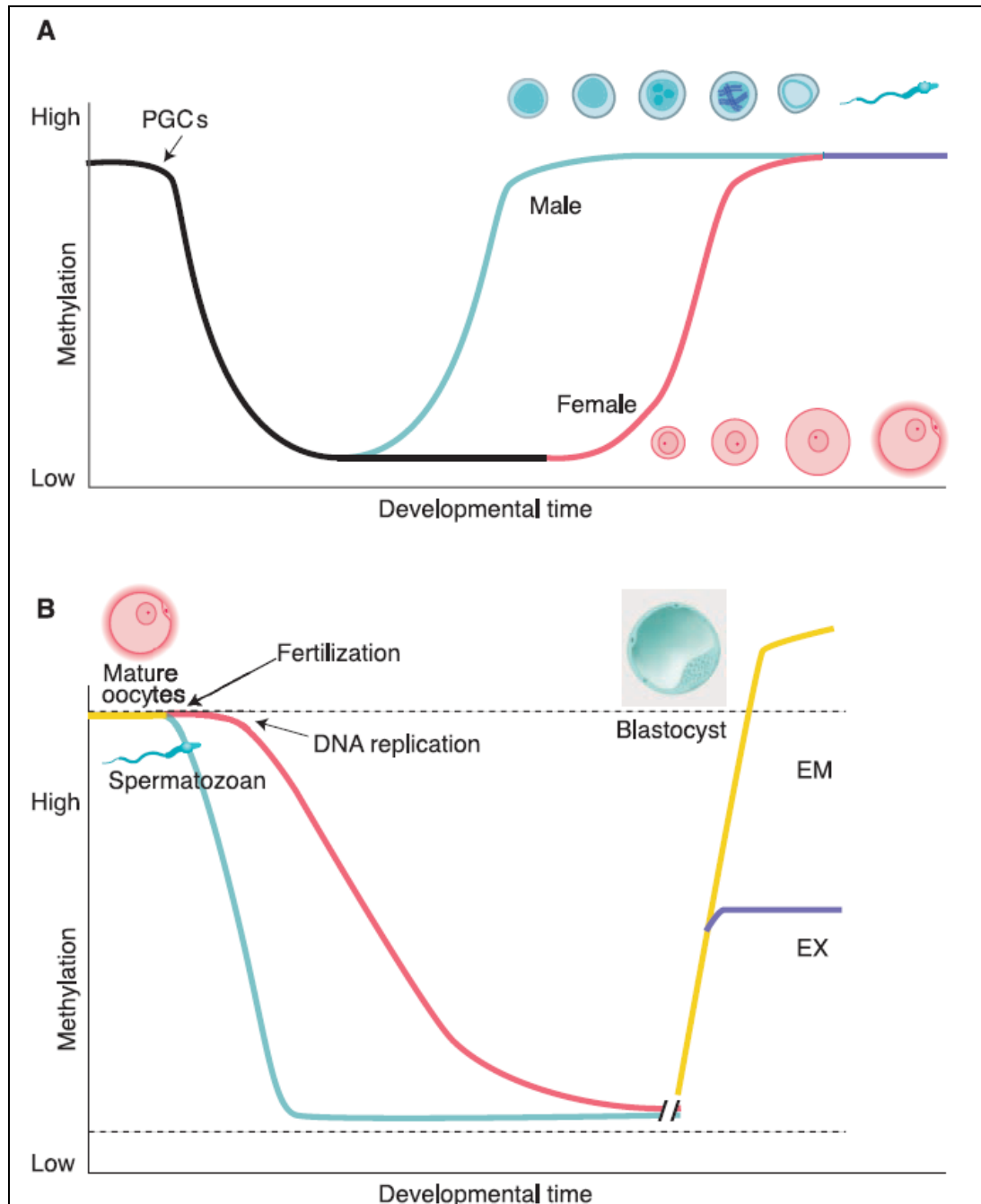
Figure 5: Life cycle of imprints and epigenetic reprogramming.
From Reik et al., 2001. Methylation reprogramming in (A) the germ line and (B) preimplantation development. (A) PGCs (Primordial Germ Cells) become demethylated early in development and subsequently acquire imprinting marks according to the gender of the fetus. This starts in prenatal stages in the male lineage, but it is a postnatal event in the females, were imprint acquisition takes places in growing oocytes. (B) The paternal genome is represented in blue and the maternal genome in red. Both suffer a wave of demethylation after fertilization, which is rapid and active in the paternal and slow and passive in the maternal pronucleus. The dashed line represents methylated imprinted genes and some repeat sequences, which do not undergo demethylation. Remethylation occurs around the time of implantation and is assymetric between the embryonic (EM) and extraembryonic (EX) lineages. (Data predominantly from mice).

3 GENOMIC IMPRINTING AND FETAL GROWTH

3.1. THE PLACENTA AS A TARGET OF THE ACTION OF IMPRINTED GENES

Genomic imprinting seems to have evolved in nature as a way of modulating the transfer of nutrients to the offspring, as it is only present in eutherian mammals and flowering plants. The placenta and the endosperm are, respectively, the organs in charge of this task (Reik et al., 2003). Many imprinted genes described so far in the mouse are expressed in the placenta and all the ones for which allelic expression has been determined are monoallelic, even though one third of them are biallelic in other fetal organs (Ferguson-Smith et al., 2006).

Many imprinted genes have been shown to have effects in placental development and function (reviewed in Frost and Moore, 2010). Some are directly involved in the conformation of the placenta, e.g. *Mash1/Ascl2* or *Peg10* (Guillemot et al., 1995; Ono et al., 2006) where null mice are embryonic lethal due to absence of a functional placenta. Others regulate the transfer of nutrients to the fetus, either by regulating storage of glycogen in extraembryonic tissues, such as *Phlda2* (Tunster et al., 2010), or directly by encoding transporters and channel proteins with roles in placental exchange mechanisms. This is the case for the maternally expressed organic cation transporters *Slc22a18, Slc22a2*, *Slc22a3* and *Impt1/Slc22a1l* or the paternally expressed amino acid transporter A3 (*Ata3*), part of the A amino acid transport system (Constancia et al., 2005).

The evolutionary need for genomic imprinting has been explained by different models. The major hypothesis is based on the prominent role of imprinted genes in the placenta: the "conflict theory" focuses on the tug of war between the parents for the allocation of nutrients to the fetus in order to achieve the best survival of their own independent genes. During prenatal development and up until weaning, the paternal genome would force the delivery of resources from the mother. This is at the expense of other littermates, of potential litters from other fathers or of the mother herself. In turn, the maternal genome would favour an equal distribution amongst the offspring while trying to preserve her survival and reproductive ability for the future (Moore, 2001). Experimental evidence on the role of particular imprinted genes has generally been supportive of this principle, but there are exceptions, such as *Rbl1*, which is maternally expressed but results in impaired growth when inactivated (Lee et al., 1996).

Other theories for the evolution of imprinting include the "supply and demand theory", which stresses the effect of imprinted genes in controlling the transfer of nutrients in the placenta and regulating request from in fetal tissues, setting an appropriate balance between both (Constância et al., 2002; Angiolini et al., 2006). The model is based on experimental data regarding the role of *Igf2* in fetal development in the mouse (Constância et al., 2002, Gardner et al., 1999, Reik et al., 2003), suggesting that circulating Igf2 produced by the fetus may have an endocrine effect on the placenta. It is currently unknown whether this model applies to humans, where the *IGF2-P0* transcript is conserved but not placental-specific (Monk et al., 2006b).

3.2. IMPRINTED GENES AND FETAL GROWTH

Experiments utilizing mice models of uniparental disomies (UPDs), the inheritance of both homologues of a chromosomal region from only one parent, and subsequent targeted deletions showed that disruption of imprinting usually has an effect on fetal growth (http://www.har.mrc.ac.uk/research/genomic_imprinting/). The particular mechanisms by which imprinted genes regulate pre- and postnatal growth have been less well investigated and appear diverse. As summarized before, many of them affect placental development and function. Others, like the maternally expressed cyclin-dependent kinase inhibitor 1c (*Cdkn1c/ p57^{Kip2}*), can act as cell cycle regulators, having direct repercussions on proliferation and tissue growth (Zhang et al., 1998). The influence of imprinted genes can extend to the postnatal period and to the co-ordination between growth and energy homeostasis. *Peg1* and *Peg3* are involved in postnatal feeding behaviour and parenting skills (Nikonova et al., 2008; Takahashi et al., 2005; Li et al., 1999), while *Grb10* and *Dlk-1* are involved in the metabolic routes of glucose metabolism and adipogenesis (reviewed in Smith et al., 2006).

3.2.1. GROWTH ANOMALIES IN IMPRINTING SYNDROMES

Many UPDs in humans (mUPD7, mUPD14, mUPD16, mUPD20 and pUPD6q24) are associated with an intrauterine growth phenotype (Devriendt, 2000; Kotzot and Utermann, 2005). In these patients, IUGR can be caused by both the interference with imprinting

mechanisms and by the confined placental mosaicism that is frequently associated. In the case of mUPD16, for example, fetal size seems to relate more to the proportion of trisomic mosaicism of the placenta than to any imprinting effects (Kalousek, 1994; Kalousek and Vekemans, 2000; Moore GE et al., 1997). Well-described imprinting syndromes like Beckwith-Wiedemann or Silver-Russell are useful models that illustrate the influence of imprinted genes on birth weight even in the absence of UPD, and clarify the epigenetic mechanisms involved in their deregulation.

Beckwith-Wiedemann syndrome is the best understood overgrowth syndrome and an underlying epigenetic defect in the imprinted clusters in 11p15.5 is the most commonly identified molecular cause (Choufani et al., 2010). Genomic mutations in *CDKN1C* also cause BWS in a minority of sporadic cases (Lam et al., 1999). Other features include abdominal wall defects, macroglosia, ear abnormalities and predisposition to developmental tumours. Half of the patients show LOM at the maternal *IC2*, while paternal UPD, seen in up to 20% of cases (Romanelli et al., 2011), involves both *IC1* and *IC2*. Isolated loss of methylation of the paternal *IC1* is less common, accounting for approximately 5% of cases. Loss of methylation (LOM) of the maternal *IC2 (KvDMR1)* detected in BWS patients would cause biallelic expression of the *KCNQ1OT1* antisense transcript (Smilinich et al., 1999) and silencing of *CDKN1C* and other genes of the cluster. Almost half of the BWS affected individuals, including some with LOI at *IC2*, display loss of imprinted expression of the *IGF2* gene, although this happens through an *H19*-dependent mechanism in only a few cases. The organs and systems affected in the disease correspond well with the pattern of *IGF2* expression, implying a pathophysiological role for this gene (Weksberg et al., 2003).

Silver-Russell syndrome is another example of epigenetic deregulation causing a growth phenotype. Patients present with pre and postnatal growth failure, triangular face and, in approximately half of the cases, hemihypertrophia (Hitchins et al., 2001, Wakeling et al., 2010) Due to phenotypic variability and somatic mosaicism, a molecular cause can be identified in around 60% of cases (Eggermann, 2010). Loss of imprinting of the *IC1* at 11p15.5 was first described by Gicquel et al. in 2005 and accounts for up to 46% of the molecular defects (Gicquel et al., 2005). The usual mechanism involves loss of methylation without cytogenetic aberrations. It is thought that this leads to biallelic *H19* expression, interference with the expression of *IGF2*, and growth failure (Eggermann, 2010). Some patients with LOM of the *H19* DMD show extended loss of methylation at other imprinted loci (Turner et al., 2010). Other genetic abnormalities have been described, such as ring chromosome 15 (Tamura et al., 1993) and maternal UPD7 (up to 5% of cases) which would alter imprinted gene dosage at 2 regions:

7p11.2-p13, containing *GRB10* (Joyce et al., 1999; Monk et al., 2000) and 7q31-qter (Hannula et al., 2001), encompassing *MEST* and *COPG2*. The underlying cause of the phenotype in these cases is unclear, as no recessive gene unmasking (Preece et al., 1999), confined placental mosaicism *(*Kalousek et al., 1996), somatic mosaicism (Monk et al., 2001) or coding or epimutations (Hitchins et al., 2001; Riesewijk et al., 1999; Blagitko et al., 1999) have been uncovered that explain either IUGR or hemihypertrophy.

These examples of human disease serve to illustrate both the paramount relevance and the complex regulation of imprinting in growth. Given the principal roles of imprinted genes in fetal development and the growth phenotypes observed in imprinting defects, there has been a recent interest in assessing if this subset of genes might play a part in isolated non-syndromic IUGR.

3.2.2. IMPRINTED GENES AND NON-SYNDROMIC IUGR

PHLDA2 is a maternally expressed gene that has been shown to act as a key determinant of placental growth in mouse models (Salas et al., 2004). It maps to the human 11p15.5 centromeric/ mouse distal chromosome 7 clusters of imprinted genes, under the regulation of the Imprinting Center 2/ *KvDMR1*. For this gene, a correlation between levels of expression in human normal term placenta and fetal size at birth has been established, while this was not the case for *IGF2*, *IGF2R* and *MEST* (Apostolidou et al., 2007).

Levels of expression of this and other imprinted genes have been investigated in placentas from patients with a clinical diagnosis of IUGR. A genome-wide study approach in a small number of IUGR placentae with maternal vascular under-perfusion found differential expression of over 400 genes (McMinn et al., 2006). Six out of the 27 assessed imprinted genes were shown to be up- (*PHLDA2*) or down- (*MEST*, *MEG3*, *GATM*, *GNAS* and *PLAGL1*) regulated. It was postulated that the apparent dysregulation of imprinted expression could be an adaptive mechanism for regions of placental hypoperfusion, designed to restrict the growth of areas receiving less than optimal blood supply. This mechanism would turn deleterious if the placental flow is globally compromised, because it would further interfere with normal development.

H19, an imprinted untranslated RNA which participates in the negative regulation of *IGF2* expression, was not represented on the array used in the previous study, but has been

analyzed separately by other groups. Some demonstrate an increase in *H19* mRNA levels (Koukoura et al., 2011), sometimes with a concomitant decrease in *IGF2* (Guo et al., 2008) in IUGR placentas, although these results have not been replicated in other cohorts with heterogeneous clinical characteristics (Apostolidou et al., 2007; Bourque et al., 2010).

Non-SRS IUGR individuals have also been recently checked for methylation defects in the *H19/IGF2* region. One study reported that, out of 45 patients referred for genetic study for IUGR/short stature without a suspicion of SRS, 2 showed loss of methylation in the *H19* DMD and 6 had methylation defects in other DMRs (1 in 11p15 IC2 without a BWS phenotype and 5 a gain of methylation in the *IGF2R DMR*) (Turner et al., 2010). Most of these patients showed other dysmorphic phenotypical features, except in the case of isolated gain of methylation of the *IGF2 DMR*, which was also found in controls, but with a significantly lower prevalence. The finding of *ICR1/H19* DMD hypomethylation in IUGR has been replicated by other researchers (Koukoura et al., 2011; Bourque et al., 2010). In studies spanning several other CpG islands (ICR2 and *CDKN1C*, *H19*, *PEG10*, *PLAGL1*, *SNRPN* and *MEST* promoters), the findings appear specific to the *H19* DMD, at least in non-pre-eclamptic IUGR placentae (Bourque et al., 2010).

3.3. EFFECTS OF ASSISTED REPRODUCTION TECHNIQUES (ART) ON IMPRINTING AND PREGNANCY OUTCOME

The first notions about the possible effects of the different steps involved in assisted reproduction techniques (ART) on the correct establishment and maintenance of imprinting came from animal studies. It was observed that culture of murine, ovine and bovine pre-implantation embryos and somatic cell nuclear transfer ("cloning") in sheep were sometimes complicated with the appearance of a "large offspring syndrome (LOS)", an overgrowth phenotype with similar traits to human BWS. LOS is related to loss of imprinting and consequent loss of expression of the *Igf2r* gene (Lau et al., 1994; Young et al., 2001), a growth inhibitor. Molecular and phenotypical aberrations have also been noticed in mice after assisted reproduction (Doherty et al., 2000; Khosla et al., 2001) and the effects are, on occasion, delayed (Mahn et al., 2004).

The process of imprint methylation establishment occurs mostly during the hormonal responsive preantral phases of follicular development (see *Figure* 5). This makes imprint

acquisition susceptible to defects if immature follicles are recruited during ovarian stimulation (Fortier et al., 2008). Animal data suggest that gamete and embryo culture could entail a variety of risks, related to culture conditions during a period of extensive epigenetic reprogramming (Doherty et al., 2000) (see also sections 2.1.1 on DNA Methylation and 2.4. on The life cycle of imprints).

Human analysis of In Vitro Fertilization (IVF)- and Intra Cytoplasmatic Sperm Injection (ICSI)- conceived children yield conflicting results (Gosden et al., 2003; Steinkampf and Grifo, 2002). It is noteworthy that reported maternal infertility or IVF treatment is not strange among the series of rare imprinting defects (for example in 2/10 patients with LOM at 6q24, Mackay et al., 2006a). In large cohort studies, it remains unclear if imprinting defects are more common in babies following ART and, if this was to be the case, if it is due to the techniques themselves or to the intrinsic characteristics of couples undergoing the treatments (e.g. older female age, subfertility). Even if imprinting defects are increased, the absolute risk appears to still be small (Bowdin el al., 2007). What seems undeniable is that some common mechanism exists that differs from the general population, as most or all of the cases of BWS and Angelman syndrome (AS) diagnosed in individuals born after ART are due to loss of methylation in the maternal imprinting control region, a rare form of these diseases in spontaneously conceived cases (50% for ICR2 and 5% for ICR1 in BWS and 5% in AS) (Arnaud and Feil, 2005). Poor results in population-based studies have also been reported regarding an excess of low and very low birth weight infants and other adverse pregnancy outcomes among those pregnancies conceived by ART, especially when female infertility was a factor (Schieve et al., 2002 and 2007). It is unknown if this could be related to epigenetic or imprinting defects.

4. *PLAGL1* AND THE 6q24.2 REGION AS CANDIDATES FOR IUGR

The 6q24.2 chromosomic region in the human is syntenic to mouse chromosome 10. It contains two imprinted genes, *PLAGL1/LOT1/ZAC1* and *HYMAI*, the latter encoding an untranslated RNA. These transcripts originate from a CpG island that is differentially methylated in gametes, being unmethylated in sperm and methylated in oocytes, a pattern which is maintained in somatic tissues (Arima et al., 2000; Smith et al., 2002).

4.1. TRANSIENT NEONATAL DIABETES MELLITUS 1 (TNDM1)

Transient Neonatal Diabetes Mellitus 1 (TNDM1) is a rare disorder caused by loss of imprinting in the 6q24.2 locus (Gardner et al., 2000, Arima et al., 2001). Affected patients suffer from severe IUGR and neonatal diabetes mellitus, characterized by hyperglycaemia in the absence of ketoacidosis. Although descriptions usually refer to term babies, at least one case has also been reported in an extreme premature (Nishimaki et al., 2008) and it might be more frequent than thought in this population, where early hyperglycemia is a common, although a usually short-lived, complication (Beardsall et al., 2005; Iglesias-Platas et al., 2009). TNDM1 patients usually require insulin treatment for approximately the first three months of life and then go into relapse. The duration of the asymptomatic period seems chronologically determined and independent of maturity, as it is the same for term and preterm children (Nishimaki et al., 2008). Bursts of hyperglycaemia can occur in times of physiological stress, like with intercurrent disease during childhood, in puberty or during pregnancy. In the majority of cases, after an average of 14 years, diabetes becomes permanent, with features more similar to type 2 diabetes, like low and intermittent requirements of insulin and presence of insulin resistance (Temple et al., 2000; Temple and Mackay, 2010). An increased incidence of type 2 diabetes has also been shown in families of the probands and some individuals with the predisposing mutations do not have a neonatal phenotype, but develop diabetes later in life. The mechanisms that might regulate expressivity of the disease are unknown.

TNDM1 patients have different molecular defects, from uniparental disomy (40%) or partial duplications (32%), both of paternal origin, to loss of maternal methylation at the *PLAGL1* DMR (28%) (Cavé et al., 2000; Temple et al., 2000; Arima et al., 2001; Diatloff-Zito et

al., 2007; Gardner et al., 2000; Mackay and Temple, 2010). Recently, TNDM1 patients have been shown to have associated defects in other imprinted loci. The first to be described was a concomitant LOM of KvDMR (Arima et al., 2005; Mackay et al., 2006b). These patients do not possess any distinguishable phenotypic characteristics compared to those with isolated 6q24 defects (Mackay and Temple, 2010). Half of the cases of multiple methylation defects in TNDM have now been shown to be due to mutations in *ZFP57* (Mackay et al., 2008).

Multi-loci loss of methylation has now also been reported for other imprinting defects, including BWS and SRS patients with IC2/IC1 hypomethylation, who show multiple LOM at maternally and paternally methylated DMRs (Azzi et al., 2009; Begemann et al., 2011).

4.2. THE 6q24.2 REGION AND FETAL GROWTH AND METABOLISM

The mouse orthologue of *PLAGL1*, *Zac1*, was first described as a transcriptional inductor of cAMP through PACAP (Spengler et al., 1993). The rat equivalent, *rLot1*, was identified by the analysis of differential expression between normal and malignant rat ovarian surface epithelial cells (Abdollahi et al., 1997).

PLAGL1 is translated into a 44kDa protein that is a zinc-finger transcription factor and acts as a regulator of both apoptosis and cell cycle arrest in G1 (Spengler et al., 1997). Due to this dual function, *PLAGL1* is cardinal regulator of normal cell proliferation and loss of its expression or heterozygosity is seen in many benign and malignant tumors (Pagotto et al., 2000; Lemeta et al., 2006; Cvetkovic et al., 2004; Bilanges et al., 1999). It exists in two alternatively spliced isoforms with 5 (isoform Δ2) or 7 zinc fingers. Both forms display a similar anti-proliferative activity, but Δ2 is more efficient at inducing G1 cell-cycle arrest and has lower pro-apoptotic activity (Bilanges et al, 2001). There are at least two different *PLAGL1* transcriptional start sites, one of them originating from the DMR with imprinted expression (P1), the other non-imprinted and starting from a different unmethylated promoter (P2). The proportion of imprinted and non-imprinted transcripts varies between tissues (Valleley et al, 2007).

Some insight into the role of *Plagl1* during embryonic development has been gained from genetic manipulation in mouse models. Inactivation of the paternal copy of this gene was indistinguishable from homozygous deleted mice and produces a 23% reduction in birth

weigth (Varrault et al., 2006). The pattern is similar to what has been observed in humans after placental insufficiency, with a preservation of brain growth at the expense of other organs, like the liver and lungs, but the placenta is not affected either regarding size or transport capacity. The animals also display alterations of gross morphology, delayed ossification and a high rate of neonatal mortality due to respiratory insufficiency. Although impaired growth was not the expected phenotype when inactivating a cell-cycle inhibitor, a similar situation had been previously reported upon deletion of functional copies of genes in the retinoblastoma family (Rbl1 and Rbl2), which are also tumour suppressors (Lee et al., 1996). Coincidentally, *RB1* has recently shown to be also subjected to imprinting and maternally expressed (Kanber et al., 2009). IUGR after alteration of a paternally expressed gene, like *Plagl1*, fits the conflict theory, while inactivation of a maternally expressed gene would be expected to enhance growth. Patients with mUPD6, which would not express *PLAGL1*, display no imprinting defects, suggesting that in humans only overexpression, but not loss of expression, gives rise to a phenotype (Lapunzina and Monk, 2011).

Recent studies have identified a differential pattern of expression between mouse and human *Plagl1/PLAGL1* during pancreas development. While expression in the mouse is localized mainly in mesenchymal tissue, the strongest signal in mRNA *in situ* hybridization studies in human fetal pancreas appears specifically in insulin positive cells (Du et al., 2011). In fact, expression of *PLAGL1* in a mouse model overexpressing a BAC transgene containing the human *PLAGL1* and *HYMAI* genes mimics the human pattern of cell-type specific expression from the transgenic construct (Ma et al., 2004). While orthotopic overexpression of *Plagl1* in the pUPD10 mouse, equivalent to human pUPD6 and TNDM1, fails to bring about any gross phenotypic changes (Smith et al., 2002), the human TNDM mouse does reproduce the glucose homeostasis defects seen in TNDM1 patients (Ma et al., 2004). In this model, excessive expression of *PLAGL1* leads to reduced β cell mass in the prenatal pancreas, with a reduced insulin content at the neonatal stage, partially compensated during the juvenile age by an increase in islet mass (Ma et al., 2004). The lack of intrauterine growth restriction in the rodent could be explained by the different involvement of insulin in prenatal growth between species, as lack of this hormone does not have a major effect on fetal size in the mouse (Efstratiadis, 1998).

Excessive expression of an antiproliferative factor like *PLAGL1* during the prenatal stages might hamper the normal developing of the tissues where it is expressed, like the pancreatic islets. Postnatally, a timely downregulation on the levels of serum Igf1 and Igf2 seems essential for the terminal differentiation of the β cell, which acquires an adult phenotype, with

increased sensitivity to glucose and the ability for a rapid release of insulin (Petrik et al., 1998; Hill et al., 2000). Some *in vitro* work on hepatocarcinoma cell lines has suggested that *PLAGL1* potentiates the enhancer activity of E2 on *IGF2* upon direct binding to it (Varrault et al., 2006). If this was also the case in β cells, and excess of *PLAGL1* would lead to lack of downregulation of *IGF2* and impair the developmental wave of apoptosis, favouring the persistence of a population of fetal β cells that lack response to increases in glucose levels after feedings. A subsequent increase in Igf1 levels seems to reactivate β cell proliferation by activating differentiation from the ductal epithelium. This could increase islet mass enough to explain an asymptomatic period, with relapse occuring later in life due to pancreatic endocrine dysfunction and loss of first phase insulin secretion (Hattersley, 2004) .

Once pancreatic development is finalized, excessive expression of *PLAGL1* would be expected to result in upregulation of the PACAP receptors and consequently in increased and not diminished insulin secretion (Filipsson et al., 2001). It is possible that the ontogenic role of *PLAGL1* is essential and that, as explained before, abnormally differentiated β cells are unable to respond normally. Alternatively, continuous upregulation of the PAC1-R could lead to a persistent influx of calcium, contributing to either depletion of intracellular insulin stores, cell toxicity or both.

Loss of imprinting in the 6q24 region creates a TNDM-associated IUGR phenotype, which has usually been attributed to the decreased secretion of insulin, one of the main growth factors during human prenatal development. Also, it has been proposed that the growth effect of *Plagl1* could be exerted through its functional relationships with other imprinted genes. It is integrated in an "imprinting network" (Varrault et al., 2006) and it has also been suggested to directly influence the expression of some of the network genes through its transcription factor activity (Arima et al., 2005).

HYPOTHESIS AND AIMS

The placenta is a key organ in powering the process of fetal growth. It is likely that, in many cases, the basis of fetal growth restriction lie in alterations in size, morphology and/or transport capacity of the placenta. Imprinted genes have been shown to influence a range of these factors and, indeed, levels of expression and/or methylation of several imprinted genes in the placenta have been shown to correlate with either fetal weight or other parameters of compromised growth, such as placental hypoperfusion or abnormal uterine and fetal Doppler flows.

The imprinted gene *PLAGL1* could take part in the determination of prenatal growth, directly through influence on insulin secretion or indirectly through the "imprinted gene network". Through its regulatory activity on glucose homeostasis, *PLAGL1* fits the "fetal insulin" hypothesis while alteration of its regulating epigenetic mechanisms could result in an effect of "fetal programming". Imprinting defects in TNDM patients are peculiar in that loss of methylation on the maternal chromosome is complete, and not mosaic like methylation defects associated with other imprinting syndromes. This epigenetic defect has been observed at low frequency in individuals without hyperglycemia (Mackay and Temple, 2010), but presenting with IUGR. Therefore, an intermediate epigenetic defect could play a role in the broad spectrum of normal and abnormal non-syndromic fetal growth.

HYPOTHESIS

We hypothesize that placental expression of imprinted genes mapping to the *PLAGL1* locus will play a role in the determination of fetal growth, whether under physiological or pathological conditions. This will reflect in changes of expression and/or regulatory mechanisms of these genes in the placentae of small and growth restricted newborns.

AIMS

The global aim of this study was to determine the presence of changes in expression and epigenetic regulatory mechanisms in the 6q24 region in relation to normal and pathologic fetal growth.

The specific aims at each step were:

1. To ascertain the expression of the transcripts in the 6q24 imprinted region during human fetal growth in the placenta and fetal tissues.

2. To define the extent of the imprinted domain at 6q24.2 by analyzing normal placental and fetal tissues. The allelic origin of expression of all transcripts and the methylation status of the promoter-associated CpG islands within this region will be investigated.

3. To determine correlations between total mRNA expression of *PLAGL1* in placentas and fetal size estimated by birth weight in term pregnancies of normal course.

4. To assess the differences between the expression of all identified imprinted genes in the region, regarding both levels of expression and maintenance of imprinting, between the placentas of pregnancies complicated by term or preterm fetal growth restriction and controls of matched gestational age.

5. To determine the relationship between levels of methylation at the regulatory Differentially Methylated Region (DMR) for imprinted transcripts on Chromosome 6 in the placenta and fetal growth parameters.

PARTICIPANTS AND METHODS

PARTICIPANTS

1. TISSUE SOURCES

The human tissues used at sequential stages of this project were obtained from two maternity hospitals located in London and Barcelona, respectively.

Moore cohort (London): One hundred and three term placental samples and matched parental bloods were selected from the Moore cohort. This collection originated at Queen Charlotte's and Chelsea Hospital following informed consent from participants. Selection was based on the pregnancy being healthy, ultrasound-dated, singleton and of white European origin. This cohort was selected to explore relationships between our gene of interest and normal fetal growth.

First trimester placental and fetal tissue samples were obtained at the same hospital from terminations of pregnancy for indications other than fetal compromise. Local ethical approval for consented collection was granted by the Hammersmith and Queen Charlotte's and Chelsea Hospitals Research Ethics Committee (registration numbers 2001/6029 and 2001/6028, respectively). Tissues were rinsed in sterile PBS to remove traces of maternal blood, snap frozen in liquid nitrogen and stored at -80°C.

Sant Joan de Déu (SJD) participants (Barcelona): One hundred participants were recruited among pregnant women that delivered their babies in Sant Joan de Déu Hospital, Barcelona, after approval of the protocol by the center´s Research and Ethics Committee (35/07). Informed consent was obtained from participants and clinical information on the pregnancy follow up was entered into a database. For the purpose of the study, subgroups were established according to the characteristics of the pregnancy and of the newborn (term or preterm, IUGR or non-IUGR, spontaneously conceived or pregnancy following assisted reproduction techniques). This cohort was used in the study of normal *versus* pathological pregnancies.

2. SAMPLE PROCESSING

BLOOD SAMPLES: Blood samples were collected in EDTA tubes and frozen at -80°C until extraction. The London cohort included maternal and paternal blood samples. For the Barcelona cohort we collected maternal peripheral blood and cord blood from the section of umbilical cord adjacent to the placenta.

PLACENTAL AND TISSUE SAMPLES: Upon delivery, the placenta was weighed and membranes stripped from the fetal side. Two fragments from two different sites around the umbilical cord were sectioned, up to approximately half the depth of the placenta. In case of peripheral or velamentous insertion of the cord, the fragments were obtained from the centre of the placenta. Samples were thoroughly rinsed in saline (NaCl 0,9%) or PBS to remove maternal blood. A section of 1 cm of umbilical cord was also obtained. All tissue samples were snap frozen in liquid nitrogen, anonymized with a correlative number and stored at -80°C until nucleic acid extraction.

3. CLINICAL INFORMATION

Moore cohort: Maternal weight, height, age, parity, baby's gender, birth weight, head circumference, placental weight, past and present medical history, mode and indication for delivery, absence of pregnancy complications, smoking, diet and alcohol consumption, and partner's medical history were collected from the mother's notes.

SJD cohort: Clinical information was retrieved by review of clinical charts, direct interview with the family or from the consultant in charge. Details were obtained regarding demographic and anthropometric data from the mother and newborn, as well as medical and obstetric history and data from the pregnancy follow-up from the pathological cases, including ultrasound scans (morphology and Doppler flow assessment) and pregnancy complications and outcomes (see *Table 3* for a detailed list). These items were codified and introduced in a database in the statistical package SPSS® (Statistical Package for Social Sciences, IBM) for further analysis.

Table 3: Clinical variables included in the study database.

Variable	Definition
ID	Correlative number assigned
Maternal age	Maternal age in years
Height	Maternal height in cm
Initial weight	Maternal weight (kg) prior to pregnancy
Post-gestation weight	Maternal weight (kg) prior to delivery
Ethnicity and country of origin	Ethnic category: White/ Hispanic/ African/ Asian (India)/ Asian (China/Japan)/ Arab (Egiptian/ Magreb)/ Mixed
Previous pregnancies/ Parity	History of previous pregnancy outcomes: Number of previous Term/ Preterm/ Miscarriage/ Life births
Obstetric history	Report of previous complications of pregnancy/ infertility
Assisted Reproduction Techniques (ART)	Spontaneous pregnancy/ Pregnancy after ART
LMP	First day of Last Menstrual Period
Delivery date	Day of delivery
Multiple	Multiple gestation/ order number
Indication of delivery	Reason for finalization of pregnancy: Spontaneous/ Maternal/ Fetal
Delivery mode	Route of delivery: Vaginal/ Caesarean section (with or without labour)
Dating of pregnancy	Best assessment of Gestational Age (LMP/ US scan in first trimester)
Gestational age at delivery	Weeks + days of gestation at delivery
Sex of the newborn	Sex of the newborn: Boy/ Girl
Placental weight	Placental weight in grams
Anthropometry of the newborn	Birthweight in grams/ Length in cm/ Head Circumference in cm
IUGR	Diagnosis of IUGR during the current pregnancy

Variable	Definition
Severity of IUGR	Classification of IUGR according to ultrasound data (see text below)
Complications of pregnancy/ Treatment	Pregnancy complications other than IUGR during the current pregnancy and treatments administered
Smoking	Presence of maternal smoking habit and number of cigarettes per day: Pre-pregnancy/ During pregnancy
Maternal conditions	Chronic maternal disease unrelated to pregnancy and treatments for this reason
Admission	Admission of baby to neonatal care
GA_group	Classification by gestational age: Term/ Late or moderate preterm/ Extremely preterm
Study_group	Classification according to study group: Appropriately grown for Gestational Age/ SGA/ IUGR

Accurate dating of the pregnancy is a pre-requisite for the assessment of fetal growth (Bryan and Hindmarsh, 2006). Pregnancies were dated by Last Menstrual Period (LMP) unless the difference with dating by first trimester ultrasound scan was bigger than 7 days, in which case ultrasound dating was applied. Recruited newborns were classified in three categories based on length of gestation: term (≥37 weeks), late and moderate preterm (>32 and <37 weeks) and extreme preterm (≤32 weeks).

Three groups were also established according to fetal growth characteristics: AGA (Appropriately grown for Gestational Age, birth weight > P10), SGA (Small for Gestational Age, birth weight between 3rd and 10th percentile without haemodynamic alteration) and IUGR (Intrauterine Growth Restricted). The diagnosis of IUGR was based on the criteria of the Obstetrics Service of the hospital, including estimated fetal weight under the 3rd percentile or under the 10th percentile with accompanying alteration of fetal haemodynamics as assessed by Doppler flow study (see Introduction, section 2: Definition, diagnosis and causes of IUGR). According to this protocol and for the purpose of the study, IUGR patients were sub-divided in mutually exclusive categories based on the most severe Doppler flow abnormality as follows:

Group I. Estimated fetal weight over 3rd percentile and under 10th percentile with no Doppler abnormalities (Small for Gestational Age).

Group II. Estimated fetal weight under the 3rd percentile with no Doppler abnormalities.

Group III. Alteration of Umbilical Artery Doppler Flow with normal Middle Cerebral Artery Doppler flow.

Group IV. Alteration of Middle Cerebral Artery Doppler flow (blood flow redistribution).

Group V. Alteration of fetal venous Doppler flow.

To allow for comparisons of growth parameters among newborns of different gestational ages, measurements were transformed into the corresponding z-scores. The recently published local growth charts for Catalunya were used for these calculations (Programa de Salut Materno Infantil, 2008). This local growth information does not include data for babies below 26 weeks. In these cases we selected the growth curves for weight from Alexander and co-workers (Alexander et al., 1996) and previous local data (Carrascosa et al., 2004) for length and head circumference for participants born at 24 and 25 weeks.

METHODS

1. NUCLEIC ACID EXTRACTION PROTOCOLS

1.1. DNA EXTRACTION FROM TISSUES AND PERIPHERAL MONONUCLEATED CELLS

1.1.1. DNA EXTRACTION: PHENOL-CLOROFORM METHOD

1. LYSIS

TISSUES: Approximately 100 mg of placental or fetal tissue was homogenised in 2.5 ml of tissue lysis buffer (NaCl 100 mM, Tris-HCl 10 mM pH 8, EDTA 25 mM) using a Polytron® (Kinematica) tissue homogenizer.

PERIPHERAL MONONUCLEATED CELLS: Cell lysis was achieved by adding 90 ml of blood lysis buffer (sucrose 0,32 M, Tris-HCl 10 mM, Magnesium chloride 5mM and 1% Triton X-100 detergent) to 10 ml of blood collected in EDTA tubes. The sample was centrifuged at 10,000 rpm for 15 minutes at 4°C in a refrigerated centrifuge (5810R, Eppendorf) with a swing-bucket rotor and the supernatant discarded. The pellet containing the nuclei was resuspended in 4.5 ml of suspension buffer (NaCl 75mM, EDTA 24 mM pH 8.0).

For both tissues and peripheral mononucleated cells extraction, SDS and proteinase K (Sigma) were added to 0.5% and 200 μl/ml final concentrations, respectively, to disrupt lipids and digest proteins. This mixture was incubated overnight in a thermoblock at 55°C.

2. DNA PURIFICATION

DNA was further purified by mixing the digested blood/tissue sample with an equal volume of phenol. This homogenate was separated into the aqueous and phenol phases by centrifuging at 10,000 rpm for 10 minutes at room temperature using Phase Lock Gel tubes® (QIAGEN). The shifting Phase Lock gel separates the aqueous phase containing the DNA from the organic phenol phase. This process was repeated twice. Phenol was removed by using an equal volume of chloroform, and the phases were separated as above.

3. DNA PRECIPITATION

The DNA was precipitated by mixing of 2 volumes of absolute ethanol with the final aqueous phase and spinning for 5 minutes at 10,000 rpm at room temperature. The pellet was then washed in 70% ethanol and left to air-dry before being re-suspended in 0.5-1 ml of TE buffer (Tris-EDTA: Tris-HCl 10mM pH 7,5, EDTA 1 mM pH 8,0).

1.1.2. COLUMN DNA EXTRACTION PROTOCOL FOR BLOOD

The DNA was extracted from small volumes of blood using the QIAamp DNA Blood Midi Kit® (QIAGEN). A starting volume of 0.3 to 2 ml of blood was adjusted to a final volume of 1 or 2 ml with 0.9% NaCl followed by lysis and proteinase K treatment. Purification was performed by the column system provided according to the manufacturer's spin protocol. After two wash steps, double elution was performed for maximum concentration yield of DNA in a final volume of 200 to 300 μL.

All DNA samples were subject to spectrophotometry, using NanoDrop technology (see below, section 1.3. Measurement of nucleic acid concentration). The DNA samples were diluted to a working concentration of 200 ng/μl in TE buffer and stored at -20°C until required.

1.2. RNA EXTRACTION

1.2.1. EXTRACTION OF TOTAL RNA

RNA procedures were carried out in a ribonuclease- free area. Surfaces were wiped with water and ethanol and pipette tips and microcentrifuge tubes were autoclaved. Solutions were made with DEPC water and equipment and reagents were kept separately, to avoid ribonuclease digestion.

A maximum of 100 mg of placental tissue was placed in 1ml TRIzol® (Invitrogen), containing phenol and guanidine isothiocyanate, homogenized and extracted according to the manufacturer´s protocol. Briefly, after incubation at room temperature for 5 minutes, 200 µl of chloroform were added to the sample and mixed by shaking. This mixture was then incubated for 5 minutes at room temperature and centrifuged at 4°C for 15 minutes at 12,000 rpm; the aqueous phase was removed and the RNA precipitated in 0.8 volumes of isopropanol for 10 minutes at room temperature. The sample was centrifuged at 12,000 rpm for 1 hour at 4°C, and the resulting pellet was washed in 70% ethanol and allowed to air-dry. The pellet was resuspended in 180µl TE.

Total RNA was then subjected to DNAse treatment to remove possible contaminating DNA using TURBO DNase (Ambion). This involved adding 20µl of reaction buffer and 2µl enzyme and incubating at 37°C for 30 minutes. The enzyme was inactivated and eliminated from the samples by TRIzol®-chloroform treatment. The precipitated RNA pellet was washed in 70% ethanol and subsequently resuspended in 25 µl of 1mM EDTA. RNA concentration was measured by NanoDrop spectrophotometry (see below, section 1.3. Measurement of nucleic acid concentration) and stored at -80°C until required.

1.2.2. GENERATION OF cDNA

A second DNase step (DNase I, Invitrogen) was undertaken to ensure complete absence of DNA contamination, following manufacturer's recommendations. The reaction was inactivated by the addition of 1 µL of 25mM EDTA (pH 8,0) and heating for 10 minutes at 65°C. One µg of total RNA per sample served as template to generate cDNA. After an initial incubation at 70°C to remove any RNA secondary structure, a mix consisting of 1 µl MMLV reverse transcriptase with 4 µl of reverse transcriptase buffer (Promega), 1 µl random hexanucleotide primers (Promega), 2µL of 100nM nucleotides, 0.25 µl of RNAase inhibitor (RNasin, Promega) and 2 µl of DEPC water was added to each sample and incubated for 90 minutes at 37 °C.

The reaction was terminated by denaturation of the enzyme at 75°C for 5 minutes. For each RNA sample, a duplicated set of reactions was performed without MMLV to serve as an RT negative control to rule out genomic DNA contamination. All cDNAs were subjected to RT-PCR using a multiplex reaction amplifying both GAPDH and β-actin housekeeping genes. The

resulting amplicons were designed to span at least and intron and they had a size of 850 bp and 150 bp respectively, to assess efficient RNA coversion and integrity. cDNAs with prominent bands were deemed efficiently converted and were either immediately used or stored at -20°C until required.

1.3. MEASUREMENT OF NUCLEIC ACID CONCENTRATION

Determination of the resulting concentration of nucleic acids after extraction was carried out by spectrophotometry, analysing absorbance at 260nm (A260). The spectrophotometric measurements were carried out either in a DNA/RNA spectrophotometer calculator (Gene Quant II, Pharmacia Biotech), or directly in a NanoDrop® ND-1000 espectrophotometer (NanoDrop Technologies, Inc).

The ratio between the readings at different wavelengths serves as an estimate for the purity of the sample. Pure DNAs had a ratio of approximately 1.8, whereas for RNAs the values were approximately 2.0.

2. PCR PROTOCOLS

2.1. POLYMERASE CHAIN REACTION (PCR)

Polymerase Chain Reaction (PCR) protocols were used for amplification of target DNA or cDNA sequences. Oligonucleotide primers flanking the fragment of interest were designed and checked against databases to ensure specificity (see Appendix for sequences and conditions). Oligonucleotides were supplied by Invitrogen (UK) and Sigma (Spain) and amplification was carried out with Biotaq® DNA polymerase (Bioline) or Hotstart Taq® DNA polymerase (Qiagen). A non-template control (blank) was included in all experiments to check for contamination. PCR cycling consisted of a first denaturation step of 94°C for 5 minutes, followed by repetitive cycles of denaturing (94°, 30 seconds), annealing (annealing temperature, 30 seconds) and extension (72°C, 30 seconds). For each pair of primers, the optimal annealing temperature was experimentally determined by performing a temperature profile and the highest possible temperature selected to ensure specificity. Successful amplification was tested by running an aliquot of the PCR reaction products on an agarose gel.

2.2. AGAROSE GEL ELECTROPHORESIS

Agarose gels were used to check for correct product size, quantity and reaction specificity after PCR amplification or after digestion of DNA with restriction enzymes. The gels were prepared by adding agarose to 1x TAE buffer (Tris-Acetate: 40 mM Tris-Acetate, 1 mM EDTA, pH 8.0) and heating in a microwave oven. A standard concentration of 1.5% was used, while higher percentages were reserved for separation of small or closely sized fragments.

The mixture was left to cool slightly and an intercalating dye (either ethidium bromide, final concentration of 0.5 mg/ml or SYBR® Safe, Invitrogen, 1:10.000 final dilution) was added to allow detection of DNA under UV light.

Orange G dye or commercial loading dye was added to all samples at 1/6 volume before loading in the precast wells. Electrophoresis was then used to separate DNA fragments depending on their charge, size and conformation. The samples were run in horizontal electrophoresis devices (H15 Standard tanks, Scie-Plas Ltd and PowerPac Basic Bio Rad power

supply) until the loading dye was two thirds from the wells. Sizes were estimated by comparing with known size standards (100 bp or 1 kb, Promega).

2.3. DYE TERMINATOR CYCLE SEQUENCING

Prior to direct sequencing, unincorporated primers, excess dNTPs and salts from the PCR reactions were removed from the sequencing templates either by the addition of an equal volume of Microclean (Mircozone Ltd) or by standard DNA precipitation with x2.5 volumes ethanol and 1/10 volume 3M Sodium acetate. Samples were centrifuged for 40 minutes at 4000 rpm before removing the supernatant. Pellets were subsequently washed in 200 µl 70% ethanol and centrifuged at 4000 rpm for 10 minutes before decanting the 70% ethanol. After air-drying the pellets, the PCR products were re-suspended in 10 µl of water.

In a 10µl sequencing reaction, approximately 10ng of PCR product was used as a template and mixed with 20 ng of primer and 4 µL of BDT3 (Applied Biosystems) mix. The reactions were carried out in a thermocycler (2720 Thermal Cycler, Applied Biosystems) with heated lid and consisted of initial denaturation at 96°C for 1 minute, followed by 28 cycles of 96°C for 30 seconds, annealing at 55°C for 15 seconds and extension at 60°C for 4 minutes. Products were precipitated using the ethanol/sodium acetate method described above, re-suspended in 10 µl of formamide and sequenced in an ABI 377 (Applied Biosystems) automated sequencer. The output electronic data were saved and analyzed using the Sequencher® computer software.

3. ASSESSMENT OF DNA METHYLATION

3.1. SODIUM BISULFITE TREATMENT OF DNA

Sodium bisulfite treatment of DNA converts all unmethylated cytosine residues, but not methylated ones, to uracil, and can therefore be used to assess methylation patterns of DNA (see *Figure 6*). Bisulfite treatment was performed adapting the original protocol by Frommer et al., (Clark et al., 1994), or with the protocol recommended with the EZ Gold kit when performed on a 96-well format.
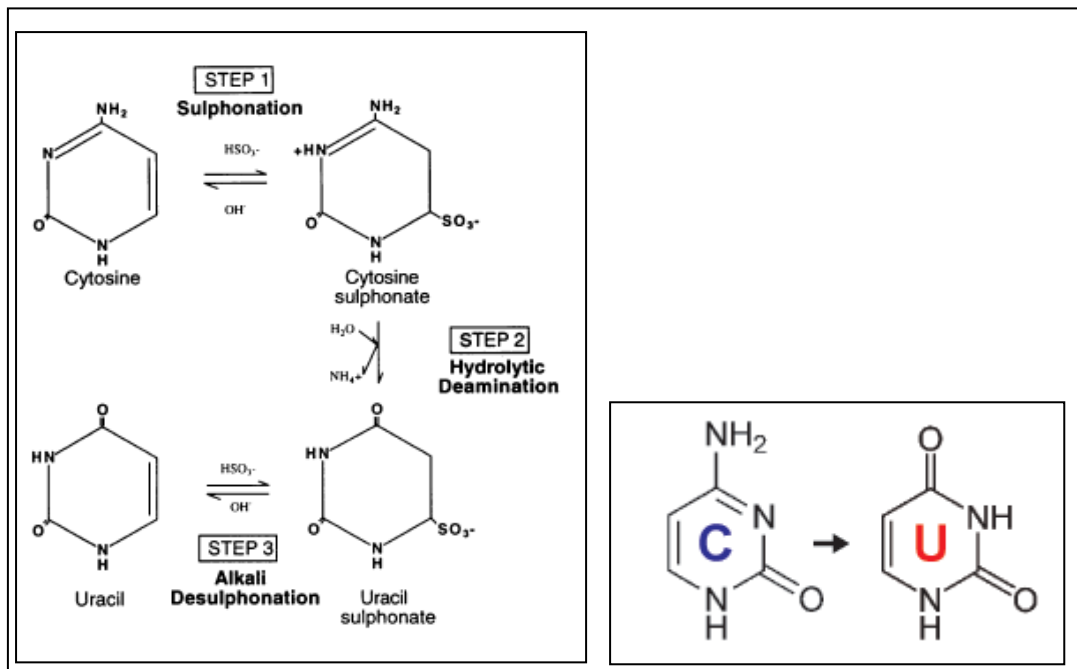
Figure 6: Conversion of unmethylated cytosine to uracil after bisulfite treatment.
Cytosine undergoes sulphonation, hydrolytic deamination and alkali desulphonation to be converted to uracil. From www.zymoresearch.com and Clark et al., 1994.

In the manual protocol, genomic DNA (2 μg) was diluted in distilled water to 50 μl final volume. For denaturation, 5.7 μl of freshly made 3M NaOH was added and incubated for 15 minutes at 37°C. Denatured DNA was then immediately mixed with 33 μl of 20 mM hydroquinone and 530 μl of 3.6M bisulfite . The mixture was incubated for 16 hours at 50°C. Desalting of the treated DNA was performed with the Wizard DNA Clean up system® (Promega) and bound DNA was eluted in 50 μl of water. Desulphonation by addition of 5.7 μl

of freshly prepared 3M NaOH and incubation at 37°C for 15 minutes was followed by neutralisation with 17 µl of ammonium acetate 10M, using glycogen as a carrier. Subsequently, the DNA was precipitated by adding 2.5 volumes of 100% ethanol and incubating at −80 °C for 30 minutes, followed by centrifugation at 12,000 rpm at 4 °C for 30 minutes. The pellet was washed in cold 70% ethanol, air-dried and re-suspended in 30 µl of DEPC water.

Alternatively, bisulfite conversion was achieved using a commercial kit that combines a shorter protocol with the possibility of high-throughput treatment in a 96-well plate format (EZ DNA Methylation-GoldTM Kit® and EZ-96 DNA Methylation-GoldTM® Kit, Zymo Research). For this, 1µg of DNA was added to each well of a conversion plate and incubated with the conversion reagent provided at 98°C for 10 minutes, followed by 64°C for 2.5 hours. Afterwards, the samples were transferred, purified and washed in DNA-binding columns and finally subject to desulphonation, washed and eluted in 30µL of elution buffer following the manufacturer's protocol.

All bisulfite-treated DNA samples were stored at -80°C, minimizing freeze-thaw cycles. A commercial control was used as reference for bisulfite-converted fully methylated DNA when needed (EpiTect Control DNA®, methylated, Qiagen).

3.2. SEQUENCING OF BISULFITE PCR PRODUCTS

The CpG islands associated with the promoters of *PHACTR2*, *SF3B5*, *UTRN* and the non-imprinted isoform of *PLAGL1* P2 were analyzed by bisulphite PCR and sequencing. Bisulphite PCR requires specific conditions for primer design:

− Sequences should be complementary to the expected converted sequences, minimizing the content of any potential CpG (C/T) (highlighted by Y or R), so that they have a higher G content.

− Due to expected DNA degradation during the treatment, the PCRs amplification is aimed at shorter fragments.

To allow individual analysis of DNA molecules, the PCR products were ligated into vectors, cloned into competent cells and sequenced as outlined below. A methylated cytosine will remain a cytosine in the converted sequence, while unmethylated cytosines will be converted to uracils and subsequently replaced with thymidines in the PCR reaction.

Ligation reaction

One microlitre of the PCR product was ligated into pGEM®-T-Easy vectors (Promega) with the provided T4 ligase. Ligation reactions contained 1x buffer, the bisulphite PCR product, 50 ng pGEM®-T-Easy vector and 1 unit T4 DNA ligase in a total volume of 10 µl. Reactions were incubated overnight at 4°C.

Transformation

Commercial JM109 competent cells (Promega) were used for cloning of the PCR products obtained from bisulphite treated cloned DNA. Approximately 50µl of competent cells were carefully mixed with 5µl of the ligation and incubated on ice for 30 minutes, followed by 45 seconds at 42°C and quenching on ice for 2 minutes. SOC medium (950 µL) was added to the cells previous to incubation for one hour at 37°C with shaking. The cells were then spread onto agar plates containing 50µg/ml of ampicilin, 40µg/ml X-gal and 50µg/ml IPTG, and incubated overnight at 37°C.

JM109 cells lack β-galactosidase activity and, since the pGEM®-T-Easy vectors contain an ampicilin-resistance gene as well as a disruptable β-galactosidase gene, the transformed cells can be selected on the basis of acquired antibiotic resistance and blue/white colour selection. The IPTG within the agar plates induces β-galactosidase, which cleaves X-gal to a blue substrate. If the *lac-Z* gene is disrupted by integration of the insert, the colony will remain white.

PCR amplification of cloned DNA

Individual white colonies were picked from the culture plates and grown in 100µl LB media at 37°C for 2 hours. These bacterial cultures were subjected to PCR, with 2 µl used as a

template to enable the inserted sequences to be amplified using M13 forward and reverse primers present in the vector. The resulting PCR amplicons were directly sequenced. Only PCR products with a conversion efficiency of greater than 95% were assessed. A low level, random distribution of unconverted non-CpG cytosines ensured absence of clonal amplification in the initial PCR reaction (Arnaud et al., 2003).

3.3. COMBINED BISULFITE RESTRICTION ANALYSIS (COBRA)

Combined bisulfite restriction analysis (COBRA) was used to assess methylation patterns and to ensure that there was no cloning bias prior to sequencing or pyrosequencing. Each bisulphite sequencing experiment was designed so that restriction enzyme sites would be incorporated in the PCR products that could differentiate methylated and unmethylated sequences. Using restriction enzymes that contained CpG in their recognition sequence, the presence of preserved cytosines (methylated CpG dinucleotides) or converted thymidines (unmethylated CpG dinucleotides) could be discriminated by digestion of the resulting PCR product (see *Table 4*). PCR products that contained unmethylated CpGs would remain uncut, while the methylated CpGs would be digested.

Table 4. Restriction enzymes commonly used for Combined Bisulfite Restriction Analysis (COBRA).
The table displays the particular sequence cut by each enzyme (restriction site) and the reaction conditions. Selective conversion of unmethylated cytosines explains why differential cutting takes place, identifyng the methylation status of the original sequence.

Enzyme	Restriction site	Sequence in methylated DNA	Sequence in unmethylated DNA	Digestion conditions
*HpyCH4=Tai*1	A/CGT	ACGT- cut	ATGT-uncut	37°C, >1h
*BstU*I	CG/CG	CGCG- cut	TGTG-uncut	60°C, >1h
*Taq*1	T/CGA	TCGA- cut	TTGA-uncut	65°C, >1h

3.4. PYROSEQUENCING

Pyrosequencing was selected for the quantitative assessment of DNA methylation at the *PLAGL1* P1 DMR. Pyrosequencing is a sequencing-by-synthesis technique that allows quantification of the relative abundance of a nucleotide in a specified position due to the generation of a bioluminometric signal that is proportional to the amount of nucleotide added. This method has been shown to be useful for the analysis of DNA methylation patterns (Tost and Gut, 2007).
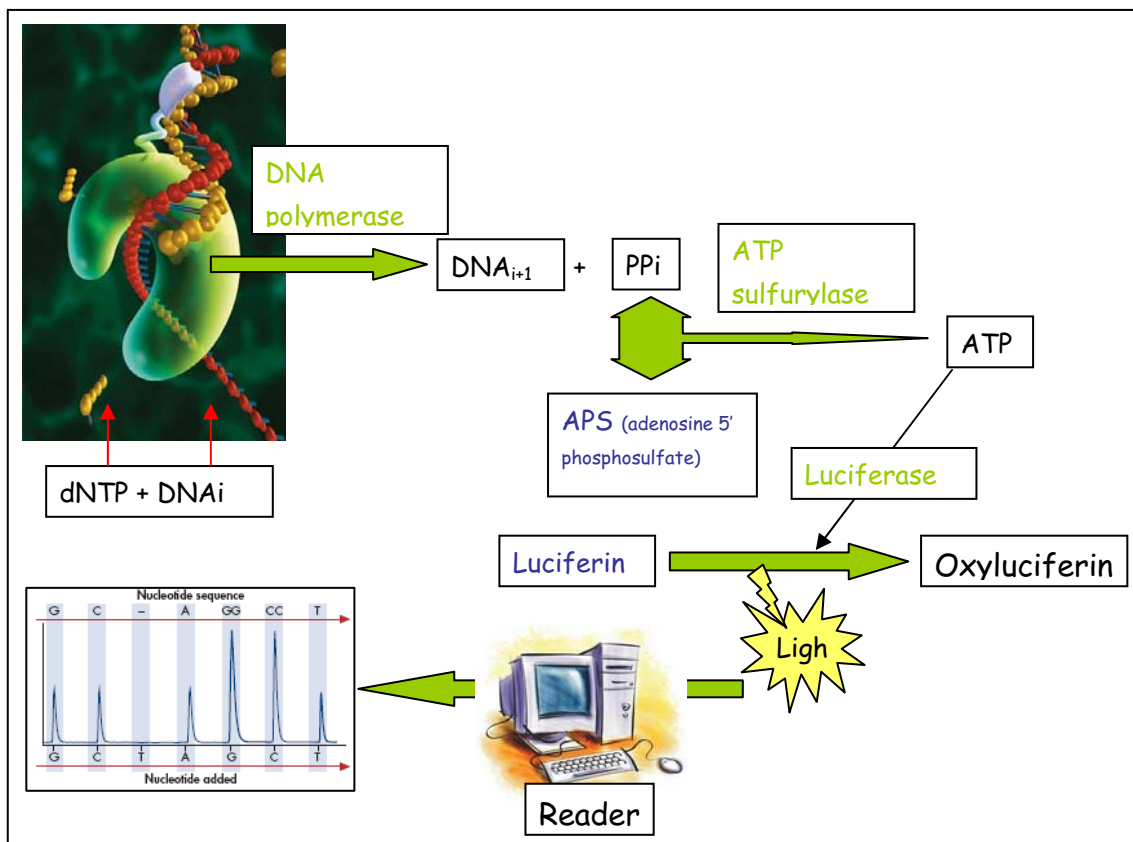
Figure 7: Principles of pyrosequencing.
The reaction mix contains four enzymes (in green: DNA polymerase, ATP sulfurylase, luciferase and apirase) and two substrates (in blue: adenosine 5'phosphosulfate- APS- and luciferin), plus the single-stranded PCR product that will serve as a template. Each one of the four nucleotides is added sequentially, so that only one of them is present at any given time. If it is complementary to the template, it will be incorporated by the DNA polymerase, releasing one molecule of pyrophosphate (PPi). This will be, in turn, transformed to ATP in the presence of ATP sulfurylase and APS. The energy of the ATP will be subsequently used by the luciferase to transform luciferin into oxiluciferin, which results in the generation of a photon. All remaining free nucleotides and ATP will be degraded by the apyrase. This way, the amount of light generated is proportionate to the nucleotide incorporation and is detected by a charge-coupled device and transformed in a graphic reading.
(http://www.pyrosequencing.com/DynPage.aspx?id=7454).

Prior to pyrosequencing, bisulfite PCR was performed as described above with the exception that the reverse primer was biotin-labelled. Immobilization of the PCR products for purification is achieved by adding streptavidin-coated sepharose beads (2 μL/sample) and binding buffer (40 μL/sample) (Qiagen), which capture the biotin molecules. After this, the PCR plate is agitated at 1400 rpm for 10 minutes at room temperature using a shaker. Further steps involve the use of the PyroMark Q24 Vacuum Prep Workstation® according to the manufacturer´s instructions for purification of samples. With the aid of the vacuum tool, the biotin-labelled DNA strands contained in each well are immobilized in a single pin of the device. The pins are then sequentially introduced in the troughs, which results in exposure of the DNA to 70% ethanol (5 seconds), denaturation solution (5 seconds) and wash buffer (10 seconds). Finally, the PCR products are dried and deposited in a fresh plate containing 25 μL of PyroMark Annealing Buffer (Qiagen) per well plus the sequencing primer. The plate is then heated to 80°C for 2 minutes and, after cooling to room temperature, is ready to undergo pyrosequencing. Internal primers were used for specific sequencing of the *PLAGL1* DMR.

3.5. METHYLATION ARRAY

After bisulfite treatment, the DNA samples were analysed with the HumanMethylation27 BeadChip® (www.illumina.com). This commercial array gives a quantitative methylation measure at the single CpG level for 27,578 CpG loci covering more than 14,000 genes, including the CpG islands associated with the promoters of *DEADC1/ADAT2*, *PEX3*, *FUCA2*, *LTV1* and *STX11*, all of them mapping within the 6q24.2 region.

The assay detects methylation by using two site-specific probes for each loci, one for the methylated (M bead type) and one for the unmethylated locus (U bead type). The probes are marked by single-base extension incorporating a labelled dNTP, which is then stained with a fluorescence reagent. The ratio of the fluorescent signals from the methylated *versus* the sum of methylated and unmethylated probes is calculated by the plate reader (see *Figure 8*).

The hybridization of the arrays was performed by CEGEN (Centro Nacional de Genotipado, National Center for Genotyping) at the CNIO (Centro Nacional de Investigaciones Oncológicas, Nacional Center for Oncologic Research). Briefly, 1μg of genomic DNA for each sample was converted by bisulfite treatment, subject to whole genome amplification (WGA)

and enzymatic fragmentation. After purification, the fragments were applied to the Bead Chips and analyzed in the array.
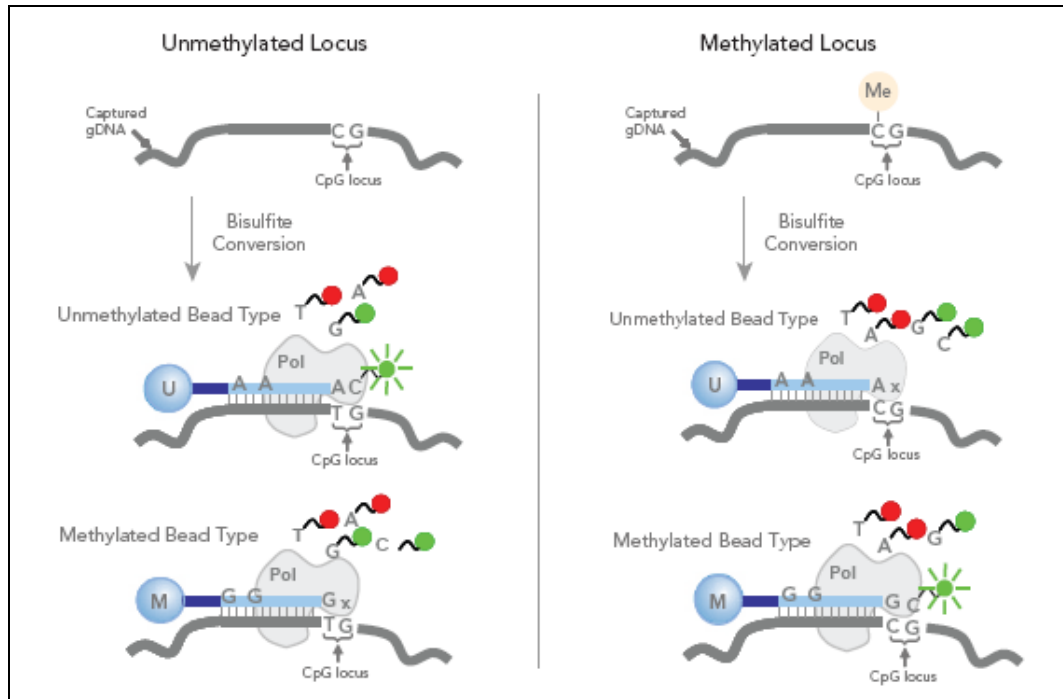
Figure 8: Representation of the principles underlying methylation arrays.
The bisulfite-converted, whole-genome amplified, enzymatically-fragmented genomic DNA is applied to the array probes. The converted methylated (right panel) or unmethylated (left panel) fragments anneal to their specific complementary sequence in the array, triggering a polymerization reaction which adds one nucleotide and produces fluorescent signal that is then read and computerized.
(http://www.servicexs.com/blobs/Illumina/HumanMethylation27_Datasheet.pdf)

4. ASSESSMENT OF EXPRESSION

4.1. ASSESSMENT OF IMPRINTED EXPRESSION

Single Nucleotide Polymorphism (SNP) analysis was performed to determine allelic expression of the transcripts of interest. SNPs within the coding sequence of the corresponding gene were identified through database search (see *Table 5*). PCR primers were designed to incorporate highly polymorphic SNPs within the amplicons. All placental and fetal DNA samples were genotyped to identify heterozygous individuals.

Expression was then analyzed in heterozygous samples by RT-PCR and sequencing of the products. A heterozygous SNP reading from the cDNA is indicative of biallelic, non-imprinted expression. Imprinting was suggested only if a single base peak was observed at the SNP site in the RT-PCR product of a heterozygous sample. In these samples, the parental origin of expression was determined by assessing parental genotypes.

Primers for RT-PCR were located in different exons, so that the PCR product crossed a splice site whenever possible. Otherwise, RT-PCR was performed on RT-positive and negative samples in order to rule out genomic contamination.

Table 5: Single Nucleotide Polymorphisms (SNPs) used for the study of the allelic expression of the genes in the human 6q24.2 region.
Av. Het: average heterozygosity.

Gene/Sequence	SNP	Sequence	Av. Het
PEX3 (NM_003630)	rs223234	TTTTGTATTTA/TTATATATATA	0,420
DEADC1/ADAT2 (NM_182503)	rs1065355	CCAGTCCAGGA/CAAGTGCTGAC	0,327
PHACTR2 (NM_001100164)	rs1082	AAAAACTTGA/CATCCAAAGTCA	0,464
	rs2073215	AAACACGACCC/AGAGAGGCTGG	0,359
FUCA2 (NM_032020)	rs3762002	CAGGACCCCAT/CTTGCCTCAGT	0,348
BC033369	rs4142502	TTATTAGCCAT/CTTGCATTTTC	0,377
LTV1 (NM_032860)	rs7454959	CAGAATTGGAA/GGGTTCTATTC	0,066

Gene/Sequence	SNP	Sequence	Av. Het
SF3B5 (NM_031287)	rs7744101	AGGAGAGTGAA/CGCCACCGCGC	0,103
STX11 (NM_003764)	rs3734228	GGCAGAGCTCC/TCGGCTTTGGT	0,262
UTRN (NM_007124)	rs4895642	CAGACGAAGAA/GGAATTTGAGA	0,500
PLAGL1 (NM_006718, NM_001080951, AJ006354, AK091707)	rs2076684	TTACCTTTCTGC/GTCCTGAATCG	0,372
HYMAI (NR_002768)	rs2281476	GTGGACCTCAT/CACCAGATAGG	0,321

4.2. ASSESSMENT OF LEVELS OF EXPRESSION BY RNA LEVELS

Levels of expression of the transcripts of interest were analyzed by Real-Time PCR using a fluorochrome (SYBR-Green®) technique and specific primer sequences. Real-Time PCR allows for quantification of the amount of specific nucleic acids in the starting sample. The reactions were set up in 11 μL total volume with 5,5 μL of SYBR Green PCR Master Mix, 0,25 μL of the forward and reverse primers at optimal concentration and 6 μL of diluted cDNA. After assessment of several housekeeping genes, the ribosomal gene *RPL19* was selected as the most stable internal control for placental tissue. Assays were carried out in triplicates and no-template controls, inter-plate controls and standard curves were included in each plate.

The reactions were carried out in a 7900HT Fast Real Time PCR System (Applied Biosystems) and the expression analysed with the SDS 2.3 software. Amplification plots and automatic baseline and threshold values were individually checked and adjusted where necessary according to guidelines (Nolan, Hands and Bustin, 2006). The DataAssist v2.0® software (Applied Biosystems) was used for exclusion of outlier replicates and for interplate comparisons. Only samples with two or more valid readings per triplicate were included. Analysis of the results was performed using the comparative ΔΔCT method (Schmittgen and Livak, 2008), normalized to an internal control gene and corrected for efficiency for each pair of primers whenever necessary to allow for comparison between the levels of different transcripts.

5. STATISTICAL ANALYSIS

Clinical and molecular data were introduced in a Statistical Package for Social Sciences (SPSS®, IBM) software v17.0 database. Comparisons between groups were evaluated with chi-square for categorical variables and t-Student test (for two groups) or ANOVA (more than two groups) for continuous variables. When the groups were small or the variables did not follow a normal distribution, non-parametric tests were applied (Fisher´s exact, Mann-Whitney U and Kruskal-Wallis, respectively).

Relationships between variables were explored by Pearson´s correlation and subsequently introduced in multiple regression models to adjust for possible interactions or confounding factors. Results were considered significant if the p value was under 0.05; values under 0.1 were considered as a trend.

RESULTS

RESULTS

1. DEFINING THE EXTENT OF THE IMPRINTED DOMAIN ON HUMAN CHROMOSOME 6q24.

Transient Neonatal Diabetes Mellitus (TNDM1) is caused by an imprinting or epigenetic defect. The most common cause is pUPD6 and paternally inherited duplications that span a candidate region of 440kb. To date, the only imprinted transcripts mapping to this interval are *PLAGL1/LOT1/ZAC1* and *HYMAI*.

Most imprinted genes associate in clusters containing multiple transcripts under the coordinate regulation of a single Imprinting Control Region (ICR), which in this case is likely to be the *PLAGL1* DMR.

In order to delineate the boundaries of the imprinted domain, we analyzed methylation profiles and allelic expression of the neighbouring genes in numerous human fetal tissues.

1.1. *PLAGL1/HYMAI* DMR IS THE ONLY DIFFERENTIALY METHYLATED REGION IN 6q24.2

The methylation status of the promoter-associated CpG islands in 6q24.2 (see *Table 6*) (*DEADC1/ADAT2*, *FUCA2*, *PHACTR2*, *LTV1*, *PLAGL1* P1 and P2, *SF3B5*, *STX11*, *UTRN*) was assessed for any pattern indicative of differential methylation suggestive of an imprinted DMR.

Table 6: Features of promoter-associated CpG islands in the 6q24.2 region.
CpG count: number of CG dinucleotides in the island. Percentage CpG: ratio of C or G nucleotide bases (twice the CpG count) to the length (www.ucsc.edu).

Gene	CpG Count	Size	C Count + G Count	% CpG	% C or G
DEADC1/ADAT2 & PEX3	47	474	307	19.8	64.8
FUCA2	52	554	356	18.8	64.3
PHACTR2	43	513	283	16.8	55.2
LTV1	62	728	463	17.0	63.6
PLAGL1 P1 & HYMAI	118	931	689	25.3	74.0
PLAGL1 P2	113	994	709	22.7	71.3
SF3B5	51	635	374	16.1	58.9
STX11	106	948	673	22.4	71.0
UTRN	190	2354	1497	16.1	63.6

Methylation levels were assessed in nine normal placental samples and a set of human tissues using the Illumina Infinium® Methylation array, which simultaneously quantifies the methylation of 27,000 CpG sites associated with 14,000 genes. Eighteen probes on the array were found to map within seven of the eleven promoter-associated CpG islands in the region (see *Table 7* and *Figure 9*).

Table 7: Relative levels of methylation (β) for the analyzed CpG islands in the HumanMethylation27 BeadChip ® array.
β is calculated as the ratio of methylated-probe signal to total locus signal intensity and expressed as a percentage.CpGI: CpG island.

Target ID	Gene	CpG position	β (%)	Probe sequence
cg21684385	*PEX3*	100bp from CpGI	1.4	CGCCACAAAAAGAAATGCATCTTCCTG GGCACGGTCCTTGGAGGTGGGTG
cg08286169	*PEX3*	CpGI	2.2	GACTGTCACCGGAGCGGCAAGGGGG CGTGGACTACAGCAAAGCAGCTACG
cg18540871	*FUCA2*	End of CpGI	4.6	TGGCCTTAGTTATGCTGAGCGATGCAG CCCTCCTGAGGTCATTCGGAACG
cg00380464	*LTV1*	CpGI	11.0	AGTAGCCAAGGTATTACCGGAAGCAG CCTGGCCTCTGCAAAACCACAGCG
cg02885771	*LTV1*	500bp from CpGI	60.5	CGGCATAAAGACACAATCCAGGGTAA GCCATTCATTGAGAGGTCACCAGA
cg17181653	*SF3B5*	1kb from CpGI	66.2	TCTTTTATGCCACAAACTCCTAAGAGA CATAGTTGGGACCAGAACTGGCG
cg17895149	*PLAGL1*	CpGI/HYMAI promoter	62.1	CGCGACAGATGCTGGGACGCTGCAAT AGGCCAAACTAACTTACCTCCTGT
cg22378065	*PLAGL1*	CpGI	73.2	CGGCCACCGCTGCCCCCAGCCCGCCC GCCGCAGCCGCGAGCACCCAAACA
cg25350411	*PLAGL1*	CpGI	43.5	CGGGCCAGGAAAAAAACAGAACAAGG AAAAGAAGAAAAAGTCTGTTCCAA
cg00702231	*PLAGL1*	CpGI	80.	CGGCATCTGCCATTTGTCATTCAGCCC GTCGGTACCGCCCCGAGCCTTGA
cg07077459	*PLAGL1*	CpGI	83.1	CGTCACCCGCAACCCAGGCAGCCCCA CCGCGAGTGCCGCCGGACCCCCTG
cg08263357	*PLAGL1*	CpGI	79.0	GTTTCTCATGTGTGATTGGGCTCTGGC GGCCCATCCTGGCGGAGACTTCG
cg12757684	*PLAGL1*	CpGI	69.0	GCGGTACCGACGGGCTGAATGACAAA TGGCAGATGCCGTGGGCTTTGCCG
cg14161241	*PLAGL1*	100bp from CpGI	36.4	CGTGAGCACTGACCGTGAGCCAGGCA CTGTCCTAAGCACTTTGCAGGTAA
cg07755653	*STX11*	CpGI	2.2	GGTTGGTCGGCAGGGTTCTGGGAAGG CGGTGCTCGGCCTCCGTGTGACCG
cg11070941	*STX11*	CpGI	2.0	CGCCAGATCCAAAATCCCACCTAAGGC ACAGCCGCGGGTCCCGAGCCTAG
cg10784341	*PHACTR2*	TSS-no CpGI	47.0	CCTTGCTGGCACACTGAGCATACTTCA TGCACTGTCTGCAGGAGACACCG
cg19205041	*PHACTR2*	Intron 1-no CpGI	47.3	CGGGCTGCAAAGGAAGCCAGCAGCTA TGAAGAATTCATGCTTGATTTACC

*DEADC1/ADAT2 share the same CpG as PEX3.

The CpGs associated to *PEX3-DEADC1/ADAT2*, *FUCA2* and *STX11* displayed less than 5% of average methylation, as determined by the β score from the BeadStudio® software (a value of 0% is unmethylated, whereas 100% is fully methylated). This was also the case for the *LTV1*-associated CpG probe cg00380464 (11.0% average methylation), although probe

cg02885771 gave a partial methylation score (60.5%). The discordant result between the two probes for this gene is due to their location, one within the body of the CpG island and the other 500bp away within the CpG shore. The score for the *PLAGL1/HYMAI* promoter CpG encompassing the DMR was on average approximately 70% of methylation when considering the probes within the limits of this CpG island. This methylation was considered allelic because of the hypermethylation in a genome-wide maternal UPD sample and relative hypomethylation in 3 paternal genome-wide UPD samples (UPD samples, kind gift from Lapunzina, Monk and Nakabayashi). Methylation values for *SF3B5* and *PHACTR2* were high, but further analysis showed that the regions tested in the array correspond to the body of the genes and not the promoter CpG islands.
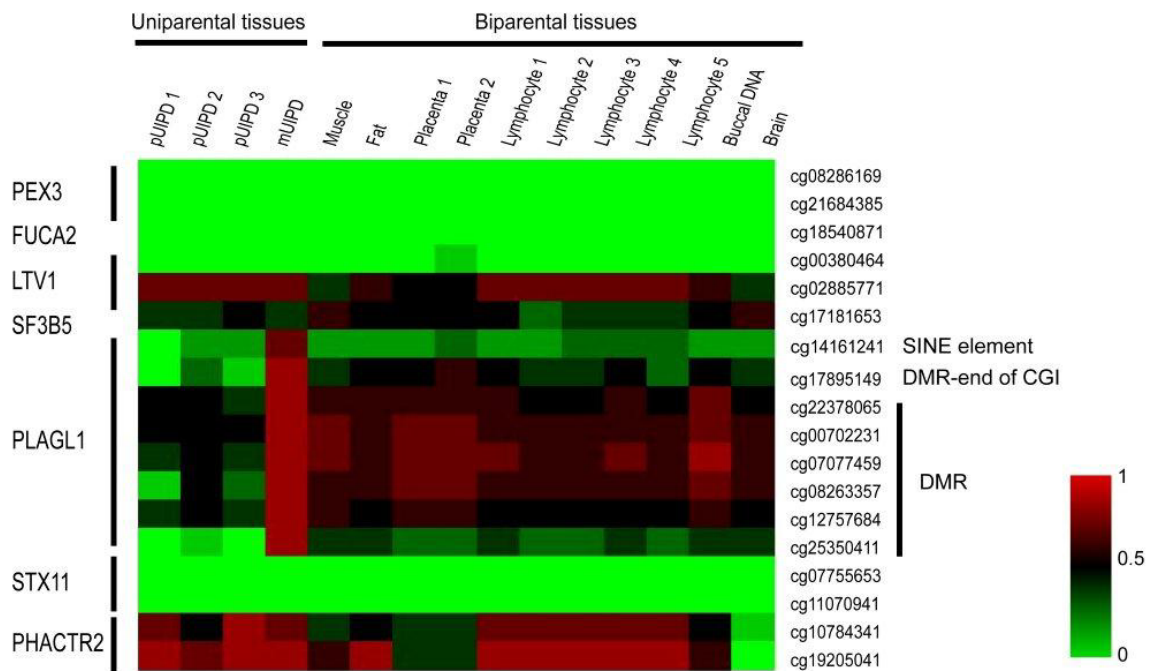
Figure 9: Heatmap representation of the methylation data of the CpG islands in 6q24.
The horizontal axis represents the different individual tissue samples. pUPD: genome-wide paternal UPD samples. mUPD: genome-wide maternal UPD. The vertical axis on the right represents the probe numbers, highlighting the ones corresponding to the PLAGL1 *DMR. The left axis details the names of the genes where each probe maps. Colour-coding: green represents complete lack of methylation, red represents a fully methylated sample.*

To determine the true methylation of *SF3B5* and *PHACTR2* CpG islands, we performed bisulfite PCR and sequencing of the corresponding regions. These revealed that both were extensively unmethylated in placenta and lymphocyte DNA. The remaining two promoter-

associated CpG islands in the region, *UTRN* and the non-imprinted *PLAGL1* isoform (P2), were also analyzed by the same technique. Both were found to be unmethylated (see *Figure 10*).
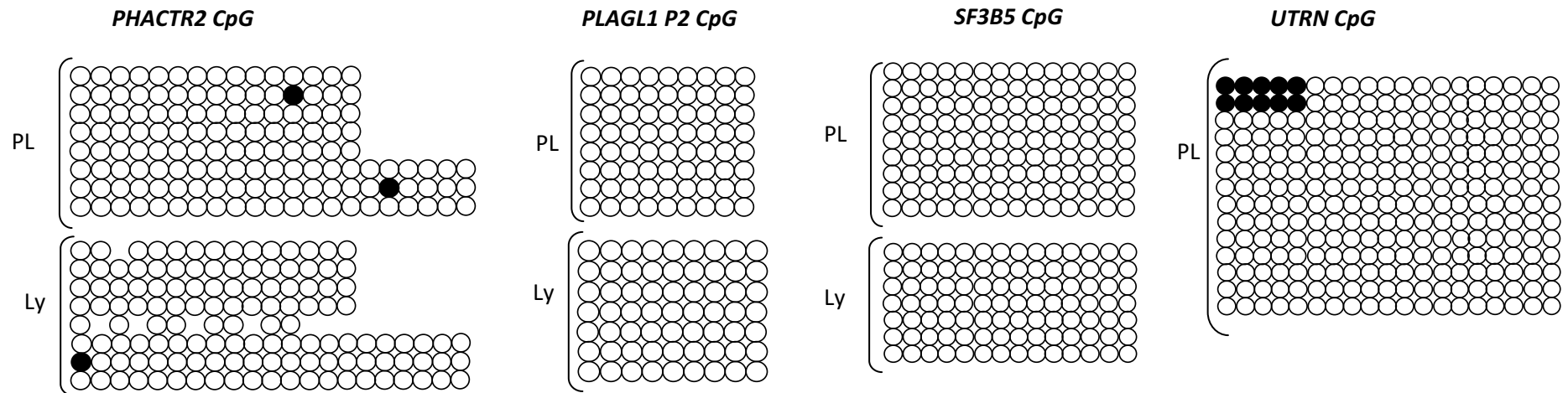
Figure 10: Analysis of the methylation status of PLAGL1 *P2 promoter,* PHACTR2, SF3B5 *and* UTRN *CpG islands by bisulfite conversion, amplification, cloning and sequencing.*

Circles stand for discrete CpG positions and they are coloured white if the cytosine was unmethylated and black if it was methylated Each row of circles represents sequencing of one clone containing an individual DNA molecule. PL: placenta. Ly: lymphocyte.

1.2. THE NEIGHBOURING GENES AROUND *PLAGL1/HYMAI* IN 6q24.2 ARE BIALLELICALY EXPRESSED

Within the 500 kb flanking *PLAGL1/HYMAI* there are 9 additional genes. Allelic expression of *ADAT2/DEADC1*, *FUCA2*, *PHACTR2*, *LTV1*, *SF3B5*, *STX11*, *UTRN* and the Expressed Sequence Tag (EST) *BC033369* was investigated by RT-PCR and SNP analysis on heterozygous first trimester fetal tissues and healthy term placentas. For this purpose, 54 fetal samples and 42 placentas were genotyped for at least one SNP within the coding sequence of the corresponding gene. RT-PCR and sequencing of the products incorporating the heterozygous SNPs was then performed (see *Table 8*) to confirm allelic origin of the transcripts.

All of the neighbouring genes showed biallelic expression in a wide range of fetal and placental tissue samples (see *Figure 11* for details).

Table 8. Summary of the samples used for imprinted expression analysis of the 6q24.2 region. Placentas and fetuses were genotyped for identification of heterozygous individuals, in which subsequent analysis of expression was undertaken in the listed tissues.

Gene	Samples
PEX3	Tissues from 4 fetuses (including 1st trimester placenta and fetal brain, intestine, lung and heart) 3 term placentas
PHACTR2	Tissues from 4 fetuses (including 1st trimester placenta and fetal lung, skin and intestine) 10 term placentas
DEADC1	Tissues from 3 fetuses (including 1st trimester placenta and fetal brain, eye, skin, muscle, intestine, lung and tongue) 3 term placentas
FUCA2	Tissues from 1 fetus (including fetal liver, skin and intestine) 1 term placenta
LTV1	Tissues from 1 fetus (including fetal brain and lung) 1 term placenta
BC033369 (LOC285740)	Tissues from 3 fetuses (including 1st trimester placenta and fetal brain and lung) 4 term placentas
UTRN	Tissues from 4 fetuses (including 1st trimester placenta and fetal brain, intestine, skin, liver, kidney and heart) 2 term placentas

Gene	Samples
SF3B5	Tissues from 2 fetuses (including 1st trimester placenta and fetal brain, spine, kidney, liver and heart)
STX11	Tissues from 4 fetuses (including 1st trimester placenta and fetal brain, heart, intestine, skin, kidney and tongue)
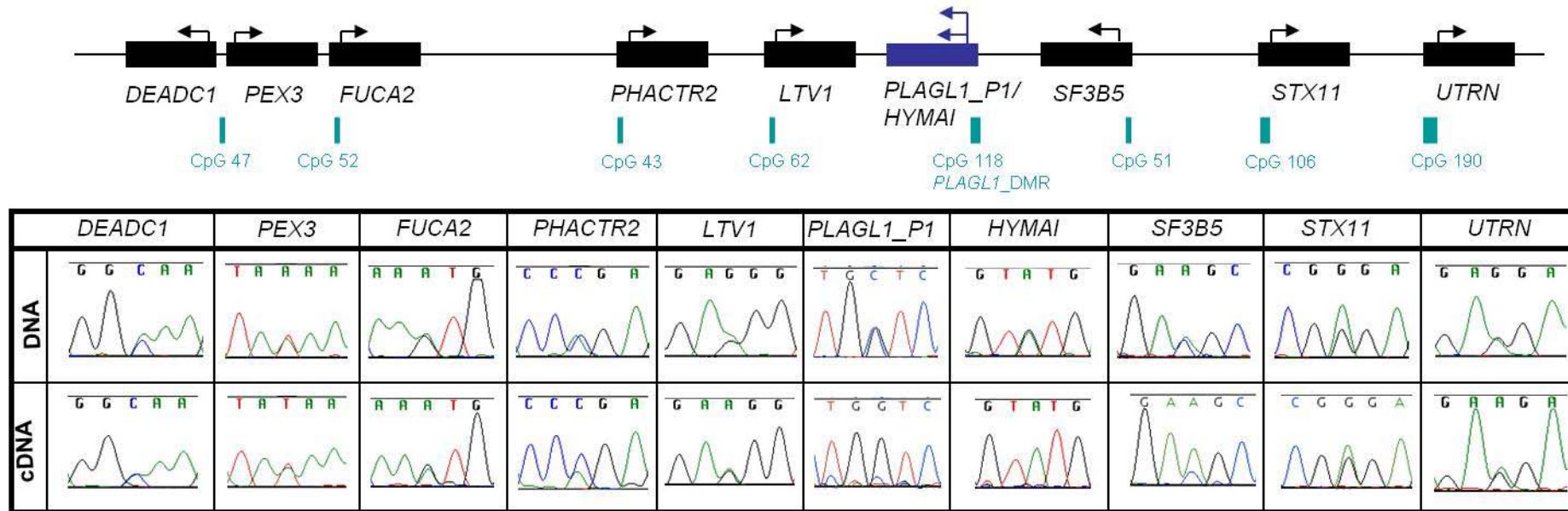
Figure 11: Allelic expression analysis of the genes that surround in the 6q24.2 region.
Bold boxes stand for genes in the region and the arrows indicate the direction of transcription. The green lines represent the relative position of the promoter-associated CpGs. The CpG numbers correspond to the identification numbers in the database, which are determined by the number of CpG dinucleotides (http://genome.ucsc.edu/). The chromatogram shows sequence traces of the analysed genomic DNA (gDNA) obtained from heterozygous placental samples in the upper row, and the corresponding ones from cDNA (complementary DNA) synthesised from RNA from the same samples in the lower row. Expression was biallelic for all genes (represented as black boxes) analyzed.

1.3. IDENTIFICATION OF ADDITIONAL *PLAGL1* TRANSCRIPTS: THE P3 AND P4 ISOFORMS

Imprinted expression of *PLAGL1 P1* was confirmed in fetal tissues (including first trimester placenta) from 4 different heterozygous individuals and in 11 placentas from healthy, term, heterozygous babies. Paternal and maternal genotypes were analyzed wherever possible and all the informative samples confirmed paternal origin of the expression. The same was true for *HYMAI* (as shown in tissues from 7 fetuses and 3 term placentas), which originates in the same DMR- associated promoter (see *Figure 11* and *Figure 12*)

As a result of human EST alignments, we identified two additional *PLAGL1* transcripts, originating from two novel promoter regions that we named P3 and P4. The Open Reading Frame (ORF) of the *PLAGL1* gene is restricted to the last two exons. The novel promoter of *PLAGL1* P3 is located 3kb 5' to the exon 5 donor site. This transcript corresponds to EST AK091707. The novel *PLAGL1* P4 (reference EST AJ006354) originates from a unique promoter region 5' to the exon 6 donor site with a UTR that extends at least 800 bp into the upstream intron. Both of these transcripts include the last exons and therefore incorporate the full-length *PLAGL1* ORF.

Using RT-PCR primers that were isoform-specific and amplified a single transcript, we analyzed the allelic expression of P3 and P4 in 11 heterozygous term placenta samples. Both were found to be monoallelically expressed. Analysis of parental genotypes, when possible, revealed that the expression was solely from the paternal allele (see *Figure 12*). This indicates that the maternal imprinting of *PLAGL1* P1 probably extends to these two newly defined isoforms.
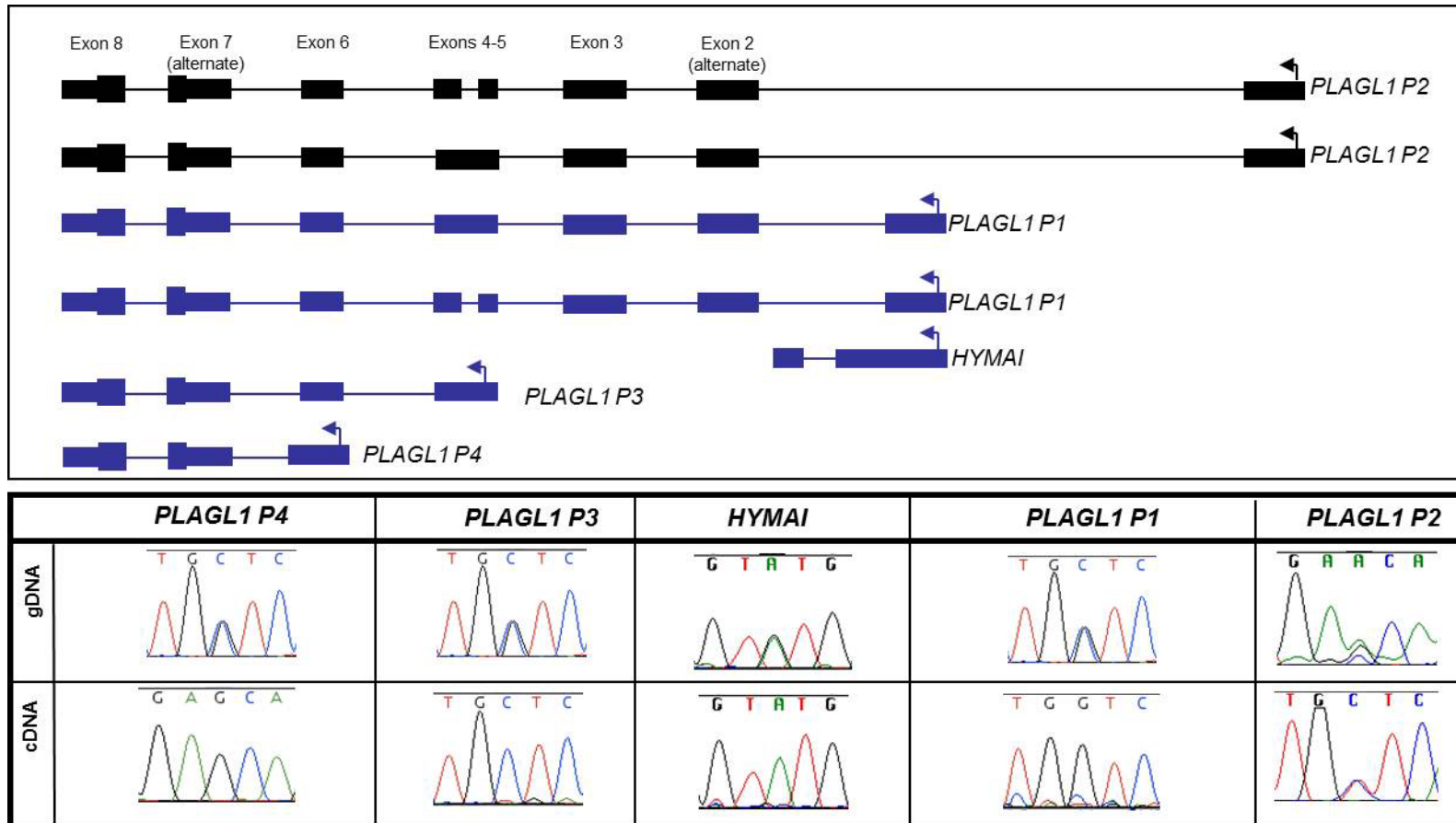
Figure 12: Analysis of allelic expression of the transcripts originated from the different human PLAGL1/HYMAI *promoters.*
Exons are represented by squares, black indicates biallelic expression, blue indicates imprinted expression from the paternal allele, as shown in the corresponding sequence traces in the table below. The areas corresponding to coding sequence are highlighted with a broader square. Allelic expression was studied in human placenta except for the P2 isoform, where the cDNA was obtained from adult blood (sequence traces for P4 cDNA and P2 DNA are in the reverse orientation).

2. EXPRESSION OF THE 6q24 IMPRINTED TRANSCRIPTS IN FETAL GROWTH

2.1. THE DIFFERENT ISOFORMS OF *PLAGL1* AND THE NON-CODING RNA *HYMAI* ARE EXPRESSED IN FETAL TISSUES AND IN THE PLACENTA THROUGHOUT GESTATION

To determine the expression profile of *PLAGL1* and *HYMAI* we performed quantitative RT-PCR in various first trimester human fetal tissues. Primers were designed to amplify small fragments of approximately 100bp. Individual *PLAGL1* isoforms had separate primers that could discriminate each transcript, with forward primers located in the unique 5'UTRs. All primers were designed to cross intron/exon splice sites and reactions were optimized using SYBR amplification followed by melt curve analysis to ensure amplicons were free of primer dimer products. In the case of P1, melt curve analysis revealed two products, which were interpreted as representative of amplicons containing the alternative second exon or not (*Figure 13*). Subsequent cloning and sequencing of the PCR products confirmed the presence of alternatively spliced transcripts.
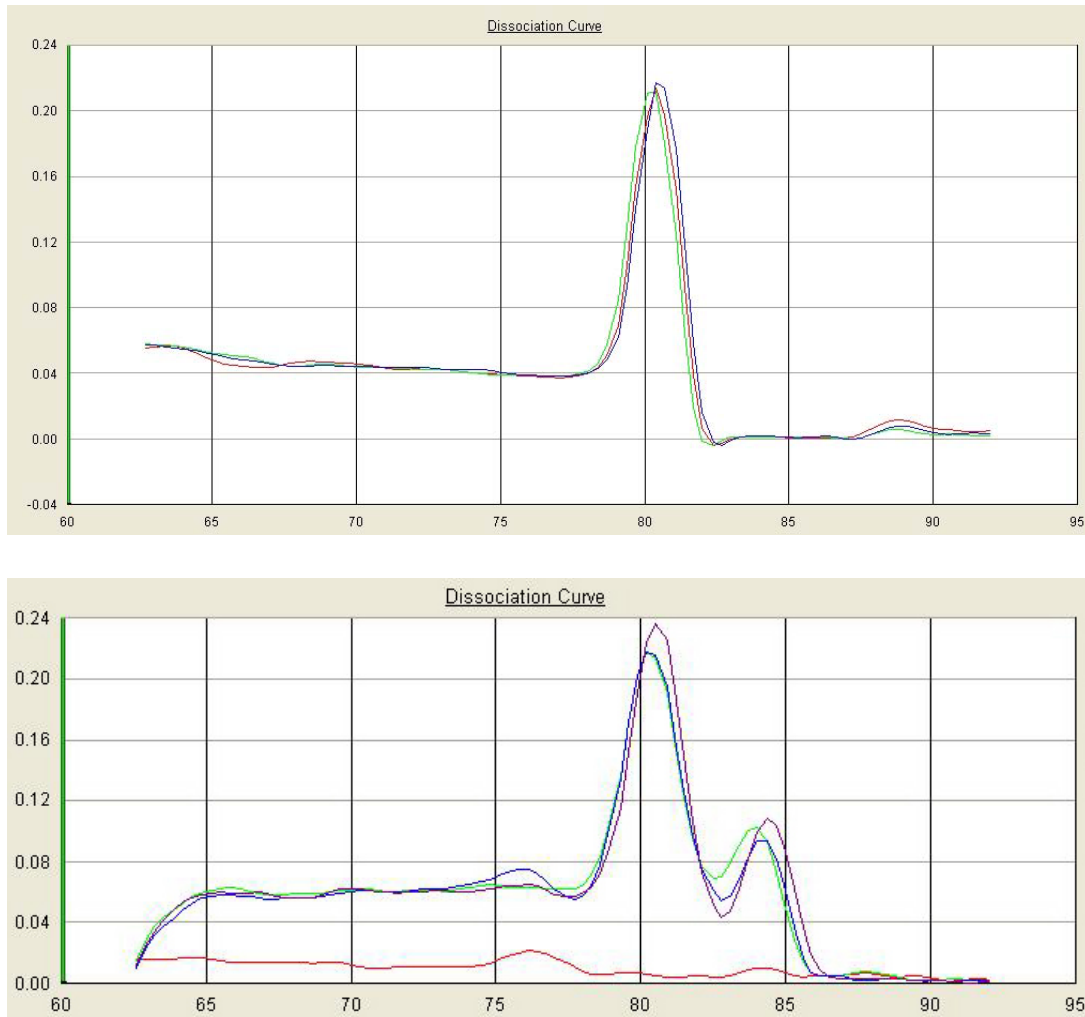
Figure 13: Dissociation curves of the PLAGL1 *reactions amplifying a fragment common to all isoforms ("*PLAGL1_All isoforms"*, upper panel) and a fragment specific to the imprinted isoform ("*PLAGL1_P1"*, lower panel).*
The two fluorescence peaks in the second case are due to alternative splicing and amplification of isoforms containing or not an alternative second exon of 40 bp, as confirmed by fragment cloning, amplification and sequencing.

2.1.1. SELECTION OF APPROPRIATE INTERNAL CONTROL GENES FOR qRT-PCR

Quantitative real time PCR (qRT-PCR) was carried out with commonly used housekeeping genes in order to identify the most suitable candidates for the comparison of gene expression across several developmental stages in tissues. We analyzed *GAPDH*, *β-ACTIN*, *GUS3*, *HPRT*, *NCL* and *MRPL19* (see Table 9). The mitochondrial ribosomal transcript *MRPL19* (*L19*) was showed the best expression stability and the closest level of expression to our

experimental transcripts in placenta, while β-actin was the most suitable for fetal tissue analysis.

Table 9: *Summary of the experimental results that based our selection of MRPL19 as the internal control gene in placental tissue.*
L19*: mitochondrial ribosomal transcript* MRPL19*.* GUS3*: glucuronidase 3.* HPRT*: Hypoxanthine guanine phosphoribosyl transferase.* NCL*: nucleolin.* GAPDH*: glyceraldehyde-3-phosphate dehydrogenase.* MRLPL19 *showed the smallest variation between placental samples and the closest amplification characteristics (Cycle Threshold, C_T) to those of our genes of interest.*

	Average C_T (AvgC_T)	Range of AvgC_T in a set of 4 placentas
β-actin	18	18.3-20.9
L19	21	21.3-22.6
GUS3	28	27.4-29.1
HPRT	25	25.7-27.4
NCL	26	23.4-29.2
GAPDH	24	23.7-25.7

PLAGL1 and *HYMAI* transcripts were detectable in multiple tissues, with predominant expression in first trimester placenta, where levels more than double the maximum in fetal tissues (*Figure 14*). We failed to detect transcription from the non-imprinted promoter *PLAGL1* P2. We observed that all *PLAGL1* isoforms had a consistently higher expression than *HYMAI* in all tissues, as this transcript was low throughout the tissue panel. Primers located in exon 8 simultaneously amplify all isoforms of *PLAGL1*, giving the highest reading. The majority of transcription originated from the P1 promoter, which is embedded within the DMR.
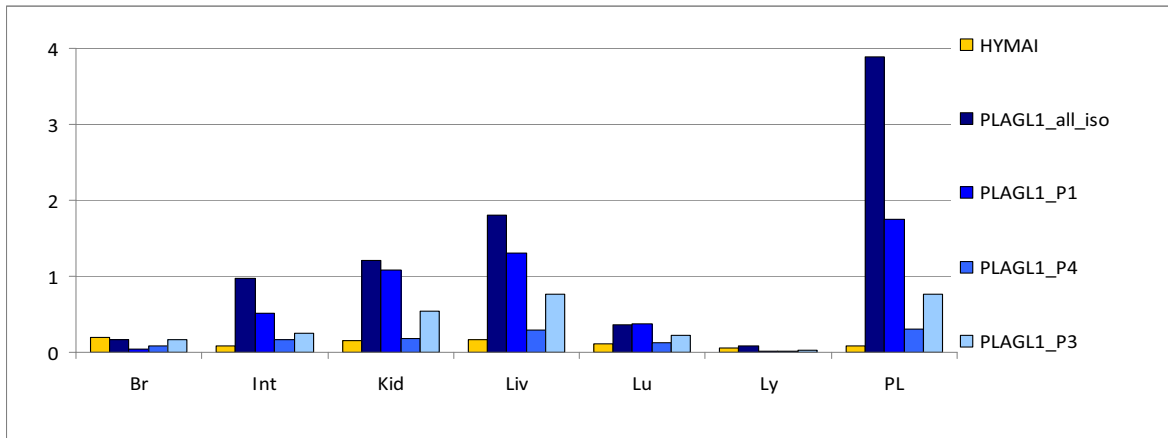
Figure 14: *Expression of HYMAI and the different isoforms of* PLAGL1 *in human fetal tissues.*
Y axis: *levels of expression in arbitrary units, normalized to an internal control gene (β-actin) and results corrected for efficiency for each pair of primers. X axis: Fetal tissues analyzed. Br: brain. Int: intestine. Kid: kidney. Ly: lymphocytes. PL: first trimester placenta. Pooled cDNA from different fetal tissues was used as a reference sample.*

2.2. ANALYSIS OF THE LEVELS OF EXPRESSION OF *PLAGL1* IN RELATION TO FETAL SIZE IN ADEQUATE FOR GESTATIONAL AGE TERM PLACENTA

2.2.1. LONDON PARTICIPANTS: THE MOORE COHORT

One hundred and three placental samples from spontaneously-conceived, singleton pregnancies of white European origin were used for this study. Mean maternal age was 34 years (SD 4,6 years) and 46,6% were primiparous. By inclusion criteria, all babies were born at term (mean gestational age 39,1 ± 1,1 weeks), with a mean birthweight of 3.432,5g (SD 622,8g). There were 48 boys and 55 girls (46,6%/53,4%, respectively). Customized birthweight percentiles, adjusted for gestational age, maternal height and weight, ethnic origin, parity and gender of the newborn, were calculated with the GROW program (Gardosi and Francis, 2009) from the NHS Perinatal Institute for Maternal and Child Health (www.gestation.net).

Two mothers developed mild preeclampsia and two others had a previous history of high blood pressure. Among them, two of the newborns had a weight below the 3rd percentile at birth. Exclusion of these patients did not influence the results of the analysis.

2.2.2. INVESTIGATION OF THE RELATIONSHIP BETWEEN EXPRESSION OF *PLAGL1* AND SIZE AT BIRTH

Expression of the *PLAGL1* isoforms was analyzed by the $\Delta\Delta$Ct ($2^{-\Delta CT}$) method using *L19* as a housekeeping gene (Schmittgen and Livak, 2008). Transcript levels were normalized by log10 transformation. Preliminary analyses were conducted to ensure no violation of the assumptions of the statistical models.

2.2.2.1. Levels of expresión of *PLAGL1* do not correlate with parameters of fetal growth in healthy pregnancies.

Since total expression of *PLAGL1* was mainly contributed by the P1 isoform, we decided to perform qRT-PCR using the assays designed to amplify solely the *PLAGL1* P1 isoform and another to simultaneously amplify all isoforms together.

We found no correlation of the levels of expression with any of the maternal or obstetric characteristics (maternal age, height, weight, gestational age) or with fetal outcomes, including placental weight, birth weight, or head circumference. Correlation was also absent when adjusting weight of the newborn by gestational age, maternal height and weight, ethnic origin, parity and gender with the use of customized weight percentiles (see *Figure 15*).

There were no significant differences (as assessed by Student´s t test) in expression between boys and girls or by parity and smoking habits. Levels of expression of *PLAGL1* were higher in the placenta if labour was present before delivery (log10 of expression: -0,94 vs -1,09, p 0,022), although this result was not replicated when the expression of *PLAGL1* P1 was analyzed separately. This might have been due to the low number of spontaneous deliveries in this cohort (29,8%). The absence of a relationship between growth parameters of the newborn and expression did not change when adjusting for the presence of labour in a multivariate analysis.
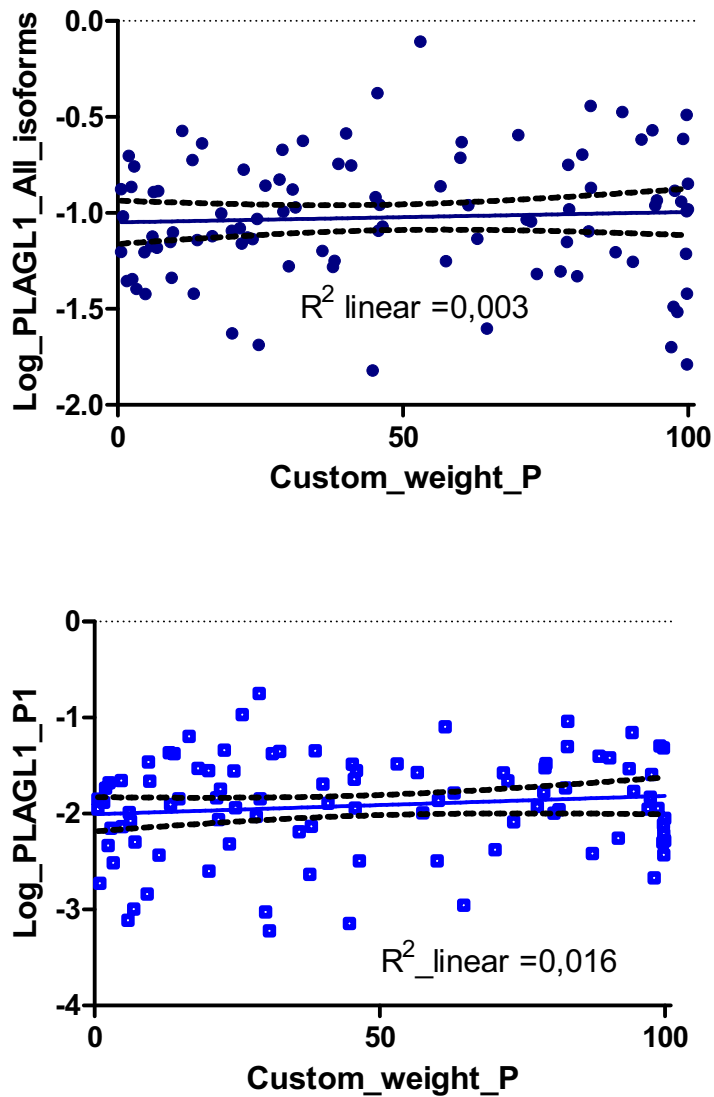
Figure 15: *Analysis of linear correlation between expression of PLAGL1 (all isoforms and P1) and the customized birth weight percentile.*
Y axis. Log_PLAGL1_(All_isoforms and P1): Log10 of the levels of expression of PLAGL1 (All isoforms and P1) as analyzed by Real-Time PCR. Expression is in arbitrary units. X axis: Customized_P_weight: Customized birthweight percentile (see text).

2.3. COMPARISON OF *PLAGL1/HYMAI* EXPRESSION AND METHYLATION LEVELS BETWEEN AGA AND IUGR PLACENTAS AT DIFFERENT GESTATIONAL AGES

Intrauterine growth restriction is a pathological process that is not only defined by a birth weight under a particular percentile. Most studies (McMinn et al., 2006; Bourque et al., 2010) demonstrating changes in the expression of imprinted genes, including *PLAGL1*, have compared normal and IUGR placentas from well clinically-characterized, complicated pregnancies. For this reason, we proceeded to establish a cohort of placental samples collected from Hospital Sant Joan de Déu and assess the role of the imprinted transcripts in the 6q24.2 region in pathologic fetal growth.

2.3.1. BARCELONA PARTICIPANTS: THE SJD COHORT

One hundred placental samples were obtained from 90 pregnancies. Demographic and anthropometric data of the mothers and babies are summarized in *Table 10* and *Table 11*. Most mothers were of Caucasian or Hispanic (91,2%) origin and were healthy before pregnancy. Among those suffering from pregnancy- unrelated conditions, 5.5% had chronic hypertension and 3,3% psychologic/psychiatric disorders (mainly anxiety and depression). Over half of the newborn babies were girls and the mean gestational age was under 36 weeks, as 49% of them were born before term age (30 were late or moderate preterms and 19 extreme preterms). The mean gestational age of the boys was significantly lower (34,8±4,5 weeks vs 36,5±3,9, p 0,046) which reflected a higher proportion of boys among the extreme prematures (13 boys and 6 girls).

Table 10: *Summary of maternal characteristics regarding demographic, anthropometric and medical data (n=90).*

	n (%)
Ethnicity	
Caucasian	68(75,6)
Hispanic	14(15,6)
Chronic conditions	
None	73 (81,1)
Chronic hypertension	
With treatment	3(3,3)
Without treatment	2(2,2)
	Mean ± SD
Age (years)	31,7 ± 5,5
Anthropometric data	
Height (cm)	162,3±7,0
Pre-pregnancy weight (kg)	64,8±14,3

Table 11: *Baseline characteristics of the newborns regarding gender, length of gestation, and anthropometric parameters (n=100).*

	n (%)
Gender	
Boys	46 (46,0)
Girls	54 (54,0)
Gestational age group (w= weeks)	
Term (≥37w)	51 (51,0)
Late/moderate premature (32 -37 w)	30 (30,0)
Extreme premature (≤ 32 w)	19 (19,0)
	Mean ± SD
Gestational age (w)	35,7± 4,2
Anthropometric data	
Birthweight (g)	2300,0±887,8
Length (cm)	44,7± 5,4
Head circumference (cm)	31,2± 3,6

Singleton pregnancies accounted for 81% of the cohort. Due to the high-risk obstetric characteristics of our population (IUGR, prematurity, complications of pregnancy), there was a high rate of caesarean section (48%) (see *Table 12*).

Table 12: *Summary of the obstetric features of the sample, including prevalence of and treatment for complications of pregnancy.*
Percentages are calculated over 90 mothers and 100 fetuses. IUGR: IntraUterine Growth Restriction. PROM: Premature Rupture of Membranes.

Obstetric characteristics of the pregnancies	n (%)
Primigesta	47 (52,2)
Number and chorionicity of pregnancy	
Singleton	81 (90)
Twins	
Bichorionic	6 (6,7)
Monochorionic	2 (2,2)
Triplets	1 (1,1)
Indication of delivery	
Spontaneous	37 (41,1)
Maternal (pre-eclampsia, maternal condition,...)	8 (8,9)
Fetal (IUGR, PROM,...)	45 (50,0)
Mode of delivery	
Vaginal	52 (52,0)
Caesarean section	48 (48,0)
Diagnosis of IUGR (number of fetuses)	43 (43,0%)
Other complications of pregnancy	
Pre-eclampsia	16 (17,7)
Premature labour	4 (4,4)
PROM	8 (8,9)
Gestational Diabetes	1 (1,1)
Treatments for complications of pregnancy	
Bethametasone	
1dose	1 (1,1)
2doses	24 (26,7)
>2 doses	2 (2,2)
Antibiotics	11 (12,2)

Obstetric characteristics of the pregnancies	n (%)
Labetalol	9 (10,0)
Magnesium sulphate	9 (10,0)
Atosiban	5 (5,6)
Nifedipine	2 (2,2)
Indomethacin	1 (1,1)

Forty-three of the fetuses were diagnosed with IUGR during pregnancy (see *Figure 16*). For the purpose of this analysis, we classified them according to the most severe ultrasound abnormality present at any time during scheduled controls (see *Table 13*). Due to the higher incidence of complications in this population, end of pregnancy for fetal indication was more frequent (83,3% vs 31,6%, p <0,0001), as was the practice of caesarean section previous to the onset of labour (44,2% vs 15,8%, p 0,002). History of pre-eclampsia (30,9% vs 8,8%, p 0,005) or chronic hypertension and self-reported smoking habit (26,5% vs 10,5%, p 0,077) were also more prevalent in mothers delivering IUGR babies. IUGR and normal growing fetuses were comparable in their remaining clinical characteristics except, by definition, size at birth both in absolute terms and relative to gestational age.
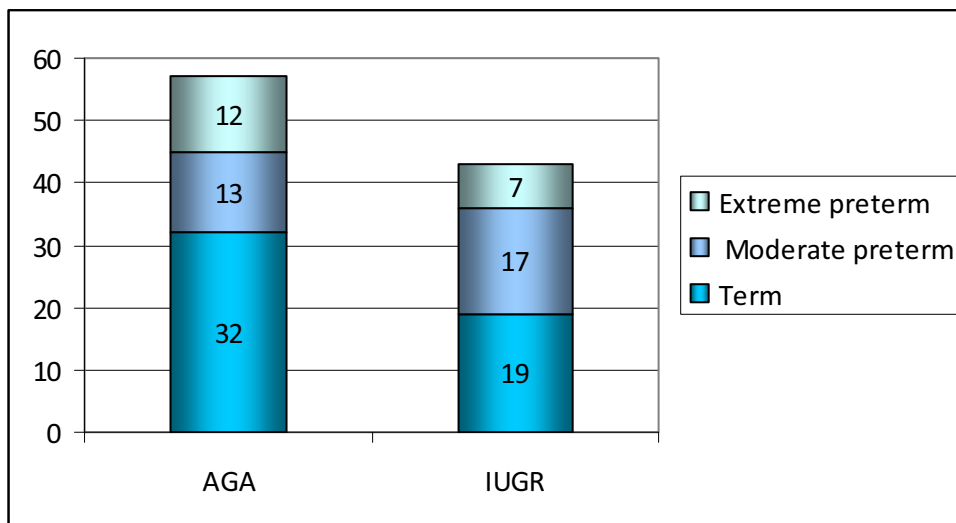
Figure 16: Distribution of the sample regarding intrauterine growth and gestational age.
AGA: Appropriate weight for Gestational Age. IUGR: Intrauterine Growth Restriction. The Y axis and the values represent number of samples in each category (n).

Table 13: *Ultrasound (US) features of IUGR fetuses regarding estimated weight and assessment of haemodinamics by Doppler flows.*
Groups were defined as mutually exclusive, so that each fetus was included in only one category according to the most severe alteration. MCA: Median Cerebral Artery.

US features of IUGR fetuses (as classified by most severe alteration)	n	% (within the IUGR group)
Estimated weight P3-10, normal Doppler evaluation	9	21,4
Estimated weight <P3, normal Doppler evaluation	11	26,2
Abnormal Umbilical Artery Doppler evaluation	5	11,9
Vascular redistribution (abnormal MCA Doppler evaluation)	13	31,0
Abnormal *ductus venosus* Doppler evaluation	4	9,5

2.3.1.1. Babies conceived by assisted reproduction in the cohort

Seven couples (7,8%) had undergone some Assisted Reproduction Technique which resulted in 12 children. In this group, the maternal age was higher (36,6±6,8 years vs 31,5±5,3, p 0,004) and multiple pregnancy was more frequent (57,1% vs 6,0%, p 0,001), as would be expected. Also, most of the ART babies recruited were premature (only an 8,6% of them had been born at term as compared to a 56,8% of the ones conceived spontaneously, p 0,002) and, consequently, gestational age (32,2±4,9 weeks vs 36,2±3,9) and weight, length and head circumference at birth were smaller. Nevertheless, there were no significant differences regarding z-scores for these parameters and the incidence of IUGR was comparable in both groups.

2.3.2. EXPRESSION OF *PLAGL1* ISOFORMS/*HYMAI* IN AGA AND IUGR PLACENTAS AT DIFFERENT GESTATIONAL AGES

Levels of expression of *HYMAI* and the different isoforms of *PLAGL1* were assessed by real-time PCR and the results analyzed by the $\Delta\Delta C_T$ ($2^{-\Delta CT}$) method with the DataAssist® v2.0 software (Applied Biosystems). *L19* was selected as a reference gene. Outliers were excluded as per system specifications (difference of more than 0.5 CTs between replicates) and samples with less than two valid CT values were discarded.

Transcript levels were normalized by log10 transformation. Statistical analysis was performed as described in Methods, section 5. Statistical Analysis.

2.3.2.1. Levels of expression of *HYMAI* are higher in IUGR placentas.

In the univariate unadjusted analysis, levels of expression of *HYMAI* were higher in the placentas of the IUGR group (mean Log10 expression 0.991 vs -0.0012, t-test p 0.018) (*Figure 17*). Although this was true for the sample as a whole, the effect was much more pronounced in male babies. A significant association between *HYMAI* levels of expression and the presence of IUGR was confirmed by standard linear regression (Standardized Beta -0,255, p 0,018).There was no correlation between *HYMAI* expression and maternal age, size or parity, or with gestational age. *HYMAI* levels were not dependent on anthropometric parameters of the baby (weigth, length or head circumference at birth), in either absolute terms or adjusted by gestational age (z-scores), but related specifically to the presence of IUGR defined by obstetric criteria. No other clinical variables (single/multiple gestation, labour, ethnicity, indication for delivery) showed any influence on *HYMAI* expression, which was homogenous between groups as assessed by t-test and one-way ANOVA.

Multivariate analysis was performed by linear regression. In order to further explore the correlation between IUGR and *HYMAI*, hierarchical multiple regression was used to adjust for other variables known to influence low size at birth, like maternal weight, parity, gestational age and gender of the baby. These additional factors did not account for the differences in *HYMAI* expression levels and the presence of IUGR was the only statistically significant factor in

the final analysis (Beta -0,268, p 0,018). This indicates that, in our cohort, levels of expression of *HYMAI* in the placenta correlated independently with the presence of IUGR after adjustment for maternal weight, parity, gestational age and gender.

We then analyzed if *HYMAI* expression levels could contribute to the presence of IUGR. For this, direct logistic regression was performed including other variables known to influence low size at birth (maternal weight, primiparity, gestational age and gender of the baby). None of the additional variables made a statistically significant contribution to the model. The strongest factor was the level of *HYMAI* expression, with an odds ratio of 18.30 (95% CI: 1.5-224,4, p = 0.023). These results indicate that high levels of expression of *HYMAI* in the placenta could be a risk factor for IUGR.

Figure 17: Comparison of levels of expression of HYMAI between the placentas of IUGR and AGA babies.
The boxes represent the interquartile range (25th to 75th percentiles) and the horizontal line corresponds to the median. The whiskers extend to the 5th and 95th percentiles of the data set. Levels of expression of HYMAI were significantly higher in IUGR placentas (Student´s t test).

2.3.2.2. Levels of expression of *PLAGL1* are lower in ART placentas.

Levels of expression of *PLAGL1* as a whole or when assessed per individual isoforms, were lower in placentas of babies conceived by Assisted Reproduction Techniques (ART) (Table 14 and Figure 18). There were no significant differences regarding *HYMAI* levels (although there was a trend for them to be higher in ART).

Table 14 and Figure 18: *Comparison of levels of expression of* HYMAI/PLAGL1 *and methylation of the DMR between placentas of babies after spontaneous or assisted conception.*
A non-parametric test (Mann-Whitney U) was selected due to small numbers in the ART group. Spont: Babies conceived without assisted reproduction techniques. Meth_DMR: Average value of methylation of the DMR as measured by pyrosequencing.

Transcript	Group	n	Mean	SD	p*
HYMAI	ART	9	0,134	0,114	0,062
	Spont	77	0,032	0,202	
PLAGL1_All isoforms	ART	9	-0,262	0,297	0,003
	Spont	78	0,064	0,271	
PLAGL1_P1	ART	9	-0,495	0,936	0,014
	Spont	77	0,0827	0,311	
PLAGL1_P3	ART	9	-0,192	0,223	0,001
	Spont	78	0,175	0,333	
PLAGL1_P4	ART	9	-0,311	0,309	0,002
	Spont	78	0,087	0,400	
Meth_ DMR	ART	11	56,755	5,077	0,334
	Spont	71	55,092	5,528	

*p value as assessed by the Mann-Whitney U test
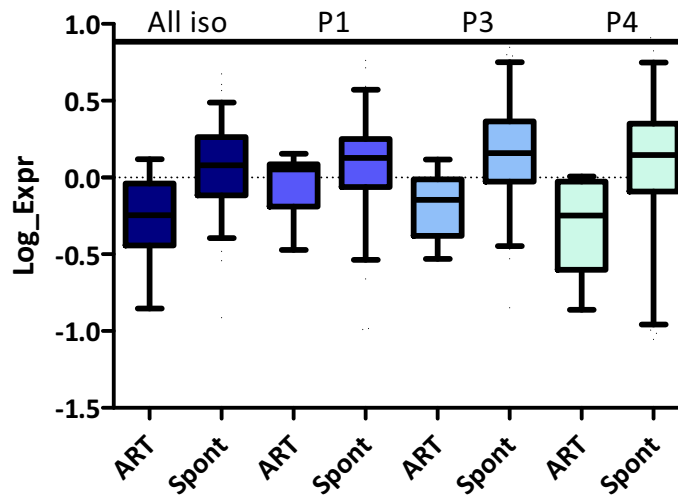
Comparison of levels of expression of HYMAI/PLAGL1 *and methylation of the DMR between placentas of babies after spontaneous or assisted conception.*
A non-parametric test (Mann-Whitney U) was selected due to small numbers in the ART group. Spont: Babies conceived without assisted reproduction techniques. Meth_DMR: Average value of methylation of the DMR as measured by pyrosequencing.

Due to the differences between these two groups regarding maternal age, prevalence of multiple pregnancy, parity, gestational age and size of the newborns (see Section 2.3.1.1. Babies conceived by assisted reproduction in the cohort), the relationship was analyzed by hierarchical multiple regression, controlling for the aforementioned factors and gender of the baby. The model was still significant (R square 0,223, p 0,007) and ART was the only factor making a relevant contribution to the variance of the expression of *PLAGL1* (R squared change 0,130, p 0,001; standardized β 0,451, p 0,001). This result indicates that, after adjustment for confounding factors (multiple pregnancy, parity, gestational age and anthropometry of the baby), levels of expression of *PLAGL1*, both globally and per each isoform, were lower in placentas of babies conceived by assisted reproduction.

2.3.2.3. Levels of expression of *PLAGL1* are lower in the placenta of IUGR girls. Gender-dependent correlation between *PLAGL1* expression and IUGR.

In the univariate analysis, expression of *PLAGL1* correlated negatively with maternal age (r= -0,232, p 0,022), probably due to the altered expression of *PLAGL1* in ART babies that were

usually born to older mothers. When ART placentas were excluded, global expression of *PLAGL1* correlated with maternal pre-pregnancy weight (r 0,232, p 0,046) and not with age. Expression of the imprinted isoform, *PLAGL1* P1, correlated with length and head circumference of the baby in non-ART placentas and with these parameters and birth weight in the sample as a whole. When using z-scores, which take into consideration gestational age, these effects disappear (see *Table 15*).

Table 15: Correlations between PLAGL1_P1 expression and anthropometric parameters of the newborns (birth weight, length and head circumference).

	Log10Expression *PLAGL1* P1	
	r	p
Raw anthropometric measurements		
Birth weight (g)	0,232	0,032
Birth length (cm)	0,310	0,006
Head circumference (HC) (cm)	0,294	0,008
Non-ART placentas		
Birth weight (g)	0,171	0,137
Birth length (cm)	0,253	0,036
Head circumference (HC) (cm)	0,241	0,045
Z-scores		
Birthweight z-score	0,039	0,721
Length z-score	0,181	0,113
HC z-score	0,110	0,334

As explored by linear regression, *PLAGL1* did not correlate with the presence of IUGR in our cohort. However, when boys and girls were analyzed separately, the global expression of *PLAGL1* was significantly lower in the placenta of IUGR girls (Log10_*PLAGL1*_All: 0,12 vs -0,08, p 0.023) when compared with their normally grown counterparts (see *Figure 19*). This was not the case in boys. There was also a negative correlation in girls between IUGR and expression of *PLAGL1*, both as a whole and from the imprinted promoter (r=-0,323, p 0,023 and r=-0,293, p= 0,041, respectively). This remained significant after adjustment for maternal age, weight and parity, length of gestation and use of assisted reproduction (Log10_*PLAGL1*_All, Beta -0,308, p= 0,018. Log10_*PLAGL1*_P1, Beta -0,257, p 0,040).
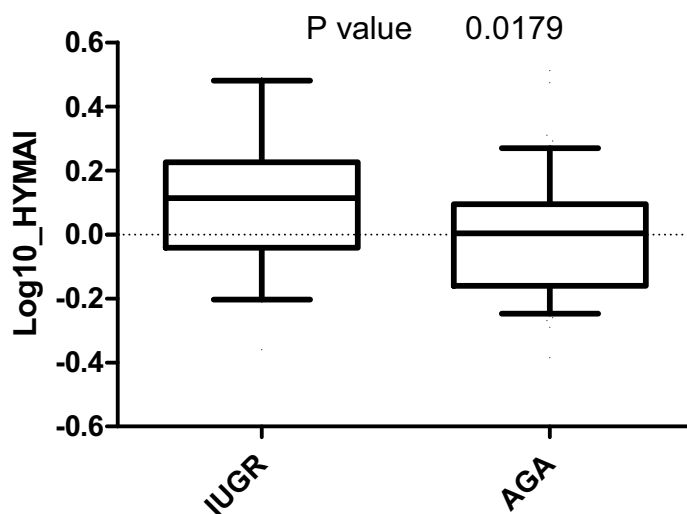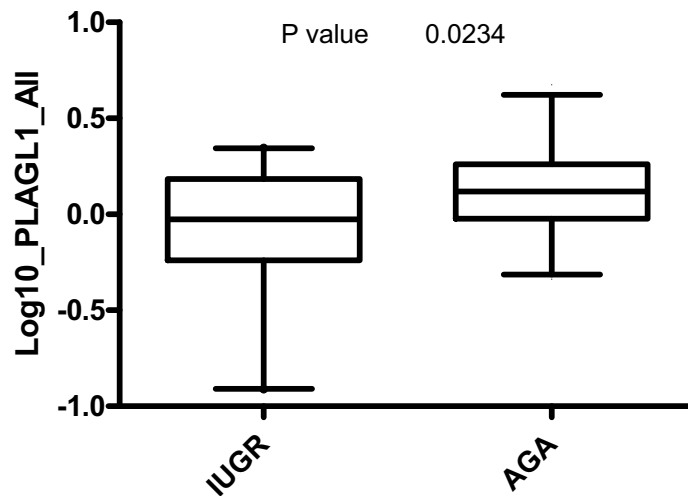
Figure 19: Comparison of global levels of expression of PLAGL1 *between the placentas of IUGR and AGA girls.*
The boxes represent the interquartile range (25th to 75th percentiles) and the horizontal line corresponds to the median. The whiskers extend to the 5th and 95th percentiles of the data set. The levels of expression of PLAGL1 were significantly lower in the placentas of IUGR girls (Student´s t test).

2.3.2.4. Changes in correlation between expression of *PLAGL1* P1 and HYMAI in IUGR

PLAGL1 P1 and *HYMAI* both originate from the same promoter region embedded in the *PLAGL1* DMR. In placentas of control babies (spontaneously conceived, normally grown), there was a correlation between the expression of both transcripts (r= 0,479, p= 0,02). However, in IUGR pregnancies this correlation is lost, due to increased *HYMAI* expression without concomitant changes in *PLAGL1* P1 (r= 0,023 and p=0,823). The increase in expression of *HYMAI* was not due to loss of imprinting, as monoallelic expression was preserved in the 4 heterozygous cases where it could be assessed (see next section).

2.3.2.5. Imprinted expression of *PLAGL1/HYMAI* is preserved in premature, IUGR and ART placentas

Allelic expression was assessed in all heterozygous individuals in the cohort. From the 12 heterozygous placental samples for the *PLAGL1* rs2076684 SNP, 7 were term, 3 moderately

premature and 2 extremely premature. Regarding growth, 4 were appropriate for gestational age, 2 SGA, 1 Large for Gestational Age (LGA) and 5 IUGR. One of the samples, corresponding to a moderately premature with adequate growth, was from a pregnancy obtained by assisted reproduction techniques (IVF with donor oocyte). Monoallelic expression was observed in all cases. Parental origin was confirmed as paternal in one sample with a homozygous mother.

Twenty samples were heterozygous for the rs2281476 SNP for *HYMAI*: 13 term, 3 moderately preterm and 4 extremely preterm. Of these 14 were AGA, 1 SGA, 4 IUGR and 1 LGA. Two babies from different mothers were conceived by assisted reproduction techniques. Expression was monoallelic in all 20 samples and identified as paternal in origin in the 3 samples for which mothers' DNA was homozygous.

3. COMPARISON OF LEVELS OF METHYLATION OF THE PLAGL1/HYMAI PROMOTER-ASSOCIATED CpG ISLAND BETWEEN AGA AND IUGR PLACENTAS

3.1. Methylation of the *PLAGL1/HYMAI* DMR does not correlate with the presence of IUGR

Levels of methylation at the *PLAGL1/HYMAI* DMR were analyzed by pyrosequencing after bisulfite conversion of the DNA extracted from placental tissues. The PCR product incorporated 10 CpG dinucleotides within the DMR. Optimisation of the amplification conditions revealed that primers amplified both the maternally methylated and paternally unmethylated strands equally when the resulting amplicons were subject to sequencing or COBRA analysis (see *Figure 20*). Subsequent pyrosequencing analysis was limited to 6 CpG dinucleotides within the PCR amplicon given the limited length of the sequence reads. The arithmetic mean of the 6 CpG dinucleotides was used as a representative measure of the level of methylation for that sample.

A commercial bisulfite converted DNA (Epitect®, QIAGEN) was used as a fully methylated control, and converted DNA from a cell line with pUPD of chromosome 6 (D3131) as an unmethylated control. The mean methylation for these controls was 90,3 and 26,4%, respectively.

Consistent with our observation of maintained imprinted expression of *PLAGL1* and *HYMAI* in all heterozygous samples, we observed no extreme deviation from the expected ~50% metylation in all samples. This suggests that loss of methylation at the *PLAGL1* DMR is not responsible for the variation in expression levels. There was also no relationship between levels of methylation at the *PLAGL1* DMR and maternal or fetal size, gestational age, presence of IUGR or any other of the clinical variables analyzed.

(A)

GAcGGGGTTGAATGATAAATGGTAGATGTCGTGGGTTTTGTCGTTCGCGGTAGTTAAGAGGATGGTTGc
GTCGAGGAGGTCGCGCGTAGGCGGGGTTCGGGAGTCGGAACGGCGCGGTCGCGAGGAGGGCGTTG
GGGTTTTTGGCGGGGGCGTTACGTGGTAGGAGGAGGTTT[1]**CG**T[2]**CG**GGGAGTTGGGGGT[3]**CG**G[4]**CG**
GT[5]**CG**AGG[6]**CG**GGGGGAGTTGAG[7]**CG**GTATTTATA[8]**CG**TTTTG[9]**CG**GGT[10]**CG**GGTTATcGGTGGGG
GTAAAGTTAAGGT

(B)

(C)
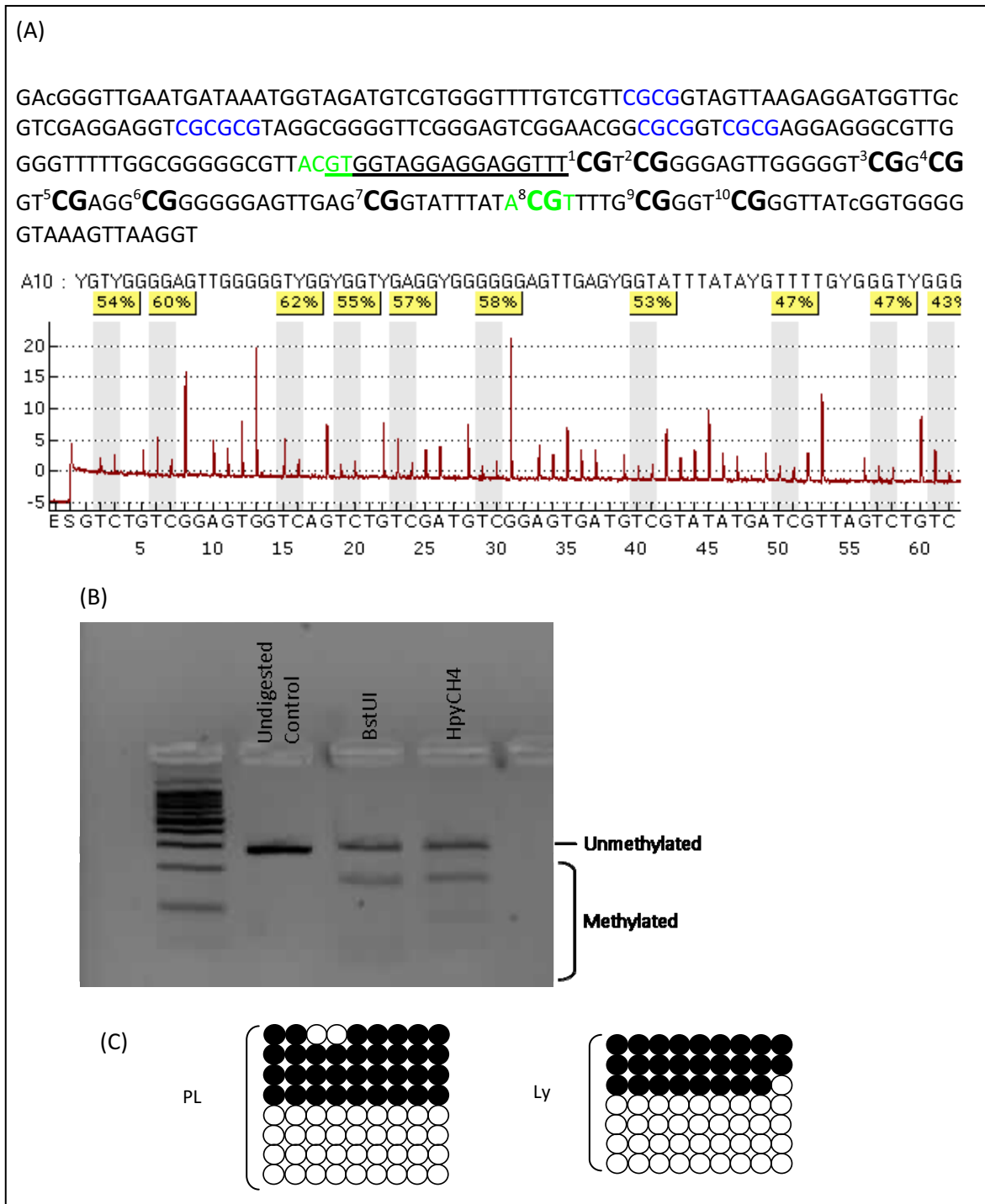
Figure 20: Analysis of the methylation status of the PLAGL1/HYMAI promoter-associated CpG island.

Panel (A): Sequence of the amplified fragment and example of a typical pyrogram. Colours represent recognition sites of the restriction enzymes (green: HpyCH4, blue: BstUI). The underlined sequence indicates the internal sequencing primer; bold type with bigger font size identifies the CpG positions analyzed by pyrosequencing. Panel (B): Combined Bisulfite-Restriction Analysis (COBRA). PCR products run in a 3% agarose gel: undigested (row 2) and digested with different restriction enzymes (rows 3 and 4). The equal intensities of the undigested unmethylated and digested fully methylated indicates equal amplification of both parental alleles. Panel (C): Representation of strand-specific sequencing, of the first nine CpG dinucleotides analysed by pyrosequencing. Key as Figure 10. PL: placenta. Ly: lymphocyte.

DISCUSSION

DISCUSSION

1. DEFINING THE BOUNDARIES OF THE IMPRINTED DOMAIN ON HUMAN CHROMOSOME 6q24.

1.1. THE DIFFERENT ISOFORMS OF *PLAGL1* AND THE NON-CODING RNA *HYMAI* ARE PATERNALLY EXPRESSED IN FETAL TISSUES AND IN THE PLACENTA THROUGHOUT GESTATION.

Imprinted genes have been shown to be important players in growth and development and, as such, they are expected to be expressed in differentiating tissues. In order to assess the role of the 6q24 imprinted transcripts in human prenatal development, we first aimed to ascertain expression of the transcripts in human fetal tissues. *PLAGL1* and *HYMAI* transcripts were detected in first trimester lung, liver, kidney and intestine and at a lower level in brain. The highest expression was found in the first trimester placenta, being more than 2-fold higher than the expression in any fetal tissue (see Results, section 2.1., Figure 14) which supports the theory that these imprinted genes, like others, could be involved in early events of placental development (Fowden et al., 2006; Tycko, 2006). It also backs the hypothesis that disruption to *PLAGL1/HYMAI* might affect normal placentation and hence influence fetal growth.

Previous studies have shown positive RNA in situ hybridization in the mouse for *Plagl1* and *Hymai* in the lung, liver, muscle and cartilage, sclerothome and placenta (Arima et al, 2001; Arima et al., 2005; Valente et al., 2005). Finding low levels of expression in the human developing nervous system was surprising, as *Plagl1* has been shown to participate in neural development in the mouse, displaying specific patterns of expression in relation to structural fate (Alam et al., 2005). Either this does not replicate in the human or the role of *PLAGL1* calls for its expression at earlier stages and is already downregulated at the gestational ages we analyzed, as it is known to take part in cell cycle arrest and apoptosis in certain early neural progenitor subpopulations, with subsequent down-regulation upon differentiation (Valente et al., 2005). Levels of expression of *Plagl1* in the mouse are highest at the final period of embryonic development, with an abrupt decline of transcription after birth (Marcelin et al., 2009). This has been suggested to reflect the coordinate down-regulation of an imprinting

network which would have a role at slowing down growth rates and determining final body size (Lui et al., 2008).

Human *PLAGL1* and *HYMAI* were first shown to be maternally imprinted and paternally expressed in several tissues, including the placenta, in methylation and expression screenings for imprinted loci (Arima et al., 2000; Kamiya et al., 2000). We interrogated parent-of-origin expression in fetal tissues and first trimester and term placenta from heterozygous healthy individuals and confirmed selective expression from the paternal allele of both transcripts originating in the DMR: *PLAGL1* P1 and *HYMAI*. A non-imprinted isoform of *PLAGL1* has been described (Valleley et al., 2007), originating from an independent promoter (P2) approximately 65 kb upstream of P1. In our experiments, expression of this isoform was below the amplification threshold in the tissues analyzed, including peripheral leukocytes, which precluded further assessment. Very low levels of expression of biallelic *PLAGL1* had also been previously reported by other authors (Kamiya et al., 2000). The most relevant role of expression from the P2 isoform seems to relate to the establishment of germline imprints. In the oocyte transcription of P2 might maintain an open chromatin conformation or recruit factors required by the *de novo* methylation machinery to act on the CpG island destined to be the DMR (Chotalia et al., 2009). Once establishted, transcription from P2 might not be necessary in somatic tissues.

Human genome database search revealed two further isoforms of *PLAGL1*, which we named P3 (AJ006354) and P4 (AK091707). They have distinct independent promoters approximately 45 kb downstream of the DMR and contain the coding exons necessary for the production of both the short (ZAC∆2, with 5 zinc fingers) and long (ZAC, 7 zinc fingers) isoforms of the PLAGL1/ZAC1 protein (Bilanges et al., 2001). After specific amplification and SNP analysis of heterozygous term placenta samples, we showed that the parent-of-origin regulation extends to these transcripts, and that they are also paternally expressed. The P3 and P4 promoters are not associated with CpG islands and the promoter CpGs are not differentially methylated (Monk D., personal communication), suggesting that monoallelic expression has to be maintained through some other mechanism.

Allelic covalent modification of histone tails in the region could be involved in the maintenance of P3 and P4 imprinting in the absence of any other identified DMRs. In the distal imprinting cluster in chromosome 7 in the mouse, placental-specific imprinting of genes 700 kb away from the imprinting control center (IC2) has been shown to relate to the deposit of allelic repressive or permissive histone modifications. This mechanism is independent of

maintenance methylation, but requires the presence of IC2 and the paternal transcription of *Kcnq1ot1* during critical stages of pre-implantation development. This brings about the recruitment of histone methyl transferases, like Ezh2 and other chromatin modifiers (G9a) and the establishment of a repressive chromatin domain in the paternal chromosome (Lewis et al., 2004). In the human, histone modifications are also involved in maintaining imprinting of the genes within this cluster that lack DMR-associated promoters, such as *PHLDA2*, *SLC22A18*, *SLC22AILS* and *CDKN1C*. Here, repressive chromatin marks (H3K27me3 and H3K9me2) are restricted to the region centromeric to the KvDMR1 in the paternal allele, which contains the silenced genes, and to the DMR itself, but they do not extend through the body of the *KCNQ1OT1* transcript (Monk et al., 2006a).

Bioinformatic evaluation through a public database (http://genome.ucsc.edu/) revealed presence of CTCF binding sites in the *PLAGL1* region (see *Figure 21*). CTCF (CCCTC binding factor) is a highly conserved 11-zinc finger protein that can bind to insulators, or specific DNA sequences, creating boundaries between different chromatin functional domains. Genome-wide studies of CTCF binding sites have revealed universal binding of this factor to gene-rich areas in a conserved manner, suggesting a central role in the organization of transcriptional regulation (Kim et al., 2007; Xie et al., 2007). CTCF boundaries can separate active (H3K27 monomethylated) chromatin from condensed (H3K27me3) chromatin immediately outside (Wallace and Fensenfeld, 2007), decouple expression of nearby promoters (Xie et al., 2007) or contribute to the organization of higher chromatin structures by interaction with nuclear matrix proteins.
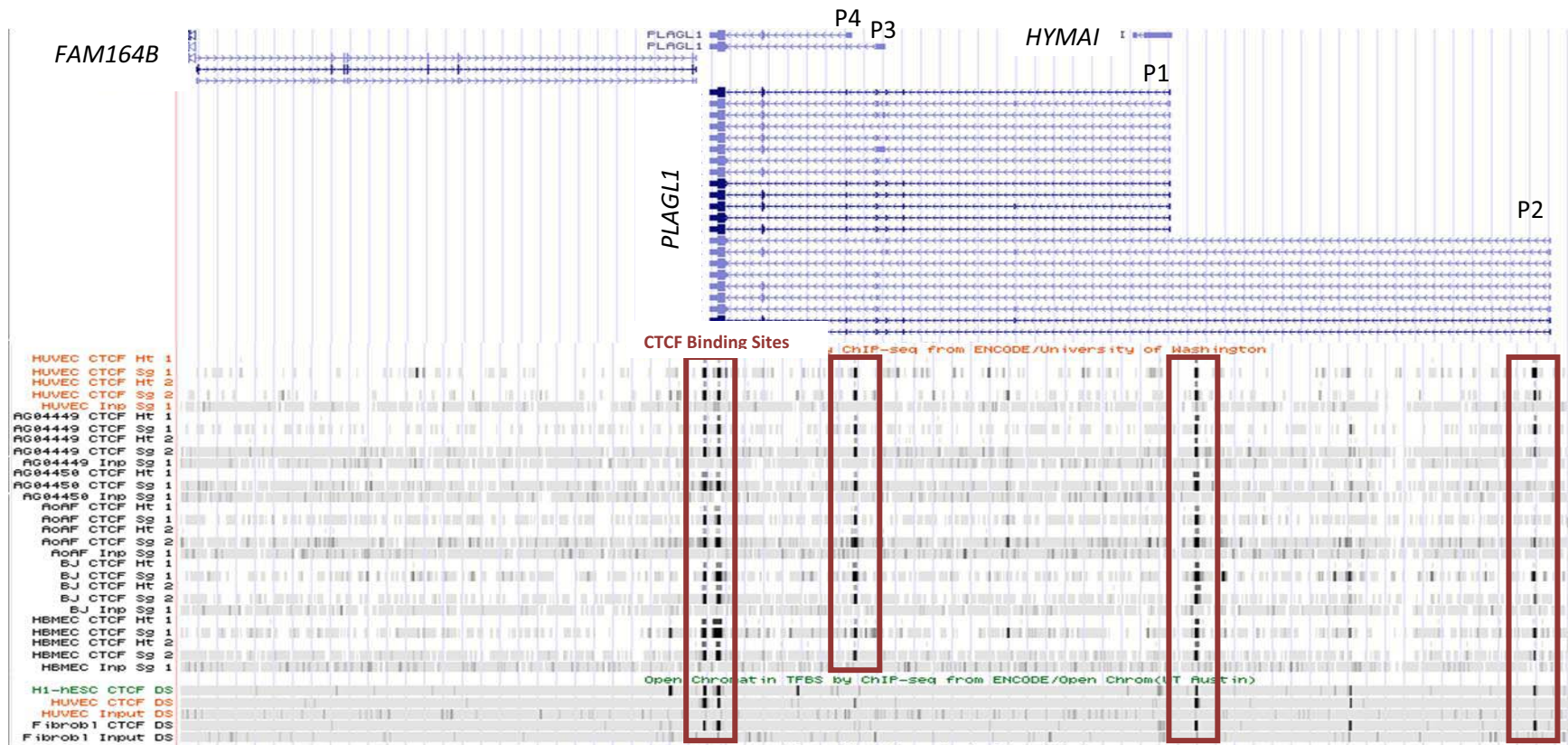
Figure 21 : CTCF binding sites in the PLAGL1/HYMAI *domain.*

CTCF binding sites as displayed with the ENC TF (ENCODE Transcription Binding Tracks) tool of the UCSC genome browser. The database includes data generated experimentally by ChiP-seq, which involves fragmenting DNA selection of the fragments bound to a certain transcription factor, and subsequent sequencing. Genes are represented in the upper panel in blue. Bold boxes indicate exons and lines with arrows indicate introns and direction of transcription. The intermediate panel shows the CpG islands, in green (associated to the P2 and P1 promoters of PLAGL1). The bottom panel contains the CTCF-binding information from the ENCODE/ University of Washington and ENCODE/Open Chromatin University of Austin. Input signal (for control) is shown as well as Hot Spots(Ht) or Density Signals (DS), which indicate abundance of the region in the immune- precipitated DNA due to CTCF binding. We selected the experimental data generated from normal tissues or cell lines, as being more relevant to our own study: HUVEC: Human Umbilical Vein Endothelial Cells, AG04449: fetal buttock/thigh fibroblast, AG04450: fetal lung fibroblast, AoAF: aortic adventicial fibroblast, BJ: skin fibroblast (from normal foreskin), HBMEC: human brain microvascular endothelial cells, hESC: human embryonic stem cells, Fibrobl: normal child (3 years) fibroblast.

The first and best described example of a role for CTCF in imprinting is in the *Igf2/H19* domain, where the ICR (IC1) acts as a methylation-sensitive insulator (Bell and Felsenfeld, 2000). Apart from being involved in the maintenance and, possibly, the setting of the differential methylation of the ICR, binding of CTCF can regulate the creation of allelic higher order chromatin structures (Lewis and Murrell, 2004). CTCF-mediated interactions between the *H19* DMD, other elements of the region and the nuclear matrix on the unmethylated maternal allele create a chromatin loop that places *Igf2* in an inactive domain, where it is inaccessible to enhancers and transcriptional machinery (Murrell et al., 2004; Kurukuti et al., 2006).

At the *PLAGL1* domain, CTCF binding sites immediately upstream of the P1 promoter and within the 3'UTR delimitate the region subjected to imprinting, so it could be speculated that, like in other clusters of the genome, this could contribute to the setting of coordinate transcriptional regulation, in this case allelic-specific transcription dictated by the *PLAGL1/HYMAI* DMR. This mechanism may act in a linear fashion, or result in chromatin looping due to dimerization or polymerization of the CTCF proteins (see *Figure 22*). More CTCF binding sites 3' to the P2 promoter and located between the P3 and P4 promoters could correspond to additional CTCF-dependent higher order chromatin structures, as seen at domains with multiple alternative promoters (Kim et al., 2007).
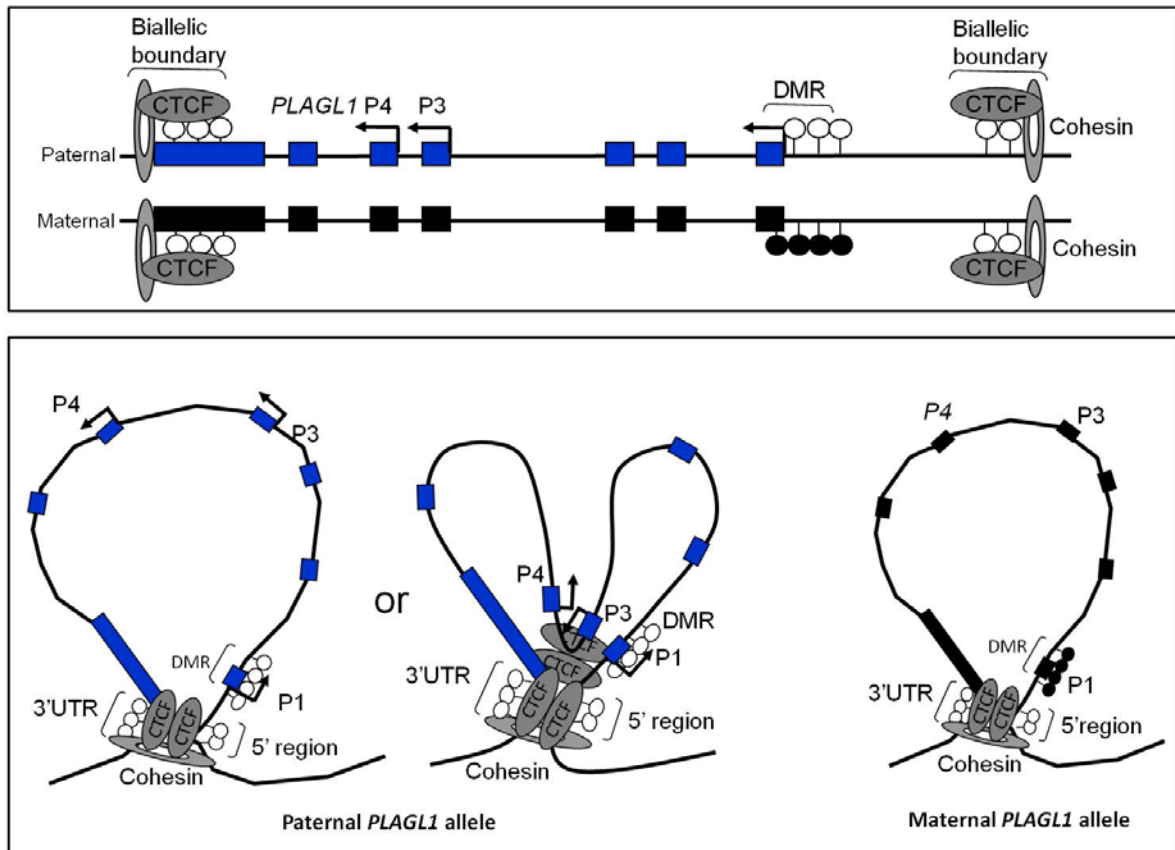
Figure 22: *Model for CTCF looping in the PLAGL1 domain*.
CTCF has binding sites in a region 5' to the P1 promoter, between the P3 and P4 promoters and between the 3' UTR of PLAGL1 and the end of FAM164B, which is transcribed in the opposite direction. This disposition of CTCF and interactions between CTCF and cohesin could help establish active (paternal) and inactive (maternal) allele-specific chromatin loops, contributing to the maintenance of imprinted expression of the different transcripts.

1.2. THE NEIGHBOURING GENES AROUND *PLAGL1/HYMAI* IN 6q24.2 ARE BIALLELICALY EXPRESSED AND THEIR PROMOTER-ASSOCIATED CpG ISLANDS ARE UNMETHYLATED.

Imprinted genes tend to be found in clusters, due to co-ordinated regulation by a common ICR (Imprinting Control Region). The number and complexity of transcripts within a cluster is very variable, as the influence of the ICR can extend over hundreds of kilobases, like the IC2 in the 11p15.5 region or the *Dlk1/Gtl2* locus, both of which include multiple genes with coordinate regulation of the same and opposite parental origin (reviewed in Lewis and Reik, 2006). It is not uncommon that loci initially described as "micro-imprinted" domains with single transcripts have later been shown to contain additional imprinted genes upon reassessment using technological advances extended to flanking regions. This has been the case for the paternally expressed human *NNAT*, embedded within the intron of *BLCAP*, which was found to undergo complex imprinting (Evans et al., 2001; Schulz et al., 2009), or for the mouse reciprocally expressed *Peg13/Kcnk9* (Smith et al, 2003; Ruf et al., 2007). A recent study in mouse embryonic and adult brain using high-throughput RNA-sequence technology suggests that the *Peg13* cluster may extend even further including several other imprinted transcrips (different *Trappc9* isoforms, several maternal ncRNAs and *Eif2c2*)(Gregg et al., 2010b). In the same analysis, discovery of parent-of-origin dependent expression of *Herc3* completed the picture of the remaining "micro-imprinted" domain, revealing that *Nap1l5* is no longer an isolated imprinted gene (Beechey, 2004; Gregg et al., 2010b). For this reason, we aimed to analyze if imprinted expression in the 6q24.2 locus extended beyond the known *PLAGL1* and *HYMAI* transcripts.

Due to the observed role of imprinting in embryonic and fetal development and to the fact that half the imprinted genes described to date are expressed and imprinted in the placenta, investigations were carried out in placental and fetal tissues. Although methylation of the ICR is found in all tissues and developmental stages, imprinted expression can be:

– Tissue-specific, e.g. *KCNQ1*, which is imprinted in early fetal and placental tissues but not in adult heart (Lee et al., 1997; Monk et al., 2006a) or *Slc38a4*, which is biallelic in adult liver but imprinted in other adult tissues, in embryonic tissue and in the mouse placenta (Smith et al., 2003).

– Stage-specific, e.g. *SLC22A3*, which exhibits imprinted expression in first trimester placenta but is biallelic in term placenta (Monk et al., 2006a).

– Isoform-specific, e.g. *Bclap/BLCAP* which has maternally (*V1)* and paternally (*V2*) expressed isoforms in brain in both mouse and human (Schulz et al., 2009) or *MEST*, for which isoform 1 is paternally expressed and isoform 2 biallelic (except in fetal kidney and placenta) (Nakabayashi et al., 2002).

– Polymorphic, e.g. human *IGF2R*, for which 10% of individuals show imprinted but most biallelic expression (Xu et al., 1993).

We determined allelic origin of expression in multiple fetal tissues of different gestational ages containing a known SNP. All transcripts analyzed in the 6q24.2 chromosomic region, except for the aforementioned *PLAGL1* isoforms and *HYMAI*, were found to be biallelically expressed.

During the course of this study, the minimal critical region for 6q24 Transient Neonatal Diabetes has been further delineated to a region of around 170 kb by the investigation of breakpoints of patients with paternal duplications (Docherty et al., 2010). The region contains only the P1 and P2 transcripts of *PLAGL1* and the non-coding RNA *HYMAI*. It was noted as well that, although not included within these limits, individuals with a single copy of the putative protein-coding *FAM164B* (C6orf94) had higher birth weight percentiles than those in which the duplication spanned the whole body of this gene. This was especially relevant to our own investigation, but the lack of expressed polymorphisms as well as the very low levels of expression of *FAM164B* in placenta and fetal tissues made it impossible to assess if this gene displays a parent-of-origin effect.

For another of the genes we analyzed, *STX11*, an Allelic Imbalance in Expression (AIE) has been shown in the mouse, favouring one of the alleles of the studied polymorphism (Marcelin et al., 2009). This phenomenon affected the shortest of its transcripts, named β, and was not related to parental origin. Only one human isoform has been described and we saw no bias in expression between alleles in the SNP assessed. The same researchers describe a secondary CpG island associated with the 3' UTR of the gene showing age-related acquisition of methylation (Marcelin et al., 2009). Because levels of methylation correlate with the abundance of transcript, it could be interpreted as a consequence of active transcription from the promoter, as seen in other genes (Jones and Takai, 2001), as opposed to a regulatory

mechanism. This was as well the case for the probes in the methylation array that mapped to CpGs located in the bodies and not in promoter-associated CpG islands of *LTV1*, *SF3B5* and *PHACTR2*, all showing high methylation percentages.

The parental origin of the *PHACTR2* transcripts was analyzed after amplification of a segment containing an expressed SNP (rs2073215) within exon 6 and our results indicated biallelic expression. High-throughput technology analysis, using both Illumina SNP and sequence technologies in search for imprinted genes in the human placenta found an imbalanced expression of *PHACTR2* consistently favouring the maternal transcript, with an approximate ratio of 70:30 (Daelemans et al., 2010). Potential imprinting of the *PHACTR2* gene would then be opposite in parent-of-origin to the neighbouring *PLAGL1/HYMAI*, which is also seen in transcripts from other imprinted clusters. The SNP used by Daelemans et al maps to the 3' UTR of the gene, which is common to all isoforms. One explanation for the difference in the results regarding allelic expression could be that our interrogated exon would be subjected to alternate splicing and, in this case, preferential expression could affect splice variants differently and be detected or not depending on the transcript being amplified. It has been shown for other transcripts, such as *Blcap*, that global analysis of expression can mask isoform-specific parent-of-origin expression of alternate isoforms with lower transcription levels (Schultz et al., 2009). Assessment of the origin of expression by Sanger sequencing, used here for *PHACTR2*, is only semi-quantitative, but no data indicated a parent-of-origin expression bias. Previous work in monochromosomal hybrid mouse cell lines, each containing a human chromosome of defined parental origin, had also shown biallelic expression of *PHACTR2* (KIAA06080) (Arima et al., 2000). A more quantitative approach, such as pyrosequencing, could be more adequate to analyze so-called "partially imprinted" transcripts. Recent work in our group suggests, however, that *PHACTR2* expression undergoes Allelic Imbalance favouring one of the genotypes, but in a parent-of-origin independent manner (Camprubí C., unpublished data). We also showed that CpG 43, the CpG island associated with the 3' most promoter of *PHACTR2* was not differentially methylated in placenta or lymphocytes, although this fact would not preclude the possibility of imprinting involving a *cis* regulated mechanism controlled by the *PLAGL1* DMR.

The CpG island associated with the *PLAGL1/HYMAI* promoter displays specific methylation of the maternal allele. The *PLAGL1* DMR was first described in a screening for imprinted genes (Kamiya et al., 2000). Further work determined that it was unmethylated in sperm (Arima el al., 2001) and that it could act as an imprinting control region (Arima et al., 2006). We confirmed that CpG 118 is differentially methylated in peripheral blood as well as in

placental tissue. The average values of percentage methylation tend to be over 50% using the methylation array, which is also seen with other techniques (Turner el al., 2010). Allelic-specific methylation was confirmed by COBRA and bisulphite sequencing and by a steep reduction in methylation (to 26,4%) values in a pUPD6 cell line. The remaining CpG islands in the region were all unmethylated in placental tissue.

2. EXPRESSION OF THE 6q24 IMPRINTED TRANSCRIPTS IN FETAL GROWTH

2.1. NORMAL FETAL GROWTH

Imprinted genes have been shown to be expressed during embryonic development in mammals and expression patterns have been subjected to extensive investigation in the mouse (http://www.eurexpress.org/). Co-ordinated down-regulation of their expression after birth has also been implicated as a control mechanism of final body size (Lui et al., 2008).

After showing that *PLAGL1* and *HYMAI* transcripts are present at early stages of development, predominantly in the placenta, we subsequently investigated the relationship between expression and fetal growth. This was undertaken by performing quantitative real time PCR (qPCR) on placenta of two clinically characterised (1) healthy and (2) IUGR cohorts of live-born babies at different gestational ages.

2.1.1. LEVELS OF EXPRESSION OF *PLAGL1* DO NOT CORRELATE WITH PARAMETERS OF FETAL GROWTH IN HEALTHY PREGNANCIES

PLAGL1 is the protein-coding transcript in the 6q24.2 region. The PLAGL1 protein is a transcription factor displaying antiproliferative activities (Bilanges et al., 2001). *Plagl1/PLAGL1* influences fetal size, but the mechanisms involved are unknown. The *Plagl1*-knock out mouse displays an IUGR phenotype (Varrault et al., 2006), which is surprising when this KO should be inactivating a gene which contributes to cell-cycle arrest and apoptosis. However, defects in placental structure and function do not seem to underlie the growth reduction in this model, which suggests a different action for this gene in the embryo.

In humans, excessive and not lack of *PLAGL1* expression could potentially contribute to the low birth weight phenotype of patients with paternal UPD or duplication of the region or LOM of the DMR. Increased expression in the placenta may negatively influence placental development and, consequently, reduce fetal growth, but the main impact might be exerted through disturbances in the production of insulin, which is a major growth factor in human prenatal development. Due to the lack of capacity of the maternal insulin to cross the

placental barrier, insulin synthesis in the fetal pancreas is essential for intrauterine growth (Beardsall et al., 2008).

In our data, we could not demonstrate a relationship between placental levels of expression of *PLAGL1* and fetal growth in a cohort of healthy Caucasian singleton pregnancies. We explored all *PLAGL1* transcripts globally and specifically the imprinted P1 that originates from the DMR. Both sets of primers were designed to amplify short and long splice variants, containing or not the alternate exon seven, which encodes the first two zinc fingers of the protein. This way, the experiment targeted transcripts originating both from the 5- (Δ2) and the 7-zinc finger isoforms of the protein, which are more efficient at inducing cell cycle arrest and apoptosis, respectively.

One study investigating other key imprinted gene involved in growth found a significant and negative correlation between placental *PHLDA2* expression and birth weight (Apostolidou et al., 2007). This gene is mainly involved in placental development in mouse models (Salas et al., 2004; Tunster et al., 2010), making it an ideal candidate to explore in placental tissue. Extrapolation from mouse data has however not always given similar results in humans. The investigations on *IGF2*, for example, have been based on the fact that it is a prime regulator of placental growth and function in the mouse, with the placental-specific isoform P0. However, association between human placental expression of *IGF2* and birthweight was not seen in a large study of normal pregnancies (Apostolidou et al., 2007). This could be due to the lack of placental-specific *IGF2* isoform in the human, where P0, also present, is expressed and imprinted in all embryonic and extraembryonic tissues (Monk et al., 2006b) or because its expression level is not important at term.

If a range of levels of expression of *PLAGL1* and its influence in endocrine pancreatic secretion were to be involved in determining size at birth, tissue-specific changes in expression might not be found in our placental samples. The only other available tissue from the newborn babies is cord blood, but unfortunately *PLAGL1* is known to be expressed at very low levels and from its biallelic P2 promoter in white blood cells (Frost et al., 2010).

True variation in *PLAGL1* levels according to birth weight could have been missed due to regional changes of expression within a given placenta, but this has previously been shown to be negligible (McMinn et al., 2006). Another possibility is that levels of expression of *PLAGL1* would exert an independent role in the placenta by its transcription factor activity during early stages of development, when placentation is taking place. We have detected high levels of expression of *PLAGL1* in first trimester placenta. In this situation, our analysis of term placental

tissue would miss the appropriate time window. Sampling of early human placentas would involve technical and ethically complex considerations.

In conclusion, placental expression of *PLAGL1* at term, both globally and from its imprinted P1 promoter, as analyzed by quantitative real time PCR, was not related to birth weight in our cohort of healthy term singleton pregnancies.

2.2. INTRAUTERINE GROWTH RESTRICTION

During the course of this study, other groups (*FAM164B*, Docherty et al., 2010) and our own (*PLAGL1* P3 and P4) identified new transcripts in the 6q24 region. *FAM164B* has a potential open reading frame (C6ORF94) and has been implicated in the IUGR phenotype of TNDM1 patients. P3 and P4 are new isoforms of *PLAGL1*, and also subjected to genomic imprinting. Due to the relevance of these findings, we decided to incorporate the study of these two isoforms in anomalies of fetal growth. We identified very low levels of expression of *FAM164B* in placenta and fetal tissues, making it unlikely that this transcript has a major relevance in human prenatal growth. These low expression levels, at the detection limits of reliable detection by qPCR also prevented further assessment of its role in IUGR.

The concept of IUGR has evolved from a definition regarding a threshold set at a certain percentile of birth weight to a complex disease affecting the blood flow and/or transfer of nutrients and oxygen from the mother to the fetus through the placenta. Analysis of placentas from IUGR pregnancies is the next logical step to unravel the underlying causes and mechanisms. Differences in expression and methylation of imprinted genes have been described in IUGR, even for some that had previously failed to show any correlation with growth parameters in normal pregnancies. IUGR might involve both processes common to normal fetal growth and others specifically altered in this condition.

For this reason, we decided to analyze our own cohort of placental samples corresponding to (1) uneventful and (2) complicated pregnancies. We aimed to compare the two groups regarding levels of expression of previously defined and newly identified transcripts in the 6q24 region.

2.2.1. LEVELS OF EXPRESSION OF *HYMAI* ARE HIGHER IN IUGR PLACENTAS.

Levels of expression of *HYMAI* were shown to be higher in IUGR placentas compared to those from normal pregnancies (p=0.018). This result continued to be significant after adjustment for variables shown to influence size at birth, like maternal size, parity and age. Some authors challenge the appropriateness of correcting birth weight data for these factors (Gluckman and Hanson, 2004), as all of them do, in fact, increase perinatal mortality, so that they might be considered to cause a reduction in fetal growth that carries adverse consequences and cannot therefore be defined as physiological (Lawn et al., 2005). In any case, our results remained unchanged in the adjusted analysis. In fact, logistic regression showed that increased levels of expression of *HYMAI* could be a risk factor for the presence of IUGR. On the contrary, levels of expression of this non-coding RNA showed no correlation with weight, birth length or head circumference at birth, suggesting a specific association with mechanisms of abnormal fetal growth *in utero* and not with anthropometric parameters at birth.

HYMAI is maternally imprinted and originates from the *PLAGL1* DMR (Arima et al., 2000). Its potential role in human disease is so far unknown. It maps to the minimal critical region of TNDM (Docherty et al., 2010) and shows LOI in TNDM patients (Arima et al., 2001; Mackay et al., 2006b), although the most obvious candidate for the phenotype is *PLAGL1*. *PLAGL1* has been shown to be expressed in the developing pancreas and seems to have a function in the perinatal secretion of insulin in humans and in animal models (Ma et al., 2004).

Long non-coding RNAs are a frequent feature of imprinting clusters and their promoters are usually associated with the ICRs. Most are expressed from the complementary allele with respect to the coding sequences they overlap and are translated from the antisense strand (O'Neill, 2005), although some originate, like *HYMAI*, from the same parental allele and DNA strand. Transcription of both strands of the same locus has been described for the mesoderm-specific transcript *MEST/PEG1* and its intronic transcript *MESTIT1* in human chromosome 7q32 (Nakabayashi et al., 2002) and the *IGF2- IGF2* antisense (*IGF2AS/ PEG8*) in human chromosome 11p15.5 (Moore T et al., 1997; Okutsu et al., 2000), which are all paternally expressed. Proposed functions for antisense transcripts include roles in transcriptional inhibition, interference with mRNA stability or with splicing, processing or nuclear export of mRNA or inhibition of translation (O´Neill, 2005). The mouse *Zfp127* and its antisense are expressed

from the paternal allele and it has been proposed that transcription from one strand precludes that on the other strand, as mutually exclusive expression of the genes has been found in different cell types during development (Jong et al., 1999). Antisense transcripts to the *IGF2* gene could act to prevent translation of *IGF2* in Wilm's tumors (Baccarini et al., 1993).

HYMAI is a unique case in that it is expressed from the same allele an in the same orientation as the overlapping *PLAGL1* P1. This fact suggests that they probably share the epigenetic mechanisms responsible for their imprinting status (maintained by the differential methylation of their promoter-associated CpG island) and even that the ncRNA might play a role in the regulation of the imprinted expression of *PLAGL1*, as seen for other clusters. The mechanisms underlying this have to be different from those proposed for the ncRNAs with opposite parental origin. Competition for promoters, enhancer elements or transcription factors is unlikely, as it would result in an opposite parent-of-origin regulation (like in the case of *Air-Igf2r*). In addition the chromatin conformation around *HYMAI* must be opened, as it does allow for transcription of *PLAGL1* from the same allele. In other imprinted clusters it has been shown that untranslated RNAs are capable of recruiting chromatin-modifying enzymes, like histone-methyl-transferases (HMT), which bring about repressive modifications (Kanduri et al., 2006). It could be speculated that *HYMAI* does recruit chromatin-remodelling complexes but of the opposite sign, like histone acetylases or other enzymes responsible for depositing permissive modifications. The overall conservation of the antisense lncRNAs involved in imprinting mechanisms is low, even for exon-intron arrangement, suggesting that expression might be more important than the actual sequence (Nakabayashi et al., 2002) or that only particular motifs, which would interact with histone modifying enzymes, have been conserved. To date, the structure of the mouse orthologue of human *HYMAI* has not been described, but the analysis of conservation of regulatory sequences as well as transcript truncation experiments would help clarify this hypothesis.

Through these or other mechanisms, *HYMAI* could affect expression of *PLAGL1* in *cis*. Transcriptional levels of *HYMAI* and *PLAGL1* were significantly and positively correlated (r= 0.479, p= 0.02) in control samples, but if the effect on growth was to be *PLAGL1*-mediated, differences in levels of expression would be also expected for this gene, which was not observed. It could be speculated that high levels of *HYMAI* in the first trimester placenta could coincide with a transient increase in the levels of *PLAGL1* at critical gestational stages but that these would have been normalized again in later gestation. As another possibility, abnormalities in regulation might occur during IUGR leading to a loss of coordination between

the expression of *PLAGL1* P1 and *HYMAI*, as suggested by the loss of correlation between their levels in the IUGR placentas (see Section 2.3.2.4. in Results).

Alternatively, *HYMAI* might exert a *PLAGL1*-independent effect on fetal development. Emerging evidence supports the role of non-coding RNAs in the regulation of gene expression by participating in modulation of the activity of chromatin-modifying enzymes or contributing to specific higher order loops (reviewed in Koziol and Rinn, 2010. See *Figure 23*). These actions can be exerted onto neighbouring sequences (in *cis*) and also affect regions located elsewhere in the genome, even in different chromosomes. If this were the case, *HYMAI* could participate in its own "imprinting network" in embryonic growth, as has been proposed for *Plagl1* (Varrault et al., 2006). The *Plagl1* knockout model which targets the last two exons of *Plagl1* leaves the orthologous *Hymai* region unaffected, causing a network effect solely attributable to *Plagl1*. If a mouse *Hymai* exists, then specific targeting experiments would be needed to assess a possible role in a similar gene network.

The changes in *HYMAI* levels of expression were not related to changes in levels of methylation of the DMR or to loss of imprinting, as we found no difference in levels of methylation at the DMR or in preservation of monoallelic expression between AGA and IUGR placentas (Section 2.3.2.5. in Results). It must then be due to the presence of anomalies in the regulatory mechanisms in the IUGR placentas, which could have also caused uncoupling between the control of *HYMAI* and *PLAGL1* P1 (see next Section).
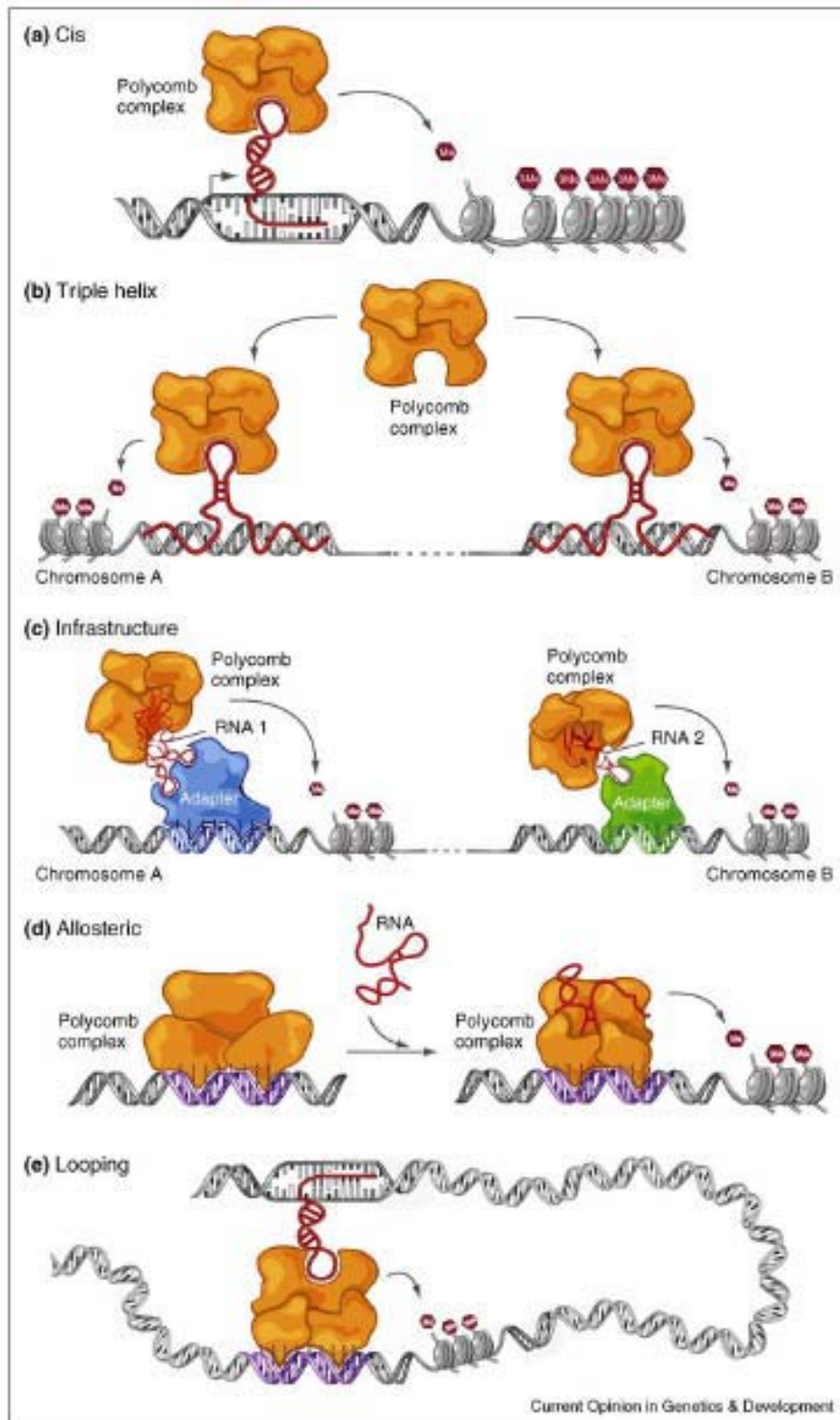
Figure 23: *Possible mechanisms of action of lncRNAs for influencing chromatin states.*
From Koziol and Rinn, 2010.   a) Recruitment of chromatin-modifying enzymes by direct sequence recognition, acting in cis *(as represented) or* trans. b) Recruitment in trans *by RNA-DNA triplex formation, not requiring sequence complementarity. c) and e) Structural adaptors between chromatin remodeling complexes and DNA binding proteins (c) or chromatin remodeling complexes and distant DNA sequences (e), forcing specific looping structures. d) Alosteric modulators of chromatin remodeling complexes.*

2.2.2. CHANGES IN CORRELATION BETWEEN EXPRESSION OF *PLAGL1* P1 AND *HYMAI* IN IUGR

A statistically significant positive correlation between the expression of *PLAGL1* P1 and *HYMAI* was apparent in placentas of control babies (spontaneously conceived, normally grown). In IUGR pregnancies expression of *HYMAI* was increased without changes in the levels of *PLAGL1* P1 and the aforementioned correlation was lost. No differences in the levels of methylation of the DMR that contains the promoter were apparent in IUGR samples (see Section 2.3.3. in Results). They would have been expected to affect both *HYMAI* and *PLAGL1* P1 in a similar manner, without modifying the relationship between them.

It seems unlikely that altered regulation leading to uncoupling of *HYMAI* and *PLAGL1* P1 expression is related to changes in transcription factors, as this would probably involve both transcripts, originating from the same promoter, in a parallel manner. Postranslational modifications or other processes affecting RNA stability could explain an increased detection of *HYMAI* without concomitant changes in *PLAGL1* P1.

2.2.3. LEVELS OF EXPRESSION OF *PLAGL1* ARE LOWER IN ART PLACENTAS.

No differences in expression of *PLAGL1* and its different isoforms were found between appropriately grown or IUGR placentas at different gestational ages in the cohort as a whole. However, levels of *PLAGL1* transcripts, both global and per individual isoforms, were lower in placentas of babies conceived by assisted reproduction techniques (ART), even after adjustment for multiple pregnancy, parity, gestational age and size and gender of the newborn. There were no significant differences regarding levels of *HYMAI* or methylation of the promoter-associated DMR.

About 1% of births and more than 30% of twin births are a result of ART in the United Kingdom (ESHRE, 2005) and these figures are similar in most developed countries. Manipulation of gametes and preimplantational embryos has been shown to carry a risk of aberrations in the epigenetic processes that take place at these critical stages of early development. Altered levels of imprinted genes have been reported in both mouse and human after the use of assisted reproduction (Fortier et al., 2008; Katari et al., 2009) and the placenta

has been suggested to have increased susceptibility, although some studies found more significant DNA methylation differences when analyzing cord blood (Katari 2009). Because of the conflicting results regarding abnormalities in the acquisition of imprints and methylation in individuals conceived by ART (see also Introduction, Section 3.3., page 46), and in the absence of strong evidence, we decided not to exclude this group from our sample collection and recorded this data as part of the clinical information for further analysis.

Decreased levels of expression of *PLAGL1* were not attributable to methylation defects. This is in agreement with other studies of imprinted gene expression after assisted reproduction. In the mouse, changes in *Igf2* mRNA levels in mid-gestation placentas, for example, was caused neither by LOM nor by LOI, although the rate of biallelic expression of *H19* (defined as >10% expression originating from the paternal allele as measured by allele-specific qPCR) was greater after hormonal treatment (Fortier et al., 2008). While altered expression of these and other imprinted genes were caused by hypomethylation of the ICRs, no epigenetic cause was found for others (Rivera et al., 2008), similar to our findings. In human samples, the presence or magnitude of expression changes could not be inferred from abnormal methylation (Katari et al., 2009). Incidentally, assessment of the mouse and human *Plagl1/PLAGL1* DMRs by bisulfite PCR sequencing or a methylation array after hormonal treatment with or without embryo transfer has demonstrated robust preservation of maternal methylation in oocytes, placenta and cord blood (Sato et al., 2007; Katari et al., 2009). We have reached the same conclusion after pyrosequencing analysis in our small subgroup of ART placentas displaying low expression of *PLAGL1*. Different steps in assisted reproduction, from hormonal treatment to gamete transfer, could be responsible for the described defects. Our sample was too small and the cycle data too general to draw any conclusions regarding this point.

2.2.4. LEVELS OF EXPRESSION OF *PLAGL1* ARE LOWER IN THE PLACENTA OF IUGR GIRLS. GENDER-DEPENDENT CORRELATION BETWEEN *PLAGL1* EXPRESSION AND IUGR.

The global expression of *PLAGL1* was significantly lower in the placenta of IUGR girls (p 0.023) but not boys (p 0,178). Downregulation of *PLAGL1* in placentas with maternal vascular

hypoperfusion had previously been suggested in a microarray screening study (McMinn et al., 2006). Gender was not specified or taken into account in the analysis. In our data, expression of *PLAGL1*, both global and from the imprinted promoter, correlated with the presence of IUGR specifically in girls and not boys in the unadjusted and adjusted analysis.

Differences in parent-of-origin expression of imprinted and non-imprinted genes have recently been shown to be a frequent feature in somatic tissues in the mouse, like liver, muscle, adipose tissue and regionally in brain (Yang et al., 2006; Gregg et al., 2010b). One of the genes involved in this divergence was *Mrpl48*, which belongs to the same family of mitochondrial ribosomal proteins as our reference gene. For this reason we decided to compare levels of expression of *MRPL19* in the placentas of male and female babies. We found no statistical difference (average CT in boys 22,05±0,93, in girls 22,33±1,14, p 0,239) to suggest that the gender-dependent correlation between *PLAGL1* expression and IUGR could have been an artefact due to differential expression of *MRPL19*.

Most of the gender-related changes in gene expression in the former studies are likely hormonal dependent, as suggested by the fact that they are only evident in post-pubertal animals (Gregg et al., 2010a). Gender differences in expression in the placenta could be explained by transient exposure to testosterone secreted by the fetal testis peaking at 13-15 weeks of pregnancy or by the sex chromosome complement, which has also been shown in other tissues to influence autosomal gene expression hormone-independently. This can involve Y-linked transcriptional regulators (mainly by the SRY transcription factor activity), functional differences between X-and Y- linked homologous alleles, gene-dosage differences through potential escape from gene inactivation in females or sequestering of rate-limiting heterochromatic factors in large regions of heterochromatin corresponding to the inactive X in females (Wijchers and Festenstein, 2011).

Whether by hormonal or genetic mechanisms, differences between male and female placental gene expression and function are progressively being uncovered and it has been suggested that the fetal gender should be accounted for when studying the placenta (Clifton, 2010). Our results support the idea that gender-specific mechanisms could apply to the placenta in intrauterine growth restriction.

2.2.5. CHANGES IN EXPRESSION IN *PLAGL1/HYMAI* ARE NOT DUE TO LOI: PRESERVED IMPRINTED EXPRESSION IN PREMATURE, IUGR AND ART PLACENTAS.

Monoallelic expression of paternal origin was confirmed in all the individuals that were heterozygous for the SNPs tested (12 for *PLAGL1*, 20 for *HYMAI*). The samples assessed spanned all groups of gestational age and intrauterine growth trajectories, as well as both spontaneous and assisted conceptions. Some degree of transcription from imprinted alleles has been described in placentas of healthy term pregnancies, usually when assessed by high-sensitivity techniques. The contribution of the silenced copy to total expression is usually under 10%, although it has been reported to be up to 50% or more in a small subset of individuals, particularly for some genes, such as *IGF2* and *PEG3* (Lambertini et al., 2008). In a cohort of 23 family trios (placenta,maternal and paternal blood) one case showed biallelic expression of *IGF2* and another of *DLK1* (Daelemans et al., 2010). These studies would predict a presumed prevalence of LOI in at least one imprinted loci in 8- 33% of normal placentas. These results have not been replicated in investigations of placentas of normal or overgrown babies when testing expression with other techniques (SNaPshot or single nucleotide primer extension, RFLP or Restriction Fragment Length Polymorphisms or Sanger sequencing) (Guo et al., 2008; Vambergue et al., 2007; Apostolidou et al., 2007) as opposed to real-time PCR and microarrays. This highlights the necessity for standardization of the term "Loss of Imprinting" when applying highly sensitive techniques for transcript detection.

A single study investigating involvement of aberrant imprinting of the 11p15.5 imprinted clusters in IUGR found *H19* LOI together with loss of methylation of the ICR of the region, but unaffected *IGF2* monoallelic expression in 1/24 SGA placentas. This sample originated from a case of spontaneous delivery at 38 weeks, a record of normal Doppler flow studies during pregnancy and an unremarkable placental pathology (Guo et al., 2008).

In summary, sporadic deregulation of imprinting mechanisms has been described in placentas of healthy and moderately growth restricted infants. Although in these reports thorough clinical evaluation of the babies had not been performed, they were collected as phenotypically normal, making the possibility of an imprinting syndrome unlikely.

Unfortunately, investigation of paired fetal samples from individuals with altered imprinted expression in the placenta was not carried out in these studies, to test if, as some experimental animal results suggest, the fetus might be more resistant to this kind of epigenetic changes (Mann et al., 2004). These studies demonstrated heterogeneous involvement of specific genes, and, when assessed, *PLAGL1* was found to maintain a consistent pattern of imprinted expression. This was also the case in our cohort for *HYMAI* and all imprinted isoforms of *PLAGL1* in both normal and complicated pregnancies.

3. COMPARISON OF LEVELS OF METHYLATION OF THE *PLAGL1/HYMAI* PROMOTER-ASSOCIATED CpG ISLAND BETWEEN AGA AND IUGR PLACENTAS

3.1. METHYLATION OF THE *PLAGL1/HYMAI* DMR DOES NOT CORRELATE WITH THE PRESENCE OF IUGR

Levels of methylation at the *PLAGL1/HYMAI* DMR were analyzed by pyrosequencing after bisulfite conversion of the DNA extracted from placental tissues. No loss of methylation was apparent at the DMR in any sample, whether IUGR, premature or ART, consistent with the maintained imprinted expression of *PLAGL1* and *HYMAI*. There was also no relationship between levels of methylation at the *PLAGL1* DMR and maternal or fetal size, gestational age, presence of IUGR or any other of the clinical variables analyzed.

Methylation changes specific to the placenta might be diluted during sampling processing if contamination by other tissues is present (Bourque et al., 2010). Special care was taken in our samples to strip membranes and avoid decidual tissue that could interfere with true methylation values, but different proportions of cell types (villous trophoblast, fetal mesenchyma or endothelium) in the biopsies could also contribute to mask any specific changes.

The CpG island constituting the *PLAGL1/HYMAI* DMR contains 118 CpG dinucleotides. We have analyzed 10 positions in the central region of the 931 base pair island (see *Figure 24*). Changes affecting the region heterogeneously or a mosaic defect in low proportion could have been missed in our experimental approach. On the other hand, changes might be indeed absent, as this DMR seems to possess a robust methylation status that is minimally susceptible to changes, as highlighted by its resistance to techniques involved in assisted reproduction as opposed to other DMRs. Moreover, coordinated mechanisms seem to be in place for the control of the whole CpG island, and altered methylation in the 6q24 region seems to be an all-or-nothing phenomenon in the TNDM patients (Mackay et al., 2005). Also, certain CpGs outside our assay might have specific roles, like binding of methylation-sensitive proteins that make their methylation status more relevant for the control of expression than the global levels throughout the island. However, previous extensive analysis throughout the CpG island in TNDM patients did not identified such specific positions (Mackay et al., 2005). Methylation of other regulatory regions outside the CpG island itself might be important in imprint maintenance, but this has not been described for the *PLAGL1* DMR (Reinhart et al., 2006).
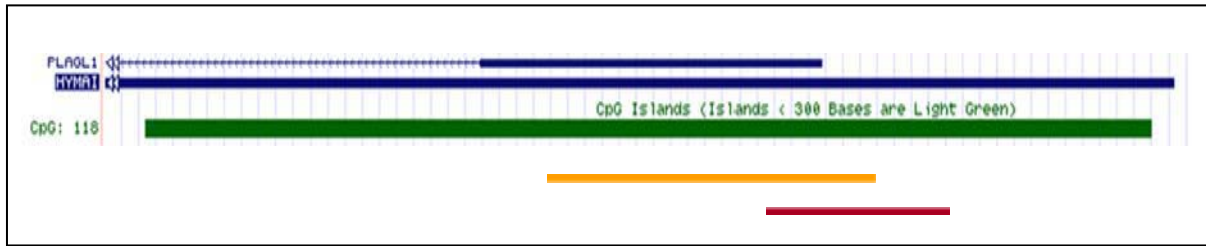
Figure 24: *Location of the regions assessed for methylation status in the 6q24 DMR.*
In orange: region assessed by bisulphite PCR sequencing in Mackay et al., 2005. In red: region analysed by pyrosequencing in the present study.

Higher levels of *HYMAI* transcripts in IUGR placentas and lower levels of *PLAGL1* in placentas of babies conceived following assisted reproduction were not paralleled by loss or gain of methylation, respectively. Most promoter-associated CpG islands are unmethylated independently of the levels of expression and absence or presence of methylation are permissive or not for expression, but not involved in fine control (Jones and Takai, 2001). Other authors have also found differences in levels of expression of imprinted genes without obvious methylation changes in the corresponding ICRs, probably reflecting transcriptional deregulation by other trans-acting factors, such as transcription factor binding (McMinn et al., 2006). There is evidence that, in postnatal life, the expression of *Plagl1* in the mouse can be down-regulated in a process that does not involve changes in methylation of the DMR (Lui et al., 2008; Marcelin et al., 2009). This could involve transcription or chromatin-remodeling factors. Expression of imprinted genes is also regulated by non-epigenetic mechanisms, e.g. *Igf2* and IMP1 (Igf2 mRNA binding protein 1) (Hansen et al., 2004).

Our results show no evidence that altered methylation of the *PLAGL1* DMR plays a role in the altered expression of *PLAGL1* and *HYMAI* in IUGR and ART placentas.

CONCLUSIONS

CONCLUSIONS

1. *PLAGL1* and *HYMAI* are expressed in human fetal tissues during development and in the term placenta.

2. *PLAGL1* and *HYMAI* are the only genes subjected to genomic imprinting in the 6q24.2 locus and the *HYMAI/PLAGL1* P1 promoter-associated CpG island is the sole differentially methylated region. The CpG islands associated to the promoters of *DEADC1/ADAT2*, *FUCA2*, *PHACTR2*, *LTV1*, *SF3B5*, *STX11* and *UTRN* and the non-imprinted promoter of *PLAGL1* (P2) are universally unmethylated. *DEADC1/ADAT2*, *PEX3*, *FUCA2*, *PHACTR2*, *LTV1*, *SF3B5*, *STX11* and the EST BC033369 are biallelically expressed in a wide range of fetal tissues and in term placenta.

   PLAGL1 displays a complex pattern of expression with two additional promoter regions downstream to the main P1 promoter (P3 and P4). These new isoforms are also paternally expressed. The promoters lack associated CpG islands.

3. Levels of expression of *PLAGL1* in the placenta do not correlate with fetal size in a cohort of healthy, singleton, term pregnancies.

4. Levels of expression of *PLAGL1* in the placenta, both globally and from the imprinted promoter P1 correlate significantly with the presence of Intrauterine Growth Restriction in girls, but not in boys or in the cohort as a whole. Global levels of expression of *PLAGL1* were also significantly lower in placentas of IUGR girls than in those from normally grown controls of the same gender.

Levels of expression of the non-coding RNA *HYMAI* are higher in the placentas of pregnancies complicated by Intrauterine Growth Restriction at different gestational ages and correlate with the presence of this complication in a multivariate analysis.

Levels of expression of the imprinted *PLAGL1* P1 transcript correlate with levels of expression of *HYMAI* in normal placentas. This correlation is lost in IUGR placentas, maybe as a result of fine changes in regulation of expression in the region.

Levels of expression of *PLAGL1* and its imprinted transcripts are lower in the placentas of pregnancies conceived by Assisted Reproduction Techniques after adjustment for confounding factors.

The abnormalities in levels of expression of *PLAGL1* and *HYMAI* in Intrauterine Growth Restricted placentas and after assisted conceptions are not due to Loss of Imprinting. Paternal monoallelic expression is preserved in all the placentas of both normal and abnormal gestations at all ages analyzed.

5. Loss of Methylation or changes in the levels of methylation at the *PLAGL1* DMR in the placenta are not related to the abnormalities in levels of expression of *PLAGL1* and *HYMAI* in Intrauterine Growth Restriction or after assisted conception. There are no significant differences in the levels of methylation of the *PLAGL1* DMR in the placenta between normal and IUGR or ART pregnancies in our cohort.

REFERENCES

Abdollahi A, Godwin AK, Miller PD, Getts LA, Schultz DC, Taguchi T, Testa JR, Hamilton TC. Identification of a gene containing zinc-finger motifs based on lost expression in malignantly transformed rat ovarian surface epithelial cells. Cancer Res. 1997: 2029-34.

Adkins RM, Somes G, Morrison JC, Hill JB, Watson EM, Magann EF, Krushkal J. Association of birth weight with polymorphisms in the *IGF2*, *H19*, and *IGF2R* genes. Ped Res. 2010; 68: 429-34.

Alam S, Zinyk D, Ma L, Schuurmans C. Members of the *Plag* gene family are expressed in complementary and overlapping regions in the developing murine nervous system. Dev Dyn. 2005; 234: 772-82.

Alexander GR, Himes JH, Kaufman RB, Mor J, Kogan M. A United States national reference for fetal growth. Obstet Gynecol. 1996; 87 (2): 163- 8.

Alvino G, Cozzi V, Radaelli T, Ortega H, Herrera E, Cetin I. Maternal and fetal fatty acid profile in normal and intrauterine growth restriction pregnancies with and without preeclampsia. Pediatr Res. 2008; 64: 615-20.

Angiolini E, Fowden A, Coan P, Sandovici I, Smith P, Dean W, Burton G, Tycko B, Reik W, Sibley C, Constancia M. Regulation of placental efficiency for nutrient transport by imprinted genes. Placenta. 2006; 27 (suppl. A, Trophoblast Research): S98-102.

Apostolidou S, Abu-Amero S, O´Donoghue K, Frost J, Olafsdottir O, Chavele KM, Whittaker JC, Loughna P, Stanier P, Moore GE. Elevated placental expression of the imprinted *PHLDA2* gene is associated with low birth weight. J Mol Med. 2007; 85: 379-87.

Arima T, Drewell RA, Arney KL, Inoue J, Makita Y, Hata A, Oshimura M, Wake N, Surani MA. A conserved impinting control region at the *HYMAI/ZAC* domain is implicated in transient neonatal diabetes mellitus. Hum Mol Genet. 2001; 10(14): 1475-83.

Arima T, Drewell RA, Oshimura M, Wake N, Surani MA. A novel imprinted gene, *HYMAI*, is located within an imprinted domain on human chromosome 6 containing *ZAC*. Genomics. 2000; 67: 248-55.

Arima T, Kamikihara T, Hayashida T, Kato K, Inoue T, Shirayoshi Y, Oshimura M, Soejima H, Mukai T, Wake N. *ZAC*, *LIT1 (KCNQ1OT1)* and *p57KIP2 (CDKN1C)* are in an imprinted gene network that may play a role in Beckwith- Wiedemann syndrome. Nucleic Acids Res. 2005; 33(8): 2650-60.

Arima T, Yamasaki K, John RM, Kato K, Sakumi K, Nakabeppu Y, Wake N, Kono T. The human *HYMAI/PLAGL1* differentially methylated region acts as an imprint control region in mice. Genomics. 2006; 88: 650-8.

Arnaud P, Feil R. Epigenetic deregulation of genomic imprinting in human disorders and following assisted reproduction. Birth Defects Res C Embryo Today. 2005; 75: 81-97.

Arnaud P, Monk D, Hitchins M, Gordon E, Dean W, Beechey CV, Peters J, Craigen W, Preece M, Stanier P, Moore GE, Kelsey G. Conserved methylation imprints in the human and mouse

GRB10 genes with divergent allele expression suggests differential reading of the same mark. Hum Mol Genet. 2003; 12: 1005-19.

Azzi S, Rossignol S, Steunou V, Sas T, Thibaud N, Danton F, Le Jule M, Heinrichs C, Cabrol S, Gicquel C, Le Bouc Y, Netchine I. Multilocus methylation analysis in a large cohort of 11p15-related foetal growth disorders (Russell Silver and Beckwith Wiedemann syndromes) reveals simultaneous loss of methylation at paternal and maternal imprinted loci. Hum Mol Genet. 2009; 18: 4724-33.

Baccarini P, Fiorentino M, D'Errico A, Mancini AM, Grigioni WF. Detection of anti-sense transcripts of the Insulin-like Growth Factor-2 gene in Wilm´s tumor. Am J Pathol. 1993; 143: 1535- 42.

Bannister AJ, Kouzarides T. Regulation of chromatin by histone modifications. Cell Res. 2011; 21: 381-95.

Barker DJ, Hales CN, Fall CH, Osmond C, Phipps K, Clark PM. Type 2 (non-insulin-dependent) diabetes mellitus, hypertension and hyperlipidaemia (syndrome X): relation to reduced fetal growth. Diabetologia. 1993; 36: 62-7.

Barker DJP, Osmond C, Forsén TJ, Kajantie E, Eriksson JG. Trajectories of growth among children who have coronary events as adults. NEJM. 2005; 353 (17): 1802-9.

Barker DJP. Adult consequences of fetal growth restriction. Clinical Obstet Gynecol. 2006; 49: 270- 83.

Beardsall K, Diderholm BM, Dunger DB. Insulin and carbohydrate metabolism. Best Pract Res Clin Endocrinol Metab. 2008; 22: 41-55.

Beardsall K, Ogilvy-Stuart AL, Ahluwalia J, Thompsom M, Dunger DB, The continuous glucose monitoring sensor in neonatal intensive care, Arch Dis Child Fetal Neonatal Ed. 2005; 90: 307-310.

Beck F, Samani NJ, Byrne S, Morgan K, Gebhard R, Brammar WJ. Histochemical localization of *IGF-I* and *IGF-II* mRNA in the rat between birth and adulthood. Development. 1988; 104: 29-39.

Beechey C. A reassessment of imprinting regions and phenotypes on mouse chromosome 6: *Nap1l5* locates within the currently defined sub-proximal imprinting region. Cytogenet Genome Res. 2004; 107: 108-14.

Begemann M, Spengler S, Kanber D, Haake A, Baudis M, Leisten I, Binder G, Markus S, Rupprecht T, Segerer H, Fricke-Otto S, Mühlenberg R, Siebert R, Buiting K, Eggerman T. Silver-Russell patients showing a broad range of ICR1 and ICR2 hypomethylation in different tissues. Clin Genet. 2011; 80: 83-88.

Beisel C, Paro R. Silencing chromatin: comparing modes and mechanisms. Nature Rev Genet. 2011; 12: 123-35.

Bell AC, Felsenfeld G. Methylation of a CTCF-dependent boundary controls imprinted expression of the *Igf2* gene. Nature. 2000; 25: 482-5.

Bernstein IM, Horbar JD, Badger GJ, Ohlsson A, Golan A, for the Vermont Oxford Network. Morbidity and mortality among very-low-birth-weight neonates with intrauterine growth restriction. Am J Obstet Gynecol. 2000; 182: 198- 206.

Bestor T. The DNA methyltransferases of mammals. Hum Mol Genet. 2000; 9: 2395-402.

Bilanges B, Varrault A, Basyuk E, Rodriguez C, Mazumdar A, Pantaloni C, Bockaert J, Theillet C, Spengler D, Journot L. Loss of expression of the candidate tumor suppressor gene ZAC in breast cancer cell lines and primary tumors. Oncogene. 1999; 18: 3979-88.

Bilanges B, Varrault A, Mazumdar A, Pantaloni C, Hoffmann A, Bockaert J, Spengler D, Journot L. Alternative splicing of the imprinted candidate tumor suppressor gene *ZAC* regulates its antiproliferative and DNA binding activities. Oncogene. 2001; 20: 1246-53.

Blagitko N, Schulz U, Schinzel AA, Ropers HH, Kalscheuer VM. *γ2-COP*, a novel imprinted gene on chromosome 7q32, defines a new imprinting cluster in the human genome. Hum Mol Genet. 1999; 8: 2387-96.

Bloomfield FH, Oliver MH, Hawkins P, Campbell M, Phillips DJ, Gluckman PD, Challis JRG, Harding JE. A periconceptional nutritional origin for noninfectious preterm birth. Science. 2003; 300: 606.

Bourc'his D, Xu GL, Lin CS, Bollman B, Bestor TH. Dnmt3L and the establishment of maternal genomic imprints. Science. 2001; 294: 2536-9.

Bourque DK, Avila L, Peñaherrera M, von Dadelszen P, Robinson WP. Decreased placental methylation at the *H19/IGF2* imprinting control region is associated with normotensive intrauterine growth restriction but not preeclampsia. Placenta. 2010; 31:197-202.

Bowdin S, Allen C, Kirby G, Brueton L, Afnan M, Barratt C, Kirkman-Brown J, Harrison R, Maher ER, Reardon W. A survey of assisted reproductive technology births and imprinting disorders. Hum Repr. 2007; 22: 3237.

Brannan CI, Bartolomei MS. Mechanisms of genomic imprinting. Curr Opin Genet Dev. 1999; 9: 164- 70.

Bryan SM, Hindmarsh PC. Normal and abnormal fetal growth. Horm Res. 2006; 65 (suppl3): 19-27.

Carrascosa A, Yeste D, Copil A, Almar J, Salcedo S, Gussinyé M. Patrones antropométricos de los recién nacidos pretérmino y a término (24-42 semanas de edad gestacional) en el Hospital Materno-Infantil Vall d´Hebron (Barcelona) (1997-2002). An Pediatr (Barc) 2004; 60: 406-16.

Cavé H, Plak M, Drunat S, Denamur E, Czernichow P. Refinement of the 6q chromosome region implicated in Transient Neonatal Diabetes. Diabetes. 2000; 49: 108-13.

Chotalia M, Smallwood SA, Ruf N, Dawson C, Lucifero D, Frontera M, James K, Dean W, Kelsey G. Transcription is required for establishment of germline methylation marks at imprinted genes. Genes Dev. 2009; 23: 105-17.

Choufani S, Shuman C, Weksberg R. Beckwith- Wiedemann syndrome. Am J Med Genet Part C Semin Med Genet. 2010; 154C: 343-54.

Clifton VL. Review: sex and the human placenta: mediating differential strategies of fetal growth and survival. Placenta. 2010; 31: S33-9.

Constancia M, Angiolini E, Sandovici I, Smith P, Smith R, Kelsey G, Dean W, Ferguson-Smith A, Sibley CP, Reik W, Fowden A. Adaptation of nutrient supply to fetal demand in the mouse

involves interaction between the *Igf2* gene and placental transporter systems. PNAS. 2005; 102: 19219-24.

Constância M, Hemberger M, Hughes J, Dean W, Ferguson-Smith A, Fundele R, Stewart F, Kelsey G, Fowden A, Sibley C, Reik W. Placental-specific *IGF-II* is a major modulator of placental and fetal growth. Nature. 2002; 417: 945- 48.

Cooper C, Javaid MK, Taylor P, Walker-Bone K, Dennison E, Arden N. The fetal origins of osteoporotic fracture. Calcif Tissue Int. 2002; 70: 391-4.

Cvetkovic D, Pisarcik D, Lee C, Hamilton TC, Abdollahi A. Altered expression and loss of heterozygosity of the *LOT1* gene in ovarian cancer. Gynecol Oncol. 2004; 95: 449-55.

Daelemans C, Ritchie ME, Smits G, Abu-Amero S, Sudbery IM, Forrest MS, Campino S, Clark TG, Stanier P, Kwiatkowski D, Deloukas P, Dermtzakis ET, Tavaré S, Moore GE, Dunham I. High-throughput analysis of candidate imprinted genes and allele-specific gene expression in the human term placenta. BMC Genetics. 2010; 11: 25.

Desforges M, Sibley CP. Placental nutrient supply and fetal growth. Int J Dev Biol. 2010; 54: 377-90.

Deter RL. Individualized growth assessment: evaluation of growth using each fetus as its own control. Semin Perinatol. 2004; 28: 23-32.

Devriendt K. Genetic control of intrauterine growth. Eur J Obstet Gynecol. 2000; 92: 29- 34.

Diatloff-Zito C, Nicole A, Marcelin G, Labit H, Marquis E, Bellanné-Chantelot C, Robert JJ. Genetic and epigenetic defects at the 6q24 imprinted locus in a cohort of 13 patients with transient neonatal diabetes: new hypothesis raised by the finding of a unique case with hemizygotic deletion in the critical region. J Med Genet. 2007; 44: 31-7.

Docherty LE, Poole RL, Mattocks CJ, Lehmann A, Temple LK, Mackay DJG. Further refinement of the critical minimal genetic region for the imprinting disorder 6q24 transient neonatal diabetes. Diabetologia. 2010; 53: 2347-51.

Doherty AS, Mann MRW, Tremblay KD, Bartolomei MS, Schultz RM. Differential effects of culture on imprinted *H19* expression in the preimplantation mouse embryo. Biol Reprod. 2000; 62: 1526.

Drake AJ, Walker BR. The intergenerational effects of fetal programming: non-genomic mechanisms for the inheritance of low birth weight and cardiovascular risk. J Endocrinol. 2004; 180: 1-16.

Du X, Rousseau M, Ounissi-Benkalha H, Marchan L, Jetha A, Paraskevas S, Goodyer C, Polychronakos C. Differential expression pattern of *ZAC* in developing mouse and human pancreas. J Mol Hist. 2011; 42: 129-36.

Dunger DB, Petry CJ, Ong KK. Genetic variations and normal fetal growth. Horm Res. 2006; 65 (suppl 3): 34-40.

Eddy SR. Non-coding RNA genes and the modern RNA world. Nature Rev Genet. 2001; 2: 919-29.

Efstratiadis A. Genetics of mouse growth. Int J Dev Biol. 1998; 42: 955-76.

Eggermann T. Russell-Silver Syndrome. Am J Med Genet Part C Semin Med Genet. 2010; 154C: 355-64.

Evans HK, Wylie AA, Murphy SK, Jirtle RL. The neuronatin gene resides in a "micro-imprinted" domain on human chromosome 20q11.2. Genomics. 2001; 77: 99-104.

Ferguson-Smith AC, Moore T, Detmar J, Lewis A, Hemberger M, Jammes H, Kelsey G, Roberts CT, Jones H, Constancia M. Epigenetics and imprinting of the trophoblast- a workshop report. Placenta. 2006; 27 (suppl. A): S122-6.

Fitzpatrick GV, Soloway PD, Higgins MJ. Regional loss of imprinting and growth deficiency in mice with a targeted deletion of KvDMR1. Nat Genet. 2002; 32: 426-31.

Fortier AL, Lopes FL, Darricarrêre N, Martel J, Trasler JM. Superovulation alters the expression of imprinted genes in the midgestation mouse placenta. Hum Mol Genet. 2008; 17: 1653-65.

Fowden AL, Sibley C, Reik W, Constancia M. Imprinted genes, placental development and fetal growth. Horm Res. 2006; 65(suppl. 3): 50-58.

Fowden AL. The Insulin-like Growth Factors and feto-placental growth. Placenta. 2003; 24: 803-12.

Freathy RM, Mook-Kanamori DO, Sovio U, Prokopenko I, Timpson NJ, Berry DJ, Warrington NM, Widen E, Hottenga JJ, Kaakinen M, Lange LA, Bradfield JP, Kerkhof M, Marsh JA, Mägi R, Chen CM, Lyon HN, Kirin M, Adair LS, Aulchenko YS, Bennett AJ, Borja J, Bouatia-Naji N, Charoen P, Coin LJM, Cousminer DL, de Geus EJC, Deloukas P, Elliott P, Evans DM, Froguel P, The Genetic Investigation of ANthropometric Traits (GIANT) Consortium, Glaser B, Groves CJ, Hartikainen AL, Hassanali N, Hirschhorn JN, Hofman A, Holly JMP, Hyppönen E, Kanoni S, Knight BA, Laitinen J, Lindgren CM, The Meta-Analyses of Glucose and Insulin-related traits Consortium (MAGIC), McArdle WL, O'Reilly PF, Pennell CE, Postma DS, Pouta A, Ramasamy A, Rayner NW, Ring SM, Rivadeneira F, Shields BM, Strachan DP, Surakka I, Taanila A, Tiesler C, Uitterlinden AG, van Duijn CM, The Wellcome Trust Case Control Consortium (WTCCC), Wijga AH, Willemsen G, Zhang H, Zhao J, Wilson JF, Steegers EAP, Hattersley AT, Eriksson JG, Peltonen L, Mohlke KL, Grant SFA, Hakonarson H, Koppelman GH, Dedoussis GV, Heinrich J, Gillman MW, Palmer LJ, Frayling TM, Boomsma DI, Smith GD, Power C, Jaddoe VWV, Jarvelin MR & McCarthy MI for the Early Growth Genetics (EGG) Consortium. Variants in ADCY5 and near CCNL1 are associated with fetal growth and birth weight. Nature Genet. 2010; 42: 430-6.

Frost JM, Moore GE. The importance of imprinting in the human placenta. PLoS Genet. 2010; 6: e1001015.

Frost JM, Monk D, Stojilkovic-Mikic T, Woodfine K, Chitty LS, Murrell A, Stanier P, Moore GE. Evaluation of allelic expression of imprinted genes in adult human blood. PLoS ONE. 2010; 5: e13556.

Gardner RJ, Mackay DJG, Mungall AJ, Polychronakos C, Siebert R, Shield JPH, Temple K, Robinson DO. An imprinted locus associated with transient neonatal diabetes mellitus. Hum Mol Genet. 2000; 9: 589-96.

Gardner RL, Squire S, Zaina S, Hills S, Graham CF. Insulin-like Growth Factor-2 regulation of conceptus composition: effects of the trophectoderm and inner cell mass genotypes in the mouse. Biol Reprod. 1999; 60: 190- 195.

Gardosi J, Francis A. Customised Weight Centile Calculator – GROW-Centile v5.15/6.4 2009.

Gardosi J. Customized Fetal Growth Standards: rationale and clinical application. Semin Perinatol. 2004; 28: 33-40.

Gestation Network, www.gestation.net/ (v6.4: bulk centiles).

Ghosh P, Dahms NM, Kornfeld S. Mannose 6-phosphate receptors: new twists in the tale. Nature Rev Mol Cell Biol. 2003; 4: 202-13.

Gicquel C, Rossignol S, Cabrol S, Houang M, Steunou V, Barbu V, Danton F, Thibaud N, Le Merrer M, Burglen L, Bertrand AM, Netchine I, Le Bouc Y. Epimutation of the telomeric imprinting center region on chromosome 11p15 in Silver-Russell syndrome. Nat Genet. 2005; 37: 1003-7.

Gicquel C., El-Osta A., Le Bouc Y. Epigenetic regulation and fetal programming. Best Pract Res Clin Endocrinol Metab. 2008; 22(1):1-16.

Giudice LC, de Zeguer F, Gargosky SE, Dsupin BA, de las Fuentes L, Cristal RA, Hintz RL, Rosenfeld RG. Insulin-like Growth Factors and their binding proteins in the term and preterm human fetus and neonate with normal and extremes of intrauterine growth. J Clinical Endocrinol Metab. 1995; 80: 1548-55.

Gluckman PD, Hanson MA. Maternal constraint of fetal growth and its consequences. Semin Fetal Neonatal Med. 2004; 9: 419-25.

Gosden R, Trasler J, Lucifero D, Faddy M. Rare congenital disorders, imprinted genes, and assisted reproductive technology. Lancet. 2003; 361: 1975-77.

Grandjean V, Yaman R, Cuzin F, Rassoulzadegan M. Inheritance of an epigenetic mark: the CpG DNA methyltransferase I is required for de novo establishment of a complex pattern of non-CpG methylation. PLoS One. 2007; 2: e1136.

Gregg C, Zhang J, Butler JE, Haig D, Dulac C. Sex-specific parent-of-origin allelic expression in the mouse brain. Science. 2010a; 329: 682-5.

Gregg C, Zhang J, Weissbourd B, Luo S, Schroth GP, Haig D, Dulac C. High resolution analysis of parent-of-origin allelic expression in the mouse brain. Science. 2010b; 329: 643-8.

Guillemot F, Caspary T, Tilghman SM, Copeland NG, Gilbert DJ, Jenkins NA, Anderson DJ, Joyner AL, Rossant J, Nagy A. Genomic imprinting of *Mash2*, a mouse gene required for trophoblast development. Nat Genet. 1995; 9: 235-42.

Guo L, Choufani S, Ferreira J, Smith A, Chitayat D, Shuman C, Uxa R, Keating S, Kingdom J, Weksberg R. Altered gene expression and methylation of the human chromosome 11 imprinted region in small for gestational age (SGA) placentae. Dev Biol. 2008; 320: 79-91.

Gupta RA, Shah N, Wang KC, Kim J, Horlings HM, Wong DJ, Tsai MC, Hung T, Argani P, Rinn JL, Wang Y, Brzoska P, Kong B, Li R, West RB, van de Vijver MJ, Sukumar S, Chang HY. Long noncoding RNA *HOTAIR* reprograms chromatin state to promote cancer metastasis. Nature. 2010; 464: 1071-6.

Hadlock FP, Harrist RB, Martínez-Poyer J. In utero analysis of fetal growth: a sonographic weight standard. Radiology. 1991; 181: 129-33.

Hannula K, Lipsanen-Nyman M, Kontiokari T, Kere J. A narrow segment of maternal uniparental disomy of chromosome 7q31-qter in Silver-Russell syndrome delimits a candidate gene region. Am J Hum Genet. 2001; 68: 247-53.

Hansen TV, Hammer NA, Nielsen J, Madsen M, Dalbaek C, Wewer UM, Christiansen J, Nielsen FC. Dawrfism and impaired gut development in insulin-like growth factor II mRNA-binding protein 1-deficient mice. Mol Cell Biol. 2004; 24: 4448-64.

Harkness UF, Mari G. Diagnosis and management of intrauterine growth restriction. Clin Perinatol. 2004; 31: 743-64.

Harrington TAM, Thomas EL, Frost G, Modi N, Bell JD. Distribution of adipose tissue in the newborn. Pediatr Res. 2004; 55: 437-41.

Hattersley AT. Unlocking the secrets of the pancreatic β cell: man and mouse provide the key. The Journal of Clinical Investigation. 2004; 114: 314- 6.

Hattersley AT, Beards F, Ballantyne E, Appleton M, Harvey R, Ellard S. Mutations in the glucokinase gene of the fetus result in reduced birth weight. Nature Genet. 1998; 19: 268-70.

Hattersley AT, Tooke JE. The fetal insulin hypothesis: an alternative explanation of the association of low birthweight with diabetes and vascular disease. Lancet. 1999; 353: 1789- 92.

Hendrix N, Berghella V. Non-placental causes of IUGR. Semin Perinatol. 2008; 36: 161-5.

Hermann A, Gowher H, Jeltsch A. Biochemistry and biology of mammalian DNA methyltransferases. Cell Mol Life Sci. 2004; 61: 2571- 87.

Hill DJ, Strutt B, Arany E, Zaina S, Coukell S, Graham CF. Increased and persistent circulating Insulin-like Growth Factor II in neonatal transgenic mice suppresses developmental apoptosis in the pancreatic islets. Endocrinology. 2000; 141: 1151-7.

Hitchins MP, Moore GE. Genomic imprinting in fetal growth and development. Expert Rev Mol Med. 2002; 4: 1-19.

Hitchins MP, Stanier P, Preece MA, Moore GE . Silver- Russell syndrome: a dissection of the genetic aetiology and candidate chromosomal regions. J Med Genet. 2001; 38: 810- 819.

Hokken-Koelega ACS, de Ridder MAJ, Lemmen RJ, den Hartog H, de Muinck Keizer-Schrama SMPF, Drop SLS. Children born Small for Gestational Age: do they catch up? Pediatr Res. 1995; 38: 267-71.

Ibáñez L, de Zegher F. Puberty after prenatal growth restraint. Horm Res. 2006; 65:112-5.

Ideraabdullah FY, Vigneau S, Bartolomei MS. Genomic imprinting mechanisms in mammals. Mutat Res. 2008: 647: 77-85.

Iglesias Platas I, Thió Lluch M, Pociello Almiñana N, Morillo Palomo A, Iriondo Sanz M, Krauel Vidal X. Continuous glucose monitoring in infants of very low Barth weight. Neonatology. 2009; 95: 217-23.

Iqbal K, Jin SG, Pfeifer GP, Szabó PE. Reprogramming of the paternal genome upon fertilization involves genome-wide oxidation of 5-methylcytosine. PNAS. 2011; 108: 3642-7.

Jarvis S, Glinianaia SV, Torrioli MG, Platt MJ, Miceli M, Jouk PS, Johnson A, Hutton J, Hemming K, Hagberg G, Dolk H, Chalmers J, on behalf of the Surveillance of Cerebral Palsy in Europe (SCPE) collaboration of European Cerebral Palsy Registers. Cerebral palsy and intrauterine growth in single births: European collaborative study. Lancet. 2003; 362: 1106-11.

Jenuwein T, Allis CD. Translating the histone code. Science. 2001; 293: 1074- 80.

Jones PA, Takai D. The role of DNA methylation in mammalian epigenetics. Science. 2001; 293: 1068- 70.

Jong MTC, Gray TA, Ji Y, Glenn CC, Saitoh S, Driscoll DJ, Nicholls RD. A novel imprinted gene, encoding a RING zinc-finger protein, and overlapping antisense transcript in the Prader-Willi syndrome critical region. Hum Mol Genet. 1999; 8: 783-93.

Joyce CA, Sharp A, Walker JM, Bullman H, Temple IK. Duplication of 7p12-2-p13, including *GRB10* and *IGFBP1*, in a mother and daughter with features of Silver-Russell syndrome. Hum Genet. 1999; 105: 273-80.

Kady SM, Gardosi J. Perinatal mortality and fetal growth restriction. Best Pract Res Clin Obstet Gynaecol. 2004; 18: 397-410.

Kalousek DK, Vekemans M. Confined placental mosaicism and genomic imprinting. Ballieres Best Practice Res Clin Obstet Gynaecol. 2000; 14: 723-30.

Kalousek DK, Langlois S, Robinson WP, Telenius A, Bernard L, Barret IJ, Howard-Peebles PN, Wilson RD. Trisomy 7 CVS mosaicism: pregnancy outcome, placental and DNA analysis in 14 cases. Am J Med Genet. 1996; 65: 348-52.

Kalousek DK. Current topic: Confined placental mosaicism and intrauterine fetal development. Placenta. 1994; 15: 219-30.

Kamiya M, Judson H, Okazaki Y, Kusakabe M, Muramatsu M, Takada S, Takagi N, Arima T, Wake N, Kamimura K, Satomura K, Hermann R, Bonthron DT, Hayashizaki Y. The cell cycle control gene *ZAC/PLAGL1* is imprinted- a strong candidate gene for transient neonatal diabetes, Hum Mol Genet. 2000; 9: 453-60.

Kanber D, Berulava T, Ammerpohl O, Mitter D, Richter J, Siebert R, Horsthemke B, Lohmann D, Buiting. The human retinoblastoma gene is imprinted. PLoS Genet. 2009; 5; 12: e1000790.

Kanduri C, Thakur N, Pandey RR. The length of the transcript encoded from the *Kcnq1ot1* antisense promoter determines the degree of silencing. EMBO J. 2006; 25: 2096-106.

Kaneda M, Okano M, Hata K, Sado T, Tsujimoto N, Li E, Sasaki H. Essential role for de novo DNA methyltransferase Dnmt3a in paternal and maternal imprinting. Nature. 2004; 429: 900-3.

Kaufmann P, Mayhew TM, Charnock-Jones DS. Aspects of human fetoplacental vasculogenesis and angiogenesis II. Changes during normal pregnancy. Placenta. 2004; 25: 114-26.

Kaufmann P, Black S, Huppertz B. Endovascular trophoblast invasion: implications for the pathogenesis of intrauterine growth retardation and preeclampsia. Biol Reprod. 2003; 69: 1-7.

Khosla S, Dean W, Brown D, Reik W, Feil R. Culture of preimplantation mouse embryos affects fetal development and the expression of imprinted genes. Biol Reprod. 2001; 64: 918-26.

Kim TH, Abdullaev ZK, Smith AD, Ching KA, Loukinov DI, Green RD, Zhang MQ, Lobanenkov VV, Ren B. Analysis of the vertebrate insulator protein CTCF-binding sites in the human genome. Cell. 2007; 128: 1231-45.

Kotzot D, Utermann G. Uniparental disomy (UPD) other than 15: phenotypes and bibliography updated. Am J Med Genet A. 2005; 136: 287-305.

Koukoura O, Sifakis S, Zaravinos A, Apostolidou S, Jones A, Hajiioannou J, Widschwendter M, Spandidos DA. Hypomethylation along with increased *H19* expression in placentas from pregnancies complicated with fetal growth restriction. Placenta. 2011;32: 51-7.

Koziol MJ, Rinn JL. RNA traffic control of chromatin complexes. Curr Opin Genet Dev. 2010; 20: 142-8.

Kurukuti S, Tiwari VK, Tavoosidana G, Pugacheva E, Murrell A, Zhao Z, Lobanenkov V, Reik W, Ohlsson R. CTCF binding at the *H19* imprinting control region mediates maternally inherited higher-order chromatin conformation to restrict enhancer access to Igf2. PNAS. 2006; 103: 10864-9.

Lala PK, Chakraborty C. Factors regulating trophoblast migration and invasiveness: possible derangements contributing to pre- eclampsia and fetal injury. Placenta. 2003; 24: 575- 587.

Lam WWK, Hatada I, Ohishi S, Mukai T, Joyce JA, Cole TRP, Donnai D, Reik W, Schofield PN, Maher ER. Analysis of germline *CDKN1C (p57KIP2)* mutations in familial and sporadic Beckwith-Wiedemann Syndrome (BWS) provides a novel genotype-phenotype correlation. J Med Genet. 1999; 36: 518-23.

Lambertini L, Diplas AI, Lee MJ, Sperling R, Chen J, Wetmur J. A sensitive functional assay reveals frequent loss of genomic imprinting in human placenta. Epigenetics. 2008; 3: 261-9.

Lapunzina P, Monk D. The consequences of uniparental disomy and copy number neutral loss-of-heterozygosity during human development and cancer. Biol Cell. 2011; 103: 303-17.

Lau MMH, Stewart CEH, Liu Z, Bhatt H, Rotwein P, Stewart CL. Loss of the imprinted *IGF2*/cation independent mannose 6-phosphate receptor results in fetal overgrowth and perinatal lethality. Genes Dev. 1994; 8: 2953-63.

Lawn JE, Cousens S, Zupan J: 4 million neonatal deaths: when? Where? Why? Lancet. 2005; 365: 891–900.

Lee MH, Williams BO, Mulligan G, Mukai S, Bronson RT, Dyson N, Harlow E, Jacks T. Targeted disruption of *p107*: functional overlap between p107 and Rb. Genes Dev. 1996; 10: 1621-32.

Lee MP, Hu RJ, Johnson LA, Feinberg AP. Human KVLQT1 gene shows tissue-specific imprinting and encompasses Beckwith-Wiedemann syndrome chromosomal rearrengements. Nat Genet. 1997: 15: 181-5.

Lees-Murdock DJ, Walsh CP. DNA methylation reprogramming in the germ line. Epigenetics. 2008; 3: 5-13.

Lemeta S, Salmenkivi K, Pylkkanen L, Sainio M, Saarikoski ST, Arola J, Heikkila P, Haglund C, Husgafvel-Pursiainen K, Bohling T. Frequent loss of heterozygosity at 6q in pheocromocytoma. Human Pathology. 2006; 37: 749-54.

Lepikhov K, Wossidlo M, Arand J, Walter J. DNA methylation reprogramming and DNA repair in the mouse zygote. Int J Dev Biol. 2010; 54: 1565-74.

Lewis A, Reik W. How imprinting centres work. Cytogenet Genome Res. 2006; 113; 81-9.

Lewis A, Mitsuya K, Umlauf D, Smith P, Dean W, Walter J, Higgins M, Feil R, Reik W. Imprinting on distal chromosome 7 in the placenta involves repressive histone methylation independent of DNA methylation. Nat Genet. 2004; 36: 1291- 5.

Lewis A, Murrell A. Genomic imprinting: CTCF protects the boundaries. Curr Biol. 2004; 6: R284-6.

Li LL, Keverne EB, Aparicio SA, Ishino F, Barton SC, Surani MA. Regulation of maternal behavior and offspring growth by paternally expressed *Peg3*. Science. 1999; 284: 330- 333.

Li X, Ito M, Zhou F, Youngson N, Zuo X, Leder P, Ferguson-Smith AC. A maternal-zygotic effect gene Zfp57 maintains both maternal and paternal imprints. Dev Cell. 2008; 15: 547-57.

Lui JC, Finkielstain GP, Barnes KM, Baron J. An imprinted gene network that controls mammalian somatic growth is down-regulated during postnatal growth deceleration in multiple organs. Am J Physiol Regul Integr Comp Physiol. 2008; 295: R189-96.

Ma D, Shield JPH, Dean W, Leclerc I, Knauf C, Burcelin R, Rutter GA, Kelsey G. Impaired glucose homeostasis in transgenic mice expressing the human transient neonatal diabetes mellitus locus, TNDM. J Clin Invest. 2004; 114: 339-48.

Mackay DJG, Temple IK. Transient Neonatal Diabetes Mellitus type 1. Am J Medical Genet C Semin Med Genet. 2010; 154(C): 335-42.

Mackay DJG, Boonen SE, Clayton-Smith J, Goodship J, Hahnemann JMD, Kant SG, Njølstad PR, Robin NH, Robinson DO, Siebert R, Shield JPH, White HE, Temple IK. A maternal hypomethylation syndrome presenting as transient neonatal diabetes mellitus. Hum Genet. 2006a; 120: 262-69.

Mackay DJG, Callaway JLA, Marks SM, White HE, Acerini CL, Boonen SE, Dayanikli P, Firth HV, Goodship JA, Haemers AP, Hahnemann JMD, Kordonouri O, Masoud AF, Oestergaard E, Storr J, Ellard S, Hattersley AT, Robinson DO, Temple IK. Hypomethylation of multiple imprinted loci in individuals with transient neonatal diabetes is associated with mutations in ZFP57. Nat Genet. 2008; 40: 949- 51.

Mackay DJG, Hahnemann JMD, Boonen SE, Poerksen S, Bunyan DJ, White HE, Durston VJ, Thomas NS, Robinson DO, Shield JPH, Clayton-Smith J, Temple IK. Epimutation of the TNDM locus and the Beckwith-Wiedemann syndrome centromeric locus in individuals with transient neonatal diabetes mellitus, Hum Genet. 2006b; 119 (1-2): 179-84.

Mackay DJG, Temple IK, Shield JPH, Robinson DO. Bisulphite sequencing of the transient neonatal diabetes mellitus DMR facilitates a novel diagnostic test but reveals no methylation anomalies in patients of unknown aetiology. Hum Genet. 2005; 116: 255-61.

Main KM, Jensen RB, Asklund C, Høi-Hansen CE, Skakkebaek NE. Low birth weight and male reproductive function. Horm Res. 2006; 65: 116-22.

Malassiné A, Frendo JL, Evain-Brion D. A comparison of placental development and endocrine functions between the human and mouse model. Hum Repr Update. 2003; 9: 531-9.

Mancini-DiNardo D, Steele SJS, Ingram RS, Tilghman SM. A differentially methylated region within the Kcnq1 functions as an imprinted promoter and silencer. Hum Mol Genet. 2003; 12, 283-294.

Mancini-DiNardo D, Steele SJS, Levorse JM, Ingram RS, Tilghman SM. Elongation of the KCNq1ot1 transcript is required for genomic imprinting of neighboring genes. Genes Dev. 2006; 20: 1268-82.

Mann MRW, Lee SS, Doherty AS, Verona RI, Nolen LD, Schultz RM, Bartolomei MS. Selective loss of imprinting in the placenta following preimplantation development in culture. Development. 2004; 131: 3727- 35.

Marcelin G, Diatloff-Zito C, Nicole A, Robert JJ. Developmental methylation program and concerted expression of Stx11 in mouse tissues. Mamm Genome. 2009; 20: 131- 9.

McGrath J, Solter D. Completion of mouse embryogenesis requires both the maternal and paternal genomes. Cell. 1984; 37: 179- 83.

McMinn J, Wei M, Sadovsky Y, Thaker HM, Tycko B. Imprinting of PEG1/MEST isoform 2 in human placenta. Placenta. 2006; 27: 119-26.

Meyer E, Lim D, Pasha S, Tee LJ, Rahman F, Yates JRW, Woods CG, Reik W, Maher ER. Germline mutation in NLRP2 (NALP2) in a familial imprinting disorder (Beckwith-Wiedemann syndrome). PLoS Genet. 2009; 5: e1000423. doi:10.1371/journal.pgen.1000423.

Miller J, Turan S, Baschat AA. Fetal growth restriction. Semin Perinatol. 2008; 32: 274-80.

Monk D, Arnaud P, Apostolidou S, Hills FA, Kelsey G, Stanier P, Feil R, Moore GE. Limited evolutionary conservation of imprinting in the human placenta. PNAS. 2006a; 103(17): 6623-8.

Monk D, Hitchins M, Russo S, Preece M, Stanier P, Moore GE. No evidence for mosaicism in Silver-Russell syndrome. J Med Genet. 2001; 38: 11-12.

Monk D, Sanches R, Arnaud P, Apostolidou S, Hills FA, Abu-Amero S, Murrell A, Friess H, Reik W, Stanier P, Constancia M, Moore GE. Imprinting of IGF2 P0 transcript and novel alternaltively spliced INS-IGF2 isoforms show differences between mouse and human. Hum Mol Genet. 2006b; 15: 1259-69.

Monk D, Wakeling EL, Proud V, Hitchins M, Abu-Amero SN, Stanier P, Preece MA, Moore GE. Duplication of 7p11.2-p13, including GRB10, in Silver-Russell syndrome. Am J Hum Genet. 2000; 66: 36-46.

Moore GE, Ali Z, Khan RU, Blunt S, Bennett PR, Vaughan JI. The incidence of uniparental disomy associated with intrauterine growth retardation in a cohort of thirty-five severely affected babies. Am J Obstet Gynecol. 1997; 176: 294-9.

Moore T, Constancia M, Zubair M, Bailleul B, Feil R, Sasaki H, Reik W. Multiple imprinted sense and antisense transcripts, differential methylation and tandem repeats in a putative imprinting control region upstream of mouse *Igf2*. PNAS. 1997; 94: 12509-14.

Moore T. Genetic conflict, genomic imprinting and establishment of the epigenotype in relation to growth. Reproduction. 2001; 122: 185-93.

Morgan AR, Thompson JMD, Murphy R, Black PN, Lam WJ, Ferguson LR, Mitchell EA. Obesity and diabetes genes are associated with being born small for gestacional age: results from the Auckland Birthweight Collaborative study. BMC Medical Genetics. 2010; 11: 125.

Morken NH, Källen K, Jacobsson B. Fetal growth and onset of delivery: a nationwide population-based study of preterm infants. Am J Obstet Gynecol. 2006; 195: 154-61.

Murrell A, Heeson S, Reik W. Interaction between differentially methylated regions partitions the imprinted genes Igf2 and H19 into parent-specific chromatin loops. Nature Genet. 2004; 36: 889- 93.

Nakabayashi K, Bentley L, Hitchins MP, Mitsuya K, Meguro M, Minagawa S, Bamforth JS, Stanier P, Preece M, Weksberg R, Oshimura M, Moore GE, Scherer SW. Identification and characterization of an imprinted antisense RNA (MESTIT1) in the human MEST locus on chromosome 7q32. Hum Mol Genet. 2002; 11: 1743-56.

Nakamura T, Arai Y, Umehara H, Masuhara M, Kimura T, Taniguchi H, Sekimoto T, Ikawa M, Yoneda Y, Okabe M, Tanaka S, Shiota K, Nakano T. PGC7/Stella protects against DNA methylation in early embryogenesis. Nature Cell Biol. 2007; 9: 64-71.

Neerhof MG, Thaete LG. The fetal response to chronic placental insufficiency. Semin Perinatol. 2008; 32: 201- 5.

Nikonova L, Koza RA, Mendoza T, Chao PM, Curley JP, Kozak LP. Mesoderm-specific transcript is associated with fat mass expansion in response to a positive energy balance. FASEB J. 2008; 22: 3925-7.

Nishimaki S, Yukawa T, Makita Y, Honda H, Kikuchi N, Minimisawa S, Yokota S. Transient neonatal diabetes mellitus in extremely preterm infant. Arch Dis Child Fetal Neonatal Ed. 2008; 93: F240-1.

Nishino K, Hattori N, Sato S, Yoshikazu A, Tanaka S, Nagy A, Shiota K. Non-CpG methylation occurs in the regulatory region of the Sry gene. J Reprod Dev. 2011; 57: 586-93.

Noguer-Dance M, Abu-Amero S, Al-Khitb M, Lefevre A, Coullin P, Moore GE, Cavaille J. The primate-specific microRNA gene cluster (C19MC) is imprinted in the placenta. Hum Mol Genet. 2010; 19: 3566-82.

Nolan T, Hands RE, Bustin SA. Quantification of mRNA using real-time RT-PCR. Nature Protocols. 2007; 1: 1559-82.

O'Neill MJ. The influence of non-coding RNAs on allele-specific gene expression in mammals, Hum Mol Genet. 2005; 14: R113- 20.

Okada Y, Yamagata K, Hong K, Wakayama T, Zhang Y. A role for elongator in zygotic paternal genome demethylation. Nature. 2010; 463: 554-8.

Okutsu T, Kuroiwa Y, Kagitani F, Kai M, Aisaka K, Tsutsumi O, Kaneko Y, Yokomori K, Surani MA, Kohda T, Kaneko-Ishino T, Ishino F. Expression and imprinting status of human *PEG8/IGF2AS*, a paternally expressed antisense transcript from the *IGF2* locus, in Wilm´s tumors. J Biochem. 2000; 127: 475-83.

Ong KK, Dunger DB. Perinatal growth failure: the road to obesity, insulin resistance and cardiovascular disease in adults. Best Pract Res Clin Endocrinol and Metab. 2002; 16: 191-207.

Ono R, Nakamura K, Inoue K, Naruse M, Usami T, Wakisaka-Saito N, Hino T, Suzuki-Migishima R, Ogonuki N, Miki H, Kohda T, Ogura A, Yokoyama M, Kaneko-Ishino T, Ishino F. Deletion of Peg10, and imprinted gene acquired from a retrotransposon, causes early embryonic lethality. Nat Genet. 2006; 38: 101-6.

Pagotto U, Arzberger T, Theodoropoulou M, Grübler Y, Pantaloni C, Saeger W, Losa M, Journot L, Stalla GK, Spengler D. The expression of the antiproliferative gene ZAC is lost or highly reduced in non-functioning pituitary adenomas. Cancer Res. 2000; 60: 6794-9.

Pardi G, Marconi AM, Cetin I. Placental-fetal interrelationship in IUGR fetuses- a review. Placenta. 2002; 23 (suppl A. Trophoblast Research): S136-41.

Pauli A, Rinn JL, Schier AF. Non-coding RNAs as regulators of embryogenesis. Nature Rev Genet. 2011; 12: 136-49.

Petrik J, Arany E, McDonald TJ, Hill DJ. Apoptosis in the pancreatic islet cells of the neonatal rat is associated with a reduced expression of Insulin-like Growth Factor II that may act as a survival factor. Endocrinology. 1998; 139: 2994-3004.

Petry CJ, Ong KK, Barratt BJ, Wingate D, Cordell HJ, Ring SM, Pembrey ME, The ALSPAC Study Team, Reik W, Todd JA, Dunger DB. Common polymorphism in H19 is associated with birthweight and cord blood IGF-II levels in humans. BMC Genetics. 2005; 6:22.

Preece MA, Abu-Amero SN, Ali Z, Abu-Amero KK, Wakeling EL, Stanier P, Moore GE. An analysis of the distribution of hetero- and isodisomic regions of chromosome 7 in five mUPD7 Silver-Russell syndrome probands. J Med Genet. 1999; 36: 457-60.

Programa de Salut Maternoinfantil, Direcció General de Salut Pública, Departament de Salut. Corbes de referència de pes, perimeter cranial i longitud en néixer de nounats d'emarassos únics, de bessons I de trigèmins a Catalunya. Generalitat de Catalunya, Departament de Salut, 2008.

Ravelli AC, van Der Meulen JH, Osmond C, Barker DJ, Bleker OP. Obesity at the age of 50 y in men and women exposed to famine prenatally. Am J Clin Nutr. 1999; 70: 811-6.

Reik W, Constancia M, Fowden A, Anderson N, Dean W, Ferguson-Smith A, Tycko B, Sibley C. Regulation of supply and demand for maternal nutrients in mammals by imprinted genes. J Physiol. 2003; 547.1: 35-44.

Reik W, Dean W, Walter J. Epigenetic reprogramming in mammalian development. Science. 2001; 293: 1089-93.

Reinhart, B., Paoloni-Giacobino, A., Chaillet, J.R. Specific differentially methylated domain sequences direct the maintenance of methylation at imprinted genes. Mol. Cell Biol. 2006; 26: 8347–56.

Rice F, Thapar A. Estimating the relative contributions of maternal genetic, paternal genetic and intrauterine factors to Offspring birth weight and head circumference. Early Hum Dev. 2010; 86: 425-32.

Riesewijk AM, Blagitko N, Schinzel AA, Hu LK, Schulz U, Hamel BCJ, Ropers HH, Kalscheuer VM. Evidence against a major role of PEG1/MEST in Silver-Russell-syndrome. Eur J Hum Genet. 1998; 6: 114- 120.

Rivera RM, Stein P, Weaver JR, Mager J, Schultz RM, Bartolomei MS. Manipulations of mouse embryos prior to implantation results in aberrant expression of imprinted genes on day 9.5 of development. Hum Mol Genet. 2008; 17: 1-14.

Romanelli V, Meneses HNM, Fernández L, Martínez-Glez V, Gracia-Bouthelier R, Fraga MF, Guillen E, Nevado J, Gean E, Martorell L, Esteban Marfil V, García-Miñaur S, Lapunzina P. Beckwith-Wiedemann syndrome and uniparental disomy 11p: fine mapping of the recombination breakpoints and evaluation of several techniques. Eur J Human Genet. 2011; 19: 416-21.

Ruf N, Bähring S, Galetzka D, Pliushch G, Luft FC, Nürnberg P, Haaf T, Kelsey G, Zechner U. Sequence-based bioinformatic prediction and QUASEP identify genomic imprinting of the KCNK9 potassium channel gene in mouse and human. Hum Mol Genet. 2007; 16: 2591-9.

Salas M, John R, Saxena A, Barton S, Frank D, Fitzpatrick G, Higgins MJ, Tycko B. Placental growth retardation due to loss of imprinting of Phlda2. Mech Dev. 2004; 121: 1199-1210.

Sankaran S, Kyle PM. Aetiology and pathogenesis of IUGR. Best Pract Res Clin Obstet Gynaecol. 2009: 23: 765-77.

Santos F, Dean W. Epigenetic reprogramming during early development in mammals. Reproduction. 2004; 127: 643-51.

Sato A, Otsu E, Negishi H, Utsunomiya T, Arima T. Aberrant DNA methylation of imprinted loci in superovulated oocytes. Hum Repr. 2007; 22: 26-35.

Schieve LA, Cohen B, Nannini A, Ferre C, Reynolds MA, Zhang Z, Jeng G, Macaluso M, Wright VC for the Massachusetts Consortium for Assisted Reproductive Technology Epidemiologic Research (MCARTER). A population-based study of maternal and perinatal outcomes associated with Assisted Reproductive Technology in Massachusetts. Matern Child Health J. 2007; 11: 517-25.

Schieve LA, Meikle SF, Ferre C, Peterson HB, Jeng G, Wilcox LS. Low and Very Low Birth Weight in infants conceived with use of assisted reproductive technology. NEJM. 2002; 346: 731-7.

Schmittgen TD, Livak KJ. Analyzing real-time PCR data by the comparative CT method. Nature Protocols. 2008; 3: 1101-8.

Schulz R, McCole RB, Woodfine K, Wood AJ, Chahal M, Monk D, Moore GE, Oakey RJ. Transcript- and tissue-specific imprinting of a tumour suppressor gene. Hum Mol Genet. 2009; 18: 118-27.

Seitz H, Royo H, Bortolin ML, Lin SP, Ferguson-Smith A, Cavaillé J. A large imprinted microRNA gene cluster at the mouse Dlk1-Gtl2 domain. Genome Res. 2004; 14: 1741-8.

Siomi MC, Sato K, Pezic D, Aravin AA. PIWI-interacting small RNAs: the vanguard of genome defence. Nat Rev Moll Cell Biol. 2011; 12: 246-58.

Sleutels F, Zwart R, Barlow DP. The non-coding Air RNA is required for silencing autosomal imprinted genes. Nature. 2002; 415: 810-3.

Smilinich NJ, Day CD, Fitzpatrick GV, Caldwell GM, Lossie AC, Cooper PR, Smallwood AC, Joyce JA, Schofield PN, Reik W, Nicholls RD, Weksberg r, Driscoll DJ, Maher ER, Shows TB, Higgins MJ.

A maternally methylated CpG island in KvLQT1 is associated with an antisense paternal transcript and loss of imprinting in Beckwith-Wiedemann syndrome. PNAS. 1999; 96: 8064-9.

Smith FM, Garfield AS, Ward A. Regulation of growth and metabolism by imprinted genes. Cytogenet Genome Res. 2006; 113: 279-91.

Smith RJ, Arnaud P, Konfortova G, Dean WL, Beechey CV, Kelsey G, The mouse Zac1 locus: basis for imprinting and comparison with human ZAC. Gene. 2002, 292: 101-12.

Smith RJ, Dean W, Konfortova G, Kelsey G. Identification of novel imprinted genes in a genome-wide screen for maternal methylation. Genome Res. 2003; 13: 558-69.

Spengler D, Villalba M, Hoffmann A, Pantaloni C, Houssami S, Bockaert J, Journot L. Regulation of apoptosis and cell cycle arrest by Zac1, a novel zinc finger protein expressed in the pituitary gland and the brain. EMBO J. 1997; 16: 2814-25.

Spengler D, Waeber C, Pantaloni C, Holsboer G, Bockaert J, Seeburg PH, Journot L. Differential signal transduction by five splice variants of the PACAP receptor. Nature. 1993; 365: 170-5.

Steikampf MP, Grifo J. Major birth defects after assisted reproduction (letter). NEJM. 2002. 347: 1449.

Surani MAH, Barton SC, Norris ML. Development of reconstituted mouse eggs suggests imprinting of the genome during gametogenesis. Nature. 1984; 308: 548-50.

Takahashi M, Kamei Y, Ezaki O. Mest/Peg1 imprinted gene enlarges adipocytes and is a marker of adipocyte size. Am J Physiol Endocrinol Metab. 2005; 288: E117-24.

Tamura T, Tohma T, Ohta T, Soejima H, Harada N, Abe K, Niikawa N. Ring chromosome 15 involving deletion of the insulin-like growth factor 1 receptor gene in a patient with features of Silver-Russell syndrome. Clin Dysmorphol. 1993; 2: 106-13.

Temple IK, Gardner RJ, Mackay DJG, Barber JCK, Robinson DO, Shield JPH. Transient Neonatal Diabetes, widening the understanding of the etiopathogenesis of diabetes. Diabetes. 2000, 49: 1359- 66.

Temple IK, Mackay DJG. Diabetes mellitus, 6q24-Related Transient Neonatal. In: Pagon RA, Bird TD, Dolan CR, Stephens K, editors. GeneReviews [Internet]. University of Washington, Seattle; 1993-. 2005 [updated 2010 Dec 23].

Thompson JMD, Clark PM, Robinson E, Becroft DMO, Pattison NS, Glavish N, Pryor JE, Wild CJ, Rees K, Mitchell EA. Risk factors for small-for-gestational-age babies: the Auckland Birthweight collaborative study. J Paediatr Child Health. 2001; 37: 369-75.

Tomizawa S, Kobayashi H, Watanabe T, Andrews S, Hata K, Kelsey G, Sasaki H. Dynamic stage-specific changes in imprinted differentially methylated regions during early mammalian development and prevalence of non-CpG methylation in oocytes. Development. 2011; 138: 811-20.

Tong PY, Tollefsen SE, Kornfeld S. The catión-independent mannose-6-phosphate receptor binds Insulin-like Growth Factor II. J Biol Chem. 1998; 263: 2585-8.

Tost J, Gut IG. DNA methylation analysis by pyrosequencing. Nature Protocols. 2007; 2: 2265-75.

Tsai MC, Manor O, Wan Y, Mosammaparast N, Wang JK, Lan F, Shi Y, Segal E, Chang HY. Long noncoding RNA as modular scaffold of histone modification complexes. Science. 2010; 329: 689-93.

Tunster SJ, Tycko B, John RM. The imprinted *Phlda2* gene regulates extraembryonic energy stores. Mol Cell Biol. 2010; 30: 295-306.

Turner CLS, Mackay DM, Callaway JLA, Docherty LE, Poole RL, Bullman H, Lever M, Castle BM, Kivuva EC, Turnpenny PD, Mehta SG, Mansour S, Wakeling EL, Mathew V, Madden J, Davies JH, Temple IK. Methylation analysis of 79 patients with growth restriction reveals novel patterns of methylation at imprinted loci. Eur J Hum Genet. 2010: 18: 648-55.

Tycko B. Imprinted genes in placental growth and obstetric disorders. Cytogenet Genome Res. 2006; 113: 271-8.

Umlauf D, Goto Y, Cao R, Cerqueira F, Wagshal A, Zhang Y,Feil R. Imprinting along the Kcnq1 domain on mouse chromosome 7 involves repressive histone methylation and recruitment of Polycomb group complexes. Nat Genet. 2004; 36: 1296- 300.

Valente T, Junyent F, Auladell C. Zac1 is expressed in progenitor/stem cells of the neuroectoderm and mesoderm during embryogenesis: differential phenotype of the Zac1-expressing cells during development. Dev Dyn. 2005; 233: 667-9.

Valleley, EM, Cordery SF, Bonthron DT, Tissue-specific imprinting of the ZAC/PLAGL1 tumour suppressor gene results from variable utilization of monoallelic and biallelic promoters. Hum Mol Genet. 2007; 16: 972-81.

Vambergue A, Fajardy I, Dufour P, Valat AS, Vandersippe M, Fontaine P, Danze PM, Rousseaux J. No loss of genomic imprinting of IGF-II and H19 in placentas of diabetic pregnancies with fetal macrosomia. Growth Horm & IGF Res. 2007; 17: 130-6.

van Weissenbruch MM, Delemarre-van de Wall HA. Early influences on the tempo of puberty. Horm Res. 2006; 65: 105-11.

Varrault A, Gueydan C, Delalbre A, Bellmann A, Houssami S, Aknin C, Severac D, Chotard L, Kahli M, Le Digarcher A, Pavlidis P, Journot L, Zac1 regulates an imprinted gene network critically involved in the control of embryonic growth. Developmental Cell. 2006; 11: 711-22.

Ventolini G, Neiger R. Placental dysfunction: pathophysiology and clinical considerations. J Obstet Gynaecol. 2006; 26: 728-30.

Verona RI, Mann MRW, Bartolomei MS. Genomic imprinting: intricacies of epigenetic regulation in clusters. Annu Rev Cell Dev Biol. 2003; 19: 237- 59.

Wakeling EL, Abu Amero S, Alders M, Bliek J, Forsythe E, Kumar S, Lim DH, MacDonald F, Mackay DJ, Maher ER, Moore GE, Poole RL, Price SM, Tangeraas T, Turner CLS, Van Haelst MM, Willoughby C, Temple IK, Cobben JM. Epigenotype-phenotype correlations in Silver-Russell syndrome. J Med Genet. 2010; 47: 760- 8.

Wallace JA, Felsenfeld G. We gather together: insulators and genome organization. Curr Opin Genet Dev. 2007; 17: 400-7.

Wang KC, Yang YW, Liu B, Sanyal A, Corces-Zimmerman R, Chen Y, Lajoie BR, Protacio A, Flynn RA, Gupta RA, Wysocka J, Lei M, Dekker J, Helms JA, Chang HY. A long noncoding RNA maintains active chromatin to coordinate homeotic gene expression. Nature. 2011; 472: 120-4.

Watanabe T, Tomizawa S, Mitsuya K, Totoki Y, Yamamoto Y, Kuramochi-Miyagawa S, Iida N, Hoki Y, Murphy PJ, Toyoda A, Gotoh K, Hiura H, Arima T, Fujiyama A, Sado T, Shibata T, Nakano T, Lin H, Ichiyanagi K, Soloway PD, Sasaki H. Role for piRNAs and noncoding RNA in de novo DNA methylation of the imprinted mouse Rasgrf1 locus. Science. 2011; 332: 848-52.

Weksberg R, Smith AC, Squire J, Sadowski P. Beckwith-Wiedemann syndrome demonstrates a role for epigenetic control of normal development. Hum Mol Genet. 2003; 12: R61-8.

Wijchers PJ, Fenstenstein. Epigenetic regulation of autosomal gene expression by sex chromosomes. Trends Genet. 2011; 27: 132-40.

Wossidlo M, Nakamura T, Lepikhov K, Marques J, Zakhartchenko V, Boiani M, Arand J, Nakano T, Reik W, Walter J. 5-Hydroxymethylcytosine in the mammalian zygote is linked with epigenetic reprogramming. Nature Comm. 2011; 2: 241.

Wutz A, Smrzka OW, Schweifer N, Schellander K, Wagner EF, Barlow DP. Imprinted expression of the Igf2r gene depends on an intronic CpG island. Nature. 1997; 389: 745-9.

Xie X, Mikkelsen TS, Gnirke A, Lindblad-Toh K, Kellis M, Lander ES. Systematic discovery of regulatory motifs in conserved regions of the human genome, including thousands of CTCF insulator sites. PNAS. 2007; 104: 7145-50.

Xu Y, Goodyer CG, Deal C, Polychronakos C. Functional polymorphism in the parental imprinting of the human *IGF2R* gene. Biochem Biophys Res Commun. 1993; 197: 747-54.

Yang X, Schadt EE, Wang S, Wang H, Arnold AP, Ingram-Drake L, Drake TA, Lusis AJ. Tissue-specific expression and regulation of sexually dimorphic genes in mice. Genome Res. 2006; 16: 995-1004.

Yanney M, Marlow N. Paediatric consequences of fetal growth restriction. Seminars Perinatol. 2004; 9: 411-8.

Young LE, Fernandes K, McEvoy TG, Butterwith SC, Gutierrez CG, Carolan C, Broadbent PJ, Robinson JJ, Wilmut I, Sinclair KD. Epigenetic change in IGF2R is associated with fetal overgrowth after sheep embryo culture. Nat Genet. 2001;27:153-4.

Yu VYH, Upadhyay A. Neonatal management of the growth-restricted infant. Seminars Perinatol. 2004; 9: 403-9.

Zeitlin J, Ancel PY, Saurel-Cubizolles MJ, Papiernik E. The relationship between intrauterine growth restriction and preterm delivery: an empirical approach using data from a European case- control study. BJOG. 2000; 107: 750-8.

Zhang J, Sundaram R, Sun W, Troendle J. Fetal growth and timing of parturition in humans. Am J Epidemiol. 2008; 168: 946-51.

Zhang P, Wong C, DePinho RA, Harper JW, Elledge SJ. Cooperation between the Cdk inhibitors p27KIP1 and p57KIP2 in the control of tissue growth and development. Genes Dev. 1998; 12: 3162-7.

Zhou H, Hu H, Lai M. Non-coding RNAs and their epigenetic regulatory mechanisms. Biol Cell. 2010; 102: 645-55.

Zhou VW, Goren A, Bernstein BE. Charting histone modifications and the functional organization of mammalian genomes. Nat Rev Genet. 2011; 12: 7-18.

Appendix 1: Primers and primer conditions

Table 16: Primer sequences and reaction conditions used for genotyping and identification of heterozygous samples in the cohort.

Gene/Sequence	Technique	Sequence (5' to 3')	T_{an} (°C)	Product size (bp)
PEX3 (NM_003630)	Genotyping	F: CAGACCAGTTTTTGTGGGC	55	280
		R: GCTGGAGAAAAGTCTGATTC		
	Sequencing	CACGTGCAAATATCAGAATTG	55	-
DEADC1/ADAT2 (NM_182503)	Genotyping	F: GGTGTCTCTCATCATTTGCTC	55	270
		R: CCTGGAGAAGGTGTTCTCAG		
	Sequencing	GCTTTTCCAGAAGCTGATTC	55	-
PHACTR2 (NM_001100164)	Genotyping	F: CCGAAAGGGGCCACTGCTGG	58	260
	Sequencing	R: GTGTCAAAGCTGAACCTGC	58	
FUCA2 (NM_032020)	Genotyping	F: CAACTTGTAGAGACAGTTTC	55	200
		R: CACATCTGGGGTGACAGTG		
	Sequencing	F: GAGACAGTTTCATGTGGAGG	55	-
Bc033369	Genotyping	F: GGAAACACACACCTTCACAC	53	315
		R: GTCACTGCCAGTCTAAGAGG		
	Sequencing	CAACTCAACACACCAAGAG	55	-
LTV1 (NM_032860)	Genotyping	F: GTCTTACTGAGTACATTTGCTTTTC	55	260
		R: GAACAGCTAAACAAGGAAGG		
	Sequencing	F: GGTATCTTTTCTCTGTTTATATTC	55	-
		R: GATCCTCCAAGGGTTCAAGG		
SF3B5 (NM_031287)	Genotyping Sequencing	F: CTGAAGCATCTTTTCCATCAAGTTG	60	320
		R: CTTCTGCGACGGCGCGGAC		
STX11 (NM_003764)	Genotyping Sequencing	F: CCCTGAACGTCATCGAGCTC	58	335
		R: CGGACGGTATCAACTAACC		
UTRN (NM_007124)	Genotyping Sequencing	F: GATGGAACTGACTGCACACC	58	160
		R: GACTGTCTGTCCATACTCTC		
PLAGL1 (NM_006718-P1, NM_001080951-P2, AJ006354-P3, AK091707-P4)	Genotyping Sequencing	F: GAGCACCATTTAAAGGAACG	55	295
		R: GGTTCTACCCAGACATGGACC		
HYMAI (NR_002768)	Genotyping Sequencing	F: GCCTACGTGCGGGTCCGGG	62	186
		R: GTTGGCGAGGTTAGAGCGCC		

Table 17: Primer sequences and conditions used for expression analysis (RT-PCR) of the previously identified heterozygous samples.
Sequencing primers are included in Table 16, unless otherwise specified.

Gene/Sequence	Technique	Sequence (5' to 3')	T_{an} (°C)	Product size (bp)
PEX3 (NM_003630)	RT-PCR	F: GTCTTTCCAGTGTCAGCCTG R: GCTGGAGAAAAGTCTGATTC	53	670
DEADC1/ADAT2 (NM_182503)	RT-PCR	F: GGGAGACCATTTCAGTGTATC R: CCTGGAGAAGGTGTTCTCAG	60	530
PHACTR2 (NM_001100164)	RT-PCR	F: CCGAAAGGGGCCACTGCTGG R: CGCCATCCACTTCATCCACC	60	258
FUCA2 (NM_032020)	RT-PCR	F: GGAGGGAAGCTGGAATCTCTG R: CACATCTGGGGTGACAGTG	58	243
Bc033369	RT-PCR	F: GGAAACACACACCTTCACAC R: GTCACTGCCAGTCTAAGAGG	53	315
LTV1 (NM_032860)	RT-PCR	F: CGGAGTATTCGATGACTTCC R: GGTCTTGATCCTCCAAGGG	58	245
SF3B5 (NM_031287)	RT-PCR	F: CTGAAGCATCTTTTCCATCAAGTTG R: CTTCTGCGACGGCGCGGAC	60	320
STX11 (NM_003764)	RT-PCR	F: CCCTGAACGTCATCGAGCTC R: CGGACGGTATCAACTAACC	58	335
UTRN (NM_007124)	RT-PCR	F: CAGAGTACAGCGCCTGAGG R: GACTGTCTGTCCATACTCTC	58	190
PLAGL1 (NM_006718-P1, NM_001080951-P2, AJ006354-P3, AK091707-P4)	RT-PCR	F: TTTGCATAGGAATCAGAGGAG F (P3): TGGAGGAATGTTTTCCTAGCTTCA F (P4): CTCTTTCCTCTTCCAAGTAGACTTC	58 56 56	282 329 406
HYMAI (NR_002768)	RT-PCR	F: GCCTACGTGCGGGTCCGGG R: GTTGGCGAGGTTAGAGCGCC	62	186
GAPDH	RT-PCR	F: GACCCCTTCATTGACCTC R: CTTACTCCTTGGAGGCCATG	58	700
β-ACTIN	RT-PCR	F: CCTGACGGCCAGGTCATCAC R: GGAGCAATGATCTTGATCTTC	58	290

Table 18: Primer sequences and conditions used for the study of levels of expression (qPCR) of the PLAGL1/HYMAI transcripts.
The mitochondrial ribosomal transcript MRPL19 (L19) *was used as the housekeeping gene for internal control.*

GENE/SEQUENCE	Technique	Sequence (5' to 3')	T_{an} (°C)	Product size (bp)
PLAGL1 (NM_006718-P1, NM_001080951-P2, AJ006354-P3, AK091707-P4)	qPCR	All isoforms_F: GTGAGGAGTGTGGGAAGAAG	58	140
		All isoforms_R: GAGGTGGTCCAGTAGCACCTC	58	
		P1_F: AGCCGTGCTCACAGCTCAG	58	200
		P1_R: AGGCAGCAGCCACATTAGAC*	58	
		P3_F: TGGAGGAATGTTTTCCTAGCTTCA	58	141
		P3_R: CCCGGATTGGCTACTGAGTGA	58	
		P4_F: CTCTTTCCTCTTCCAAGTAGACTTC	58	163
		P4_R: AGATTCAAACAAGATTAACTCCTCTGA	58	
HYMAI (NR_002768)	qPCR	F: ATTGGGCTGTGTTCACCCACCA	58	127
		R: GGGAGGCCA AGGCGGGTGGATC		
MRPL19 (NM_000981)	qPCR	F- GCGGAAGGGTACAGCCAAT	58	
		R- GCAGCCGGCGCAAA		

Table 19: *Primer sequences and conditions used for the analysis of the methylation status of the 6q24 CpG islands by bisulfite sequencing (*PHACTR2, SF3B5, PLAGL1 *P2,* UTRN*) and pyrosequencing (*PLAGL1_*P1)*.

Gene/ Sequence	Technique	Sequence (5' to 3')	T$_{an}$ (°C)	Product size (bp)
PHACTR2 (NM_001100164)	Bisulfite sequencing	F: GATTTTAGTTATGGGTTAGATTT	53	243
		R: CTAAATCCCAAAAAACATTCCTCT	53	
		Nest_R: CTACCTCTAAAATTTCTCC	53	194
SF3B5 (NM_031287)	Bisulfite sequencing	F: TGGTAAGGTAGAGTTTTAGTTTTTT	53	242
		R: AACACCTACAATCCAAATACATC	53	
		Nest_F: TGAAGTATTTTTTTTATTAAGTTGAAG	53	187
PLAGL1 (NM_006718-P1, NM_001080951-P2, AJ006354-P3, AK091707-P4)	Bisulfite sequencing	F_P2: GTTTTTATTAGGGGAGTTTTGTTTT	53	182
		R_P2: AAAATCTCAAATACCAACTTAACCC		
		Nest_R_P2: CTCCCAAAAACTAAATTAAT	53	155
	Pyrosequencing (P1) Bisulfite sequencing-COBRA	F: GAyGGGTTGAATGATAAATGGTAGATG	54	268
		R: Biotin-GAyGGGTTGAATGATAAATGGTAGATG		
		Seq_F: GTGGTAGGAGGAGGTTT		
UTRN (NM_007124)	Bisulfite sequencing	F: TGGGTTAGTGATTTGTAAGAGG	53	305
		InR: CTATCCCCTCAATCTCTCCAAAACCGC		